Carinthia II

Part 3

Nature Tech

Published since 1811
215th Year of Carinthia



Volume 2

Issue 2

2025 Verlag des Naturwissenschaftlichen Vereins für Kärnten

IMPRINT

First Edition

PUBLISHER: Natural Science Association for Carinthia, Carinthia University of Applied Sciences

ADDRESS OF PUBLISHER:
Natural Science Association for Carinthia
Museumgasse 2, 9020 Klagenfurt am Wörthersee, Austria
Telephone: +43(0)50 536-30574
E-Mail: nwv@landesmuseum.ktn.gv.at
Website: www.naturwissenschaft-ktn.at

All rights reserved.

Authors are responsible for the contents of their articles.

EDITORS: Susanne Aigner, Michael Jungmeier

EDITORIAL OFFICE: Daniel Dalton, Lilia Schmalzl, Ilja Svetnik

EDITORIAL BOARD: Susanne Aigner, Adrijana Car, Daniel Dalton, Gregory Egger, Wilfried Elmenreich, Peter Granig, Michael Jungmeier, Hanns Kirchmeir, Andreas Kleewein, Christian Komposch, Kirsten von Elverfeldt, Gernot Paulus, Franz Rauch, Tamara Schenekar, Lilia Schmalzl, Ilja Svetnik, Helmut Zwander

LAYOUT, TYPESETTING AND GRAPHICS: Alice Burger Grafik+Typografie, 9020 Klagenfurt am Wörthersee

COVER IMAGE: Adobe Stock | KAMOSTOCK

ISSN: 3061-0370 (online)

DOI's for current volume:
Vol 2 / Issue 1: https://doi.org/10.71911/cii-p3-nt-2025-02-01
Vol 2 / Issue 2: https://doi.org/10.71911/cii-p3-nt-2025-02-02

FONT: Univers LT Pro

RECOMMENDED CITATION:
ex.: J. Cao, H. Hochmair, G. Paulus, and C. T. Callaghan, "Assessment of biodiversity patterns based on iNaturalist observation data from Carinthia," *Carinthia Nature Tech*, vol. 2, issue 2, 2025, Klagenfurt, p. 7–26, doi: 10.71911/cii-p3-nt-2025221

Produced with support from the Province of Carinthia

LAND KÄRNTEN
Kultur

Published with the support of the Austrian Science Fund (FWF): 10.55776/PUZ10

FWF Österreichischer Wissenschaftsfonds

CONTENT

PREFACE

Making science visible – On the third issue of *Carinthia Nature Tech* 4

FULL ARTICLES

Assessment of biodiversity patterns based on iNaturalist observation data from Carinthia 7

Applying a slime mold-inspired algorithm to network planning challenges in the Carinthian region 27

SHORT ARTICLES

Predictive maintenance in infrastructure: Utilizing 3D point clouds for efficient damage detection 47

Assessing forest structure with LiDAR: A method benchmark in the Rohrach Natural Forest Reserve 56

SHORT NOTES

Development and field testing of a portable eDNA water sampler 73

Establishment of the Miyawaki forest at Carinthia University of Applied Sciences in Villach 78

Restoring ecosystems, advancing science: The Metschacher Moos outdoor lab 84

BOOK REVIEWS

Handbuch Naturschutzfachkraft: a guide to getting things done in conservation 94

Monitoring biodiversity: Hitting the nail on the head with *Conservation Technology* 96

"Tage der Biodiversität 2025" – Collection of abstracts 98

CARINTHIA NATURE TECH AUTHOR GUIDELINES 100

Making science visible – On the third issue of *Carinthia Nature Tech*

Susanne Aigner, Michael Jungmeier

We are pleased to present the third publication of the journal Carinthia Nature Tech with this issue. While the first release marked the achievement of launching this journal after a long process, the second release provided an opportunity to consolidate certain workflows, results, and presentations. Now, the current issue demonstrates that *Carinthia Nature Tech* has already evolved into a series. Many more issues are planned to showcase and communicate the potential of new technologies for capturing, monitoring, and conveying nature in general, and biodiversity in particular. In doing so, we know we are in distinguished company worldwide.

This summer for example, the Schmidt Ocean Institute (SOI), a non-profit foundation "established to advance oceanographic research, discovery, and knowledge, and catalyze sharing of information about the oceans," reported reaching 4 million viewers through live broadcasts of dives conducted by the remotely operated vehicle SuBastian (https://schmidtocean.org). SOI explored the Mar del Plata Canyon, one of Argentina's largest deep sea trenches, which reaches a depth of 3,500 meters. Equipped with state-of-the-art technology, the dives likely led to the discovery of up to 40 species new to science. A global audience had the opportunity to follow the scientists' work up close and in real time via "dive streams."

Through this form of communication, SOI aims to explore new ways of conveying scientific knowledge. It allows a broad audience to experience the persistent efforts, enthusiasm, daily routines (in this case, aboard a research vessel), challenges, setbacks, and successes of scientists. This approach can also spark interest in nature and highlight the importance of its protection.

More generally, many new technologies offer expanded opportunities to communicate research activities and findings, as well as to make the research process itself more understandable and visible.

And on a more localized scale, the potential of new technologies becomes evident. For example, we fondly recall the large-format, iconic image of the Vellacher Au, which was displayed during the biodiversity exhibition at the Carinthian State Museum. This high-resolution aerial photograph by Ulf Scherling from the Carinthia University of Applied



Fig. 1

Figure 1:
The river landscape of the Vellacher Au. The image illustrates the patterns of a dynamic river course, shaped by the interplay of erosion and deposition as well as succession and disturbances. The figure is composed of 2,300 photos taken with a DJI Phantom 4RTK drone and subsequently stitched together. The resolution is 3.3 cm per pixel, with an individual photo resolution of 4864 × 3648 pixels; the total area captured encompasses approximately 4.9 km × 0.7 km. (Photo: Ulf Scherling, October 10th, 2022; portion of the photo)

Abbildung 1:
Die Flusslandschaft der Vellacher Au. Das Bild zeigt die Muster eines dynamischen Flusslaufes, der durch das Wechselspiel von Abtragung und Anlandung sowie durch Sukzessionen und Störungen geprägt ist. Die Abbildung besteht aus 2300 Fotos, die mit einer DJI Phantom 4RTK Drohne aufgenommen und anschließend zusammengefügt wurden. Die Auflösung beträgt 3,3 cm/pixel, die Einzelfotoauflösung 4864 x 3648 Pixel; die insgesamt erfasste Fläche umfasst etwa 4,9 km x 0,7 km. (Foto: Ulf Scherling, 10. Oktober 2022, Ausschnitt des Bildes)

Sciences was indeed the result of capturing the perfect time of day and year, but it also required significant technical effort and high-performance equipment. This made one of Carinthia's most beautiful river landscapes "accessible" to a broader audience. The image not only allows for ecological, geomorphological, and vegetation analyses, as well as studies of succession, but also showcases the beauty of the area and its outstanding riverine landscape (Figure 1).

Naturally, a journal—especially a young one—can only present exemplary studies and applications of technologies. The current issue features peer-reviewed studies on the implementation of UAV-mounted sensors applied to collect data in urban landscapes and natural areas. The interested reader will find a peer-reviewed contribution on the use of iNaturalist for citizen science observations. An innovative laboratory experiment is featured, comparing slime mold-inspired algorithms with the growth of the real organism, forecasting potential improvements to transportation systems. In the short notes section, the reader can learn about the establishment of a Miyawaki forest, recent developments at an outdoor laboratory for ecological research, and innovations in environmental DNA sampling. Three book reviews are provided, giving the reader a glimpse into the state-of-the-art of biodiversity monitoring technologies, active biodiversity research in Austria, and applied techniques to promote nature in engineering.
Let yourself be inspired by these contributions. We warmly invite you to submit your own articles or short notes to support the development of the journal while also increasing its reach and visibility. By contributing, you can help shape the future of this journal and share your work with a growing audience.
An important contribution to the further development of the journal will be made by an FWF-funded project, which will enable the implementation of a professional editorial management system. This system will provide a platform to streamline workflows, making the review process more efficient and user-friendly, improve analytics, and provide readers easy access to current and archived articles.
Finally, we would like to express our gratitude to the authors, the anonymous reviewers, the Editorial Office, the Editorial Board, and last but not least, the layout designer, who once again crafted this volume with expertise, dedication, and attention to detail.

ZUSAMMENFASSUNG

Wissenschaft erfahrbar machen – zur dritten Ausgabe des Carinthia Nature Tech

Die Herausgeber:innen freuen sich, dass mit der mittlerweile dritten Ausgabe der Carinthia Nature Tech der Charakter der Zeitschrift als fortlaufende Serie deutlich sichtbar wird. Ziel der Zeitschrift ist es, das Potenzial neuer Technologien zur Erfassung, zum Monitoring und zur Vermittlung von Biodiversität aufzuzeigen.
Ein anschauliches Beispiel für diese Möglichkeiten bieten die „Divestreams" des Schmidt Ocean Institute (https://schmidtocean.org
). Dabei ermöglichen ferngesteuerte Tauchroboter durch Live-Übertragungen faszinierende Einblicke in Lebensräume in mehreren tausend Metern Tiefe. Diese Übertragungen erreichen ein Millionenpublikum und vermitteln auf eindrucksvolle Weise sowohl die Forschungsanstrengungen als auch die erzielten Ergebnisse.
Auch in unserem unmittelbaren Umfeld gibt es Beispiele dafür, wie moderne Technologien neue Perspektiven auf Natur und Biodiversität eröffnen können. So sei etwa auf ein drohnenbasiertes Luftbild der Vellacher Au verwiesen, das auch großformatig im Kärnten:Museum ausgestellt war.
Die Herausgeber:innen hoffen, dass die Beiträge in diesem Band der Carinthia Nature Tech die geschätzte Leserschaft erreichen und inspirieren. Potenzielle Autorinnen und Autoren sind herzlich eingeladen, weitere Beiträge einzureichen und so zur Weiterentwicklung und Bekanntheit dieser jungen Zeitschrift beizutragen.
Ein herzlicher Dank gilt allen Autor:innen, Reviewer:innen, dem Editorial Office, dem Advisory Board sowie – einmal mehr – der Grafikerin für die liebevolle und präzise Gestaltung des Erscheinungsbildes der Zeitschrift.

ABOUT THE AUTHORS

Susanne Aigner
Board member of *Natural Science Association for Carinthia*, Klagenfurt am Wörthersee, Austria
E-mail: office@oekologiebuero-aigner.com

Michael Jungmeier
Chairholder of UNESCO Chair on Sustainable Management of Conservation Areas, *Carinthia University of Applied Sciences*, Villach, Austria
E-Mail: m.jungmeier@cuas.at

BACK TO CONTENT

Full Articles

Assessment of biodiversity patterns based on iNaturalist observation data from Carinthia

Jiping Cao, Hartwig Hochmair, Gernot Paulus, Corey T. Callaghan

ABSTRACT

This study examines the spatial and temporal patterns of citizen science contributions to biodiversity monitoring in Carinthia, Austria, utilizing iNaturalist research-grade observations collected from 2015 to 2022. It investigates potential data collection biases, such as time of day and season, as well as species phenology, including seasonal life cycles, which manifest in temporal patterns of data contributions. Additionally, the study explores how land cover and other variables influence observation counts across 5 × 5 km² grid cells, employing a negative binomial regression model with Eigenvector Spatial Filtering. The temporal analysis also analyzes seasonal shifts in the internationality of iNaturalist contributors in Carinthia. The results reveal significant effects of time of day, season, and land cover on observed species and biodiversity. Most taxonomic families were primarily recorded in forested and semi-natural areas during the summer months. Although artificial surfaces, such as urban fabric, contribute fewer observations in total, they exhibit a bias due to ease of access and longer observation hours during winter, aided by artificial lighting. The study also highlights that iNaturalist contributions in Carinthia during the summer months are predominantly from users who tend to contribute more frequently outside of Austria, suggesting that the summer period attracts more internationally active contributors, such as foreign tourists. This research expands on prior studies of biodiversity monitoring by integrating both local and global scales of contributor behavior.

KEYWORDS

- citizen science
- seasonality
- land cover
- contribution bias

Bewertung von Biodiversitätsmustern auf Basis von iNaturalist-Beobachtungen in Kärnten

ZUSAMMENFASSUNG

Diese Studie untersucht die räumlichen und zeitlichen Citizen Science Beobachtungen für Biodiversitätsmonitoring in Kärnten, Österreich, basierend auf iNaturalist Daten von 2015 bis 2022. Sie behandelt sowohl systematische Effekte in der Datensammlung, wie z. B. Tageszeit oder Jahreszeit, als auch die Phänologie von Pflanzen und Tieren, wie z. B. saisonale Lebenszyklen, die sich im zeitlichen Ablauf der Beobachtungen widerspiegeln. Darüber hinaus untersucht sie die Beziehungen zwischen Landnutzung und den Beobachtungszahlen in einem 5 × 5 km² Raster, unter Verwendung eines negativen Binomial-Regressionsmodells mit Eigenvector Spatial Filtering. Die zeitliche Analyse umfasst weiters saisonale Veränderungen des globalen Beobachtungsverhaltens von iNaturalist-Nutzern, die in Kärnten Beobachtungen durchgeführt haben. Die Ergebnisse zeigen einen starken Einfluss von Tageszeit, Jahrenzeit und Landnutzung auf die beobachteten Arten und deren Biodiversität. Die größte Biodiversität wurden hauptsächlich in Wald- und Wiesengebieten und während des Sommers beobachtet. Während in absoluten Zahlen versiegelte Flächen, so wie z. B. städtische Umgebungen, eine geringere Anzahl von iNaturalist Beobachtungen als einige andere Landnutzungstypen verzeichnen, weisen sie aufgrund der leichten Erreichbarkeit und der längeren Beobachtungszeiträume während des Winters (aufgrund der künstlichen Beleuchtung) einen systematischen Effekt auf. iNaturalist-Beobachtungen, die in Kärnten während des Sommers erfasst wurden, stammen überwiegend von Nutzer:innen, die eher dazu tendieren, auch außerhalb Österreichs Daten zu sammeln als diejenigen Nutzer, die in Kärnten während des Winters iNaturalist-Beobachtungen erfassen. Das lässt darauf schließen, dass erstere Nutzergruppe international aktiver ist, wie z.B. ausländische Touristen. Diese Forschungsarbeit liefert neue Einblicke im Bereich des Biodiversitätsmonitoring, indem sie sowohl lokale als auch globale Ebenen des Nutzerverhaltens berücksichtigt.

INTRODUCTION

In recent years, citizen science has emerged as a powerful tool for biodiversity monitoring and conservation efforts worldwide. Citizen science platforms have revolutionized the way researchers collect and analyze species occurrence data, allowing for unprecedented spatial and temporal coverage [1]. The engagement of citizens in scientific research not only contributes to data collection, but also fosters environmental awareness and scientific literacy among participants [2]. In addition, long-term citizen science data can be used to observe temporal trends and changes in phenology due to climate change and global warming [3], [4]. iNaturalist stands out as one of the largest unstructured biodiversity citizen science survey projects globally, with over 197 million observations of plants, animals, fungi, and other organisms worldwide as of July 2024 [5]. The platform

allows users to upload an observation (e.g., photo, identification, sound) of an organism. These observations are being used for biodiversity monitoring, species distribution modeling, and phenological research [6]. Citizen science platforms, such as iNaturalist, add to a range of state-of-the-art tools for biodiversity monitoring including unmanned aerial systems technology and real-time remote sensing applications [7]. The integration of citizen science biodiversity data with advanced spatial modeling techniques has further enhanced our ability to analyze and interpret biodiversity patterns across various landscapes.

Data contributed to citizen science platforms have been used to augment traditional, structured sources of biodiversity data [3], [4]. These efforts increase the number of species records in large geographic areas and lead to a more accurate reflection of species composition compared to traditional scientific references [8]. However, the opportunistic nature of biological recordings via citizen science leads to various biases, including spatial, temporal, and taxonomic [9]. Where people live–or where they visit–could have strong implications for the spatial locations of the data collected, and the interactions between humans and the environment introduce complex spatial and temporal dynamics that shape contribution patterns over time. Understanding contribution patterns to citizen science platforms is crucial for optimizing data collection strategies and addressing potential biases in citizen science datasets. For example, researchers might prefer to use observations from more active users who are more likely to record an exhaustive sample of a particular taxonomic group of interest in a specific area, excluding low-activity users that will not heavily affect sample size [10], [11].

Studies have shown that citizen science data are often biased toward areas with higher population density and greater accessibility [12], [13]. Road networks, in particular, have been linked to increased contribution rates in both eBird [14] and iNaturalist [15] datasets, as the presence of roads can increase the likelihood of chance encounters with wildlife [16]. Proximity to roads has been identified as a strong predictor of iNaturalist contribution abundance, often diminishing the apparent influence of elevation [15]. Collection hotspots are frequently associated with sites that organize public surveys or are regularly visited by recording societies [9]. In addition, protected areas and parks tend to attract more observers, likely due to their perceived biodiversity value and recreational appeal [17]. However, the relationship between protected areas and citizen science contributions varies across regions and taxa [13]. In some cases, remote protected areas or those managed primarily for biodiversity conservation receive relatively few observations despite their ecological importance, as seen in native wetlands and wet and dry forests in Hawaii [18]. Similarly, a comparison of the proportion of pixels with observed versus expected iNaturalist records across the conterminous U.S. revealed a higher-than-expected number of observations in developed areas, with the opposite pattern observed for shrublands and grasslands [10], [11]. There is growing evidence that the type of environment, particularly the distinction between urban and rural settings, influences observers' behavior and engagement with biodiversity. One study found that urban residents generally have lower species identification skills and weaker emotional connections to nature than rural residents [19] which may (or may not) contribute to reduced participation in citizen science biodiversity mapping. Similarly, residents living greater than 10 km from the nearest forest patch performed worse in bird identification tasks than those living closer [20]. A review of urban biodiversity research over the past 30 years also revealed that most studies remain spatially and temporally limited. Broader use of citizen science and remote sensing could help overcome these limitations and close existing knowledge gaps in urban biodiversity research [21].

Temporal patterns in iNaturalist contributions indicate that user activity peaks globally between May and September, with additional spikes during organized events such as the City Nature Challenge in late April and various bioblitzes [10], [11]. Contributions are also generally higher on weekends compared with weekdays. Similar patterns have been observed in other biodiversity-focused citizen science platforms, such as Artportalen, alongside long-term trends and weather-related effects [22].

Daily and seasonal cycles further shape temporal observation patterns, as they are closely linked both to human activity, such as the preference for data collection on weekends [23], and to phenology, that is, the timing of biological events in plants and animals [24]. Examining the seasonality and hourly distribution of observations in conjunction with environmental factors, such as land cover, can provide valuable insights into these temporal patterns and their associated biases, for example, longer daily observation windows in urban areas due to artificial lighting. Temporal analysis can also reveal unusual phenological events, such as regional flowering peaks, or highlight biases, such as the tendency to record plants during their flowering phase [25]. Furthermore, multi-year analyses of citizen science data aimed at detecting phenological shifts over time must account for systematic effects. For instance, a recurring sampling date, such as the first Saturday in June, shifts one day earlier each year and resets approximately every seven years [23].

In addition to spatial and temporal biases, citizen science datasets are also subject to taxonomic biases, meaning that some species are over- or under-represented. For instance, a comparison between collections-based bee biodiversity monitoring and research-grade iNaturalist observations showed that a small group of well-trained participants systematically collecting bees documented biodiversity more effectively than thousands of individual iNaturalist contributors [26]. On iNaturalist, the basic unit of data is the verifiable observation, which includes a date, georeference, photos or sounds, and excludes captive or cultivated organisms. Observations achieve research-grade status when at least two-thirds of community identifiers agree on a species-level or lower identification. Analyses of bird observations on iNaturalist indicate that large-bodied species, common species, and those occurring in large flocks tend to be over-represented [27]. Users also often specialize in particular taxa, such as plants or insects, rarely submit repeat observations of the same species, and tend to record species common in human-influenced areas, such as monarch butterflies or mallards [10]. Conversely, species that are often hidden, highly mobile, evasive, or difficult to photograph without specialized equipment are typically undersampled [28], [29]. Socio-economic constraints and health limitations, such as those affecting older individuals, have also been identified as barriers to participation in conservation-related citizen science activities [30]. To address such sampling biases in species distribution models, corrective methods including spatial filtering and background sampling techniques have been developed [31].

Participants in biodiversity projects tend to prefer areas with higher species richness and greater taxonomic diversity [32]. Consequently, seasonal variation in observable biodiversity may influence travel patterns, such as the distance traveled to observation sites for participation in citizen science projects. While other georeferenced crowd-sourced data, such as tweets [33], have been used to study global mobility patterns, they lack the biodiversity context that platforms like iNaturalist provide. Analyzing iNaturalist data enables researchers not only to track user movements but also to understand the motivations behind these movements in the context of nature observation. Only a few previous studies have addressed this research gap. For example, an analysis of iNaturalist observations in Hawaii indicated that most contributors were likely visitors [18] while

another study found that average travel distances to parks were greater for certain park management types, such as National or State Parks, compared with city or county parks [34].

This study aims to analyze the contribution patterns to iNaturalist, using Carinthia as a case study. As an Alpine region, Carinthia offers diverse opportunities for citizen science engagement due to its rich biodiversity, sensitive ecosystems [35], [36], and distinct winter and summer seasons [37]. Accordingly, the study provides insights into local contribution characteristics for this specific Alpine region, in line with previous local studies that have, for example, identified urban biodiversity hotspots [38]. Using a range of analytical approaches, the study addresses the following objectives: (1) Identify the key environmental factors associated with the spatial distribution of iNaturalist research-grade contributions in Carinthia, and (2) examine hourly and seasonal contribution patterns, including the distribution of contributions across species and taxonomic kingdoms, the influence of land cover on user contributions, and the effect of seasonality on the share of domestic versus international data collection efforts by iNaturalist contributors in Carinthia.

METHODS

Data

iNaturalist observations

Research-grade iNaturalist data were obtained through the Global Biodiversity Information Facility (GBIF) website [39] in CSV format. GBIF provides access to biodiversity data from numerous sources, either by hosting datasets directly or by indexing those maintained by external providers. Among the citizen science contributions for Carinthia available through GBIF during the 2015-2022 study period, iNaturalist ranked fourth, accounting for 15.8% (31,974) of all GBIF records (202,368). Other major contributors include the Biodiversitätsdatenbank Nationalpark Hohe Tauern (17.7%, 35,819 records), the Biodiversitätsdatenbank Salzburg (17.0%, 34,492 records), and Pl@ntNet (16.4%, 33,089 records). Because users may contribute to multiple citizen science platforms–sometimes under different usernames–combining datasets could lead to duplicate observations. Moreover, some platforms focus on specific taxonomic groups. For example, Pl@ntNet primarily targets plants. To ensure taxonomic breadth and maintain consistency while avoiding potential double counting, this study limits its analysis to a single comprehensive source of citizen science data, iNaturalist.

The downloaded iNaturalist research-grade data included georeferenced coordinates, timestamps, species identification, anonymized observer IDs, taxonomic information, observation quality, and URLs to associated photographic evidence. These data were stored in a PostgreSQL database for further analysis, with observations from January 1, 2015, to January 1, 2023, considered. Because observations initially marked as "Needs ID" require time for verification and potential upgrading to research-grade status, we focused on the time period of 2015–2022 to ensure the use of stabilized annual datasets that had sufficient time for community validation. Research-grade observations are particularly valuable for scientific research, as they provide reliable species occurrence data at a scale previously unattainable through traditional methods [40].

Other geospatial data

The following data were used in either spatial regression or temporal analysis. Road polyline data were obtained from the Carinthia Transportation Department through Carinthia University of Applied Sciences. This dataset distinguishes between 12 road

classes, which were divided into those with and without car access, followed by the computation of the total length of vehicular and pedestrian-only accessible roads within each 5 × 5 km² grid cell. Next, OpenStreetMap (OSM) road data were downloaded (https://download.geofabrik.de/europe/austria.html), and the direct distance of a grid cell to the nearest OSM primary road was computed. A land cover vector dataset was extracted from the CORINE Land Cover (CLC) 2018 version which was obtained from the Copernicus Land Monitoring Service (https://land.copernicus.eu/en/products/corine-land-cover). It comes with a minimum mapping unit of 25 ha at a scale of 1:100,000. The CLC nomenclature includes 44 land cover types, organized hierarchically in three levels. For this study, the first-level classification with five categories including artificial surfaces, agricultural areas, forest and semi-natural areas, wetlands, and water bodies (Figure 1) was used for regression, whereas the second-level classification with 12 categories was used for charting temporal contribution patterns. Artificial surfaces comprise continuous and discontinuous urban fabric, industrial and transport units, as well as artificial, non-agricultural vegetated areas, such as parks and sport facilities.

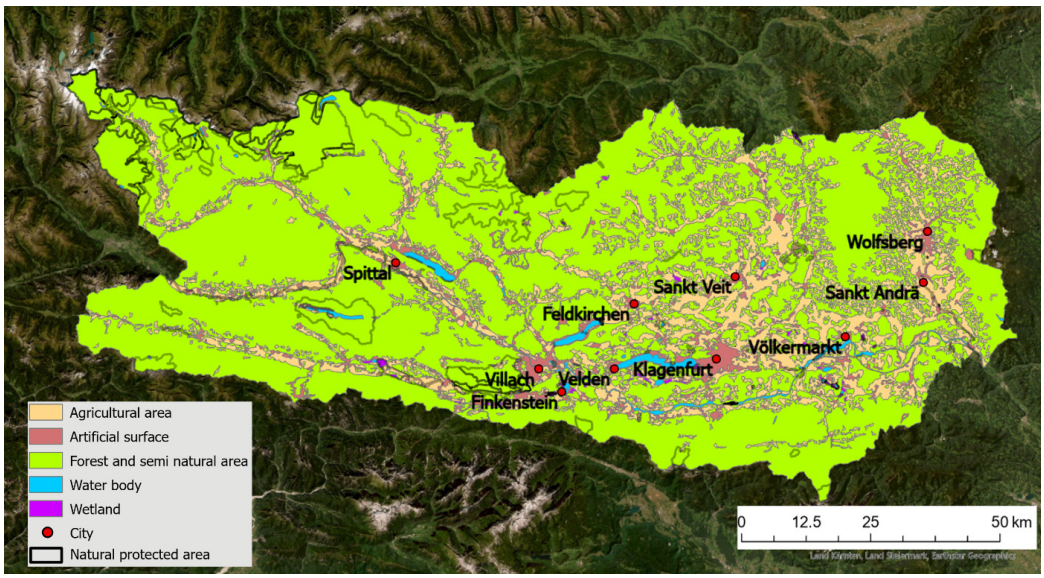


Fig. 1

Figure 1: First-level classification of CORINE land cover, protected areas and cities/towns in Carinthia

Abbildung 1: *Oberste Ebene der CORINE-Landnutzungsklassen, Naturschutzgebiete und Städte/Gemeinden in Kärnten*

Shapefiles delineating protected areas in Carinthia (see Figure 1) were obtained from multiple sources, including the Austrian Federal Ministry for Climate Action, Environment, Energy, Mobility, Innovation and Technology. This national-scale dataset served as the foundation for extracting protected areas specific to Carinthia. Additional data were manually sourced from regional environmental authorities in Carinthia, leading to 687 protected areas intersecting with Carinthia and covering 837 km².

A 10 × 10 km² elevation raster was obtained from the Austrian Open Government Data portal, and its mean elevation and slope were resampled to the 5 × 5 km² analysis grid.

The locations of the ten largest cities and towns in Carinthia as of 2020 (see Figure 1) were obtained from the Federal Statistical Office of Austria ("Statistics Austria"), with population sizes ranging from approximately 9000 to 102,000 residents. For the regression analysis, the distances between each grid cell and the nearest city (town) and protected area, respectively, were computed.

Modeling spatial contribution patterns

A negative binomial regression model was developed to predict the number of observations per nominal 5 × 5 km² grid cell where the size of grid cells is smaller along

the boundary of the study area. Published literature provides several suggestions for the grid size to be used for quadrant count analysis. One method, for example, considers study area size and number of events, which gives a recommended grid size of 2 × 2 km^2 for our dataset [41]. However, this grid size results in numerous empty cells, poor model fit of the negative binomial regression, and only a few significant coefficients. It also leads to excessive computation time when incorporating Eigenvector Spatial Filtering (ESF). Therefore, the 5 × 5 km^2 grid struck an optimal balance between preservation of spatial details in contribution patterns and computational efficiency.

Besides grid size, contribution counts per cell were also considered in data preparation. Counting observations in the 5 × 5 km^2 grid raster revealed that some "super users" had contributed disproportionately large numbers of observations (several thousands) concentrated within local areas, which could not be explained by environmental variables. These isolated contribution hotspots could not be predicted through regression analysis and were therefore mitigated as follows to avoid biased model results. Within each grid cell, the number of contributions per unique user were computed. These values were then sorted across all grids. The 95th percentile was set as a threshold that was then applied to each grid cell, capping the maximum number of observations any single user could contribute to any cell. Capping contributions from super users is a common practice when modeling activity rates from crowd-sourced data. For example, this can be done by retaining only one record when multiple images are taken within the same minute or by excluding photos with identical coordinates and owner IDs, as applied in Flickr datasets [42], [43].

Candidate predictors, computed for each grid cell, included mean elevation, slope, supply of pedestrian-only and car-accessible roads, distance to nearest city and nearest protected area, and proportion of the first four land cover types shown in Figure 1, with wetland as the default land cover category. The land cover-related variables underwent a logarithmic transformation to remove non-normality. In addition, the model included an offset term (log of cell size in km^2) to account for the varying size of grid cells in which iNaturalist observations were taken. To address spatial autocorrelation among regression residuals, ESF was employed [44], using the R packages spdep and sf.

The negative binomial regression model, incorporating land cover and other predictor variables as well as spatial eigenvectors (EVs), can be expressed as:

$$\log(\lambda) = \beta_0 + \beta_1 X_1 + \beta_2 X_2 + \ldots + \beta_n X_n + \text{offset}(\log(\text{area})) + \gamma_1 EV_1 + \ldots + \gamma_m EV_m + \varepsilon \quad (1)$$

where λ is the expected count of observations, $X_1 \ldots X_n$ are the predictor variables, $EV_1 \ldots EV_m$ are EVs, indexed β and γ symbols represent coefficients for predictor variables and eigenvectors, respectively, which are to be estimated, and ε is the error term.

To construct the final negative binomial regression with selected eigenvectors, a forward stepwise selection procedure was implemented based on the Akaike Information Criterion (AIC), which balances model fit and complexity. Variables with a Variance Inflation Factor (VIF) > 5 were flagged for potential removal due to multicollinearity among predictors. Spatial autocorrelation in model residuals was evaluated using Moran's I, and McFadden's R-squared was calculated to assess overall model fit.

Seasonal and daily variations in observation patterns

The temporal analysis examined changes in contribution patterns, including data abundance, number of taxa and users, proportion of taxonomic groups, and most frequently observed species, (1) across the four seasons; and (2) throughout the day. Some analyses were performed separately for different land cover types. For both seasonal and hourly analyses, abundance and taxonomic composition were aggregated from

multi-year data (2015-2022) into four seasonal periods and 24-hour intervals, respectively. Additional descriptive statistics, such as the number of hours per day accounting for 90% of observations for each land cover type and season, were calculated to provide further insight into temporal variation in data abundance across different land cover types.
Seasons were defined as spring (March through May), summer (June through August), fall (September through November), and winter (December through February). Chi-square tests were performed on different types of hourly and seasonal contribution data to identify the statistical significance of hourly or seasonal changes in the proportion of contribution to different kingdoms, taxonomic categories, and land cover types, respectively. A small number of observations, i.e., 50 in spring, 557 in summer, 56 in fall, and 15 in winter, with a timestamp of exactly "00:00:00" were excluded from all hourly-related analyses, because they lacked actual timestamp information.

Taxonomic variety in observation patterns

Related analyses report the number of unique families and genera across different land cover types and seasons. Finally, comparisons of the three most frequently observed species for each land cover type and season illustrate the phenological patterns of recorded species throughout the year.

RESULTS

Spatial contribution patterns

Tab. 1

Variable	Estimate	IRR	p-value
(Intercept)	1.472	4.358	< 0.001
LC proportion: Artificial surface (log)	0.226	1.253	< 0.001
LC proportion: Forest and semi-natural area (log)	-0.737	0.479	< 0.001
LC proportion: Water body (log)	0.130	1.138	< 0.001
LC proportion: Agriculture (log)	-0.218	0.804	< 0.001
Nearest distance to city [km]	-0.212	0.809	< 0.001
Nearest distance to primary road [km]	-0.136	0.873	< 0.05
EV2	-3.032	0.048	< 0.001
EV4	5.490	242.138	< 0.001
EV5	-2.816	0.060	< 0.001
EV6	-2.553	0.078	< 0.001
EV7	4.047	57.226	< 0.001
EV9	-4.339	0.013	< 0.001
EV10	-4.382	0.013	< 0.001
EV14	-3.745	0.024	< 0.001
EV15	-3.763	0.023	< 0.001
EV16	3.970	53.000	< 0.05
EV17	2.105	8.207	< 0.001
Other 53 selected Eigenvectors			
Number of observations	456		
Moran's I of residuals	0.005		0.377
McFadden's R-squared	0.12		
McFadden's adjusted R-squared	0.10		

Table 1:
Significant predictors for iNaturalist observations in Carinthia

Tabelle 1:
Signifikante Prädikatoren von iNaturalist-beobachtungen in Kärnten

Regression analysis

The final model (Table 1) shows significant predictors after removal of predictors due to multicollinearity and only a subset of significant coefficients associated with EVs for conciseness. Most EVs included in the model exhibit VIF values close to 1, underlining their effectiveness in capturing spatial autocorrelation without introducing multicollinearity. The residuals from the model without EVs demonstrated significant spatial autocorrelation (Moran's I = 0.198, $p < 0.0001$) which was mitigated after incorporating EVs (Moran's I = 0.005, $p = 0.377$). Elevation and the distance to protected areas were non-significant. The contribution densities in forested areas, artificial surfaces, and protected areas are 1.85 points/km², 11.34 points/km², and 4.25 points/km², respectively. This suggests that protected areas may function as transitional zones between artificial surfaces and forested land cover types, exhibiting neither particularly high nor low contribution densities, which likely renders this variable non-significant.

The model results indicate that the proportion of artificial surfaces and water bodies are positively associated with iNaturalist observations, while the proportion of forested areas and agricultural lands in a 5 × 5 km² cell shows negative associations. Proximity to cities and primary roads is linked to increased observation counts. Since the link function of a negative binomial model is the natural log, the interpretation of regression coefficients (e.g., β_1), is that each one-unit increase in the mean of a predictor (e.g., $\bar{x}1$) increases the mean number of observations contributed to a 5 × 5 km² cell by a multiplication factor $\exp(\beta_1)$, which gives the incidence rate ratio (IRR). For example, using the mean of 18.585 km for the "nearest distance to city" predictor across all cells, an increase of the distance by 1 km results in an IRR of $e^{-0.212} = 0.809$ and will lead, on average to a decline of (1-0.809) = 19.1% of observations in a cell. The effect sizes of the model variables with their 95% confidence intervals are expressed as IRR in Figure 2 (intercept and eigenvectors excluded), revealing the largest effect of log-transformed forest and semi-natural areas among significant predictors.

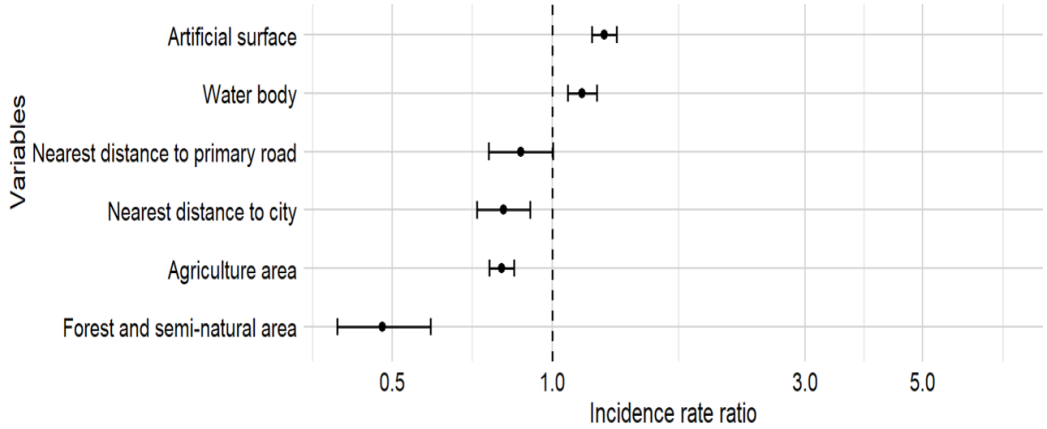


Fig. 2

Figure 2: Effect size of predictor variables

Abbildung 2: *Effektgrößen der Regressionsvariablen*

Contributions to land cover types

Users who contributed at least one iNaturalist observation in Carinthia during summer between 2015 and 2022 added observations to 2.78 CORINE land cover types (level 2, 12 types) on average (median: 2, maximum: 11). The right-tailed distribution (Figure 3a) and the log-log plot (Figure 3b) indicate that most users concentrated their observations on a few land cover types and that the number of contributors exhibited a power law relationship with the number of land cover types contributed to ($R^2 = 0.919$).

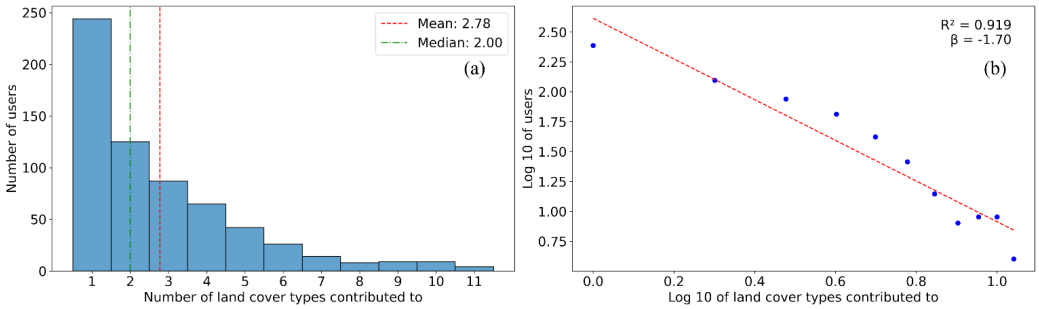


Fig. 3

Figure 3: Distribution of land cover types contributed to expressed as histogram (a) and log-log plot (b)

Abbildung 3: *Statistische Verteilung der Anzahl von Landnutzungsklassen mit Beobachtungen pro Nutzer, visualisiert als Histogram und Punktdiagramm mit logarithmischer Achsenskalierung*

Temporal contribution patterns

Seasonality of contributing individuals

Of the 825 iNaturalist users who contributed iNaturalist observations in Carinthia between 2015 and 2022, 68.3% contributed data in only a single season, 18.1% in two seasons, 6.9% in three seasons, and 6.7% in all four seasons (in any year). The first group represents typical seasonal visitors and one-time contributors, where the last group represents committed and probably local contributors taking observations throughout the year.

Contributions to biodiversity across days and seasons

The proportion of contributions to different kingdoms varies by hour and season (Figure 4). At the 12 pm peak in summer, Animalia comprises 45.4% of contributions, Plantae 51.8%, and Fungi 2.7%, whereas in fall the proportion of Animalia (63.1%) and Fungi (16.3%) increases but drops for Plantae (20.6%). Kingdom Animalia generally dominates the daily tails of early morning and late evening hours across seasons, often reaching 90-100% of observations, possibly due to nocturnal animal activity. Protozoa and Bacteria appear only sporadically in small numbers, e.g., with 1 observation for Protozoa between 8:00-9:00 in summer and 1 observation between 11:00-12:00 in fall, and 1 observation for Bacteria between 10:00-11:00 in both summer and fall. Summer exhibits the highest overall activity with a maximum of about 250 unique users contributing around 2000 observations per hour around noon, whereas winter is the opposite with a maximum of about 40 unique users contributing around 120 observations per hour around noon.

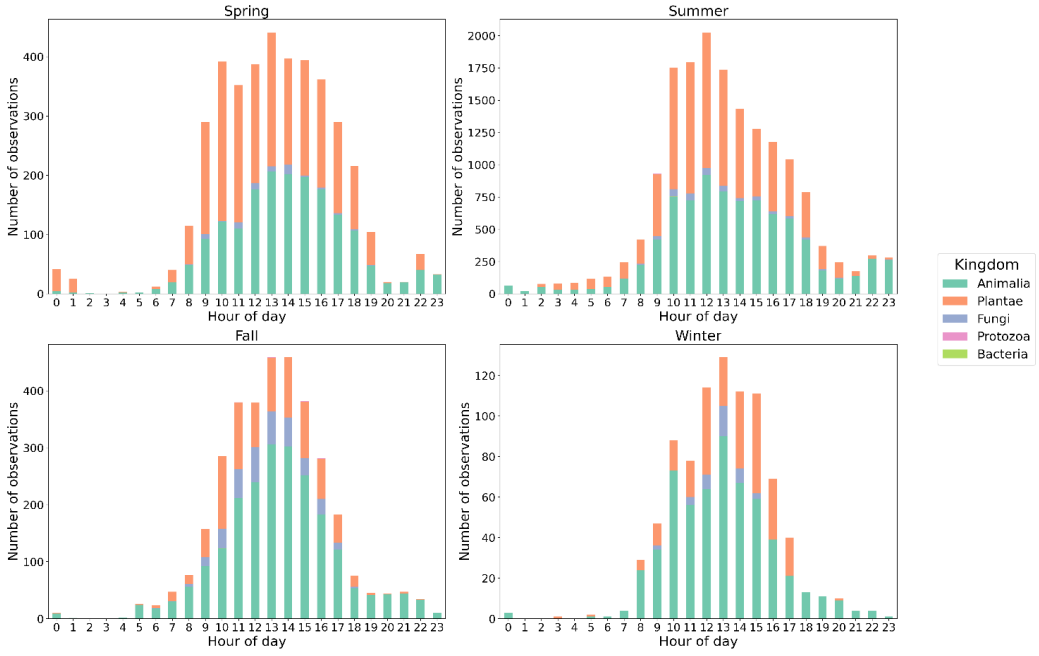


Fig. 4

Figure 4: Hourly distribution of kingdoms by season in Carinthia

Abbildung 4: *Anzahl der stündlichen Beobachtungen in Kärnten, unterteilt nach Reich*

Results of chi-square tests based on number of observations in Figure 4 show that the change in the hourly proportion of observations falling into different kingdoms is statistically significant for spring ($X^2 = 2127.01$, df = 23, $p < 0.001$), summer ($X^2 = 7336.29$, df = 23, $p < 0.001$), fall ($X^2 = 2019.01$, df = 23, $p < 0.001$), and winter ($X^2 = 603.08$, df = 23, $p < 0.001$). The proportions of kingdoms also vary significantly between seasons. For instance, Plantae dominates in spring (51.7%) and summer (51.8%), while Animalia is more prevalent in fall (63.1%) and winter (56.1%).

Seasonality of contribution patterns across land cover types

Table 2 lists the three most frequently observed species in four land cover types across four seasons. Some apparent patterns emerge, such as the predominance of butterfly and other insect observations during summer and fall for agricultural areas, followed by a shift toward more observations of birds during winter. This pattern aligns with natural phenological changes and shifts in species visibility [25], [45]. Artificial surfaces show a mix of urban-adapted species, with birds and insects dominating. Forest and semi-natural areas display high biodiversity, featuring a variety of plants, insects, and amphibians, with notable seasonal shifts from spring flowers to summer butterflies and fungi (fly agaric) in fall. Water bodies demonstrate a clear focus on aquatic species observed in summer, and birds during the remaining seasons. Each land cover type reflects its unique ecological characteristics, with seasonal variations in the most frequently observed species, highlighting the diverse habitats and seasonal dynamics of the region. The wetland habitat land cover type was excluded due to its limited number of recorded species.

Tab. 2

Season	Artificial surfaces	Forest and semi natural areas	Agricultural areas	Water bodies
Spring	common blackbird *Turdus merula* (15)	white butterbur *Petasites albus* (24)	common bugle *Ajuga reptans* (12)	Eurasian coot *Fulica atra* (4)
	common bugle *Ajuga reptans* (14)	common wall lizard *Podarcis muralis* (21)	meadow clary *Salvia pratensis* (12)	great crested grebe *Podiceps cristatus* (4)
	greater celandine *Chelidonium majus* (14)	coltsfoot *Tussilago farfara* (20)	fumewort *Corydalis solida* (11)	sedge warbler *Acrocephalus schoenobaenus* (3)
Summer	Japanese oak silk moth *Antheraea yamamai* (22)	silver-washed fritillary *Argynnis paphia* (102)	silver-washed fritillary *Argynnis paphia* (35)	Wels catfish *Silurus glanis* (245)
	Himalayan balsam *Impatiens glandulifera* (18)	heath spotted orchid *Dactylorhiza maculata* (86)	meadow brown *Maniola jurtina* (33)	European perch *Perca fluviatilis* (35)
	silver-washed fritillary *Argynnis paphia* (16)	common frog *Rana temporaria* (55)	European peacock *Aglais io* (29)	pumpkinseed *Lepomis gibbosus* (25)
Fall	western conifer seed bug *Leptoglossus occidentalis* (48)	fly agaric *Amanita muscaria* (23)	western conifer seed bug *Leptoglossus occidentalis* (31)	mute swan *Cygnus olor* (13)
	Asian lady beetle *Harmonia axyridis* (31)	fire salamander *Salamandra salamandra* (22)	European peacock *Aglais io* (16)	mallard *Anas platyrhynchos* (8)
	common blackbird *Turdus merula* (16)	Alpine chough *Pyrrhocorax graculus* (16)	Asian lady beetle *Harmonia axyridis* (16)	common darter *Sympetrum striolatum* (7)
Winter	common blackbird *Turdus merula* (15)	European beech *Fagus sylvatica* (12)	Eurasian blue tit *Cyanistes caeruleus* (10)	mallard *Anas platyrhynchos* (9)
	great tit *Parus major* (11)	Norway spruce *Picea abies* (8)	common blackbird *Turdus merula* (10)	Eurasian coot *Fulica atra* (9)
	daddy long-legs spider *Pholcus phalangioides* (10)	common hazel *Corylus avellana* (7)	common chaffinch *Fringilla coelebs* (8)	Eurasian beaver *Castor fiber* (6)

Legend: bird butterfly other insect flowering plant tree fish amphibian reptile fungus arachnid mammal
Silhouettes sourced from PhyloPic (https://www.phylopic.org), all public domain (CC0).

Table 2:
Top three observed species in four land cover types across four seasons

Tabelle 2:
Die am häufigsten drei beobachteten Arten in vier Landnutzungsklassen während der vier Jahreszeiten

Table 3 presents the typical daily observation window lengths, showing the number of hours per day that account for 90% of observations across different land cover types and seasons. The data indicate that summer generally provides the longest observation windows for iNaturalist data collection, with the exception of water bodies, which exhibit slight deviations. In winter, the longest observation window (11 hours) occurs on artificial surfaces, likely due to the influence of artificial lighting. In contrast, during summer, the longest observation window is observed in agricultural areas (17 hours), possibly attributed to minimal canopy cover and fewer obstructions to sunlight, resulting in extended natural daylight.

Tab. 3

Season	Artificial surfaces	Forest and semi natural areas	Agricultural areas	Water bodies	Wetlands
Spring	11.00	10.00	13.55	12.05	11.00
Summer	15.00	16.00	17.00	11.00	12.00
Fall	14.00	8.00	11.00	11.80	8.00
Winter	11.00	8.00	8.35	9.00	5.00

Table 3:
90% observation hour ranges across seasons and land cover types

Tabelle 3:
90% Beobachtungs-fenster während der vier Jahreszeiten in fünf Landnutzungsklassen

The number of observations across the five land cover types by hour of the day and season are plotted in Figure 5 and summarized in Table 4. The relative abundance of contributions is highest in forest and semi-natural areas during spring (44.3%), summer (57.5%), and fall (36.7%), which also correspond to the highest biodiversity levels among all land cover types in these seasons (Figure 6). In winter, agricultural surfaces show the highest relative abundance of contributions (35.4%) and the greatest biodiversity for that season (see Figure 6). The proportion of contributions from artificial surfaces is lowest in summer (13.5%), suggesting that observers spend more time exploring natural areas outside of urban environments during this period. A chi-square test of independence indicates that the distribution of observations across different land cover types varies between seasons ($X^2 = 1349.86$, df = 12, $p < 0.0001$). Furthermore, the proportion of contributions to different land cover types varies significantly by hour of day for spring ($X^2 = 898.46$, df = 4, $p < 0.001$), summer ($X^2 = 1886.91$, df = 4, $p < 0.001$), fall ($X^2 = 1263.45$, df = 4, $p < 0.001$), and winter ($X^2 = 494.37$, df = 4, $p < 0.001$).

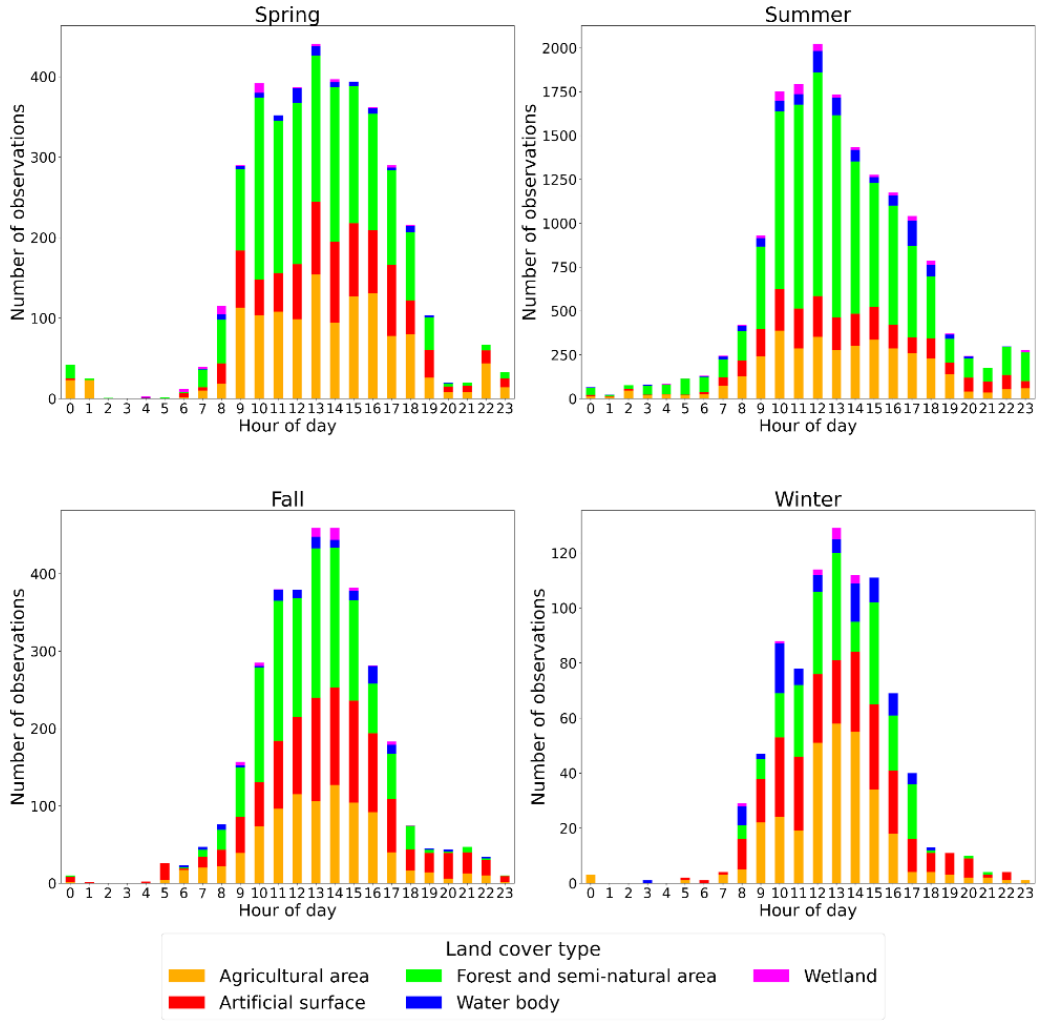


Figure 5:
Hourly contribution numbers for different land cover types across four seasons

Abbildung 5:
Stündliche Beobachtungszahlen in fünf Landnutzungsklassen während der vier Jahreszeiten

Fig. 5

Tab. 4

Land cover type	Spring	Summer	Fall	Winter
Agricultural surface	1270 (31.3%)	3772 (22.0%)	939 (27.1%)	**314 (35.4%)**
Forest and semi natural area	**1798 (44.3%)**	**9830 (57.5%)**	**1272 (36.7%)**	216 (24.4%)
Artificial surface	848 (20.9%)	2308 (13.5%)	1081 (31.2%)	264 (29.8%)
Water body	94 (2.3%)	874 (5.1%)	123 (3.6%)	81 (9.1%)
Wetland	45 (1.1%)	325 (1.9%)	47 (1.4%)	11 (1.2%)

Table 4: Number and percentage of observations falling into five different land cover types for four seasons (numbers in bold indicate land cover with highest proportion of contributions)

Tabelle 4: *Anzahl und Prozentanteil der Beobachtungen, unterteilt in fünf Landnutzungsklassen und vier Jahreszeiten (fettgedruckte Zahlen beziehen sich auf die Landnutzungsklasse mit dem höchsten Beobachtungsanteil)*

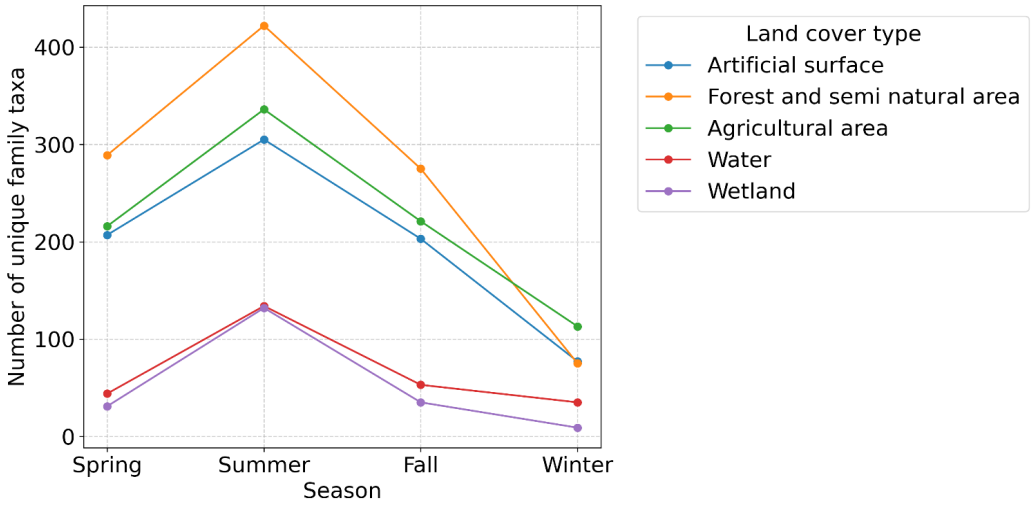


Fig. 6

Figure 6: Number of different family taxa observed across four seasons and five land cover types

Abbildung 6: *Anzahl der verschiedenen Familien in Beobachtungen während der vier Jahreszeiten in fünf Landnutzungsklassen*

Taxonomic variety of contributions

The number of contributed family-level taxa across land cover types for all four seasons is illustrated in Figure 6. Forest and semi-natural areas exhibited the highest taxonomic diversity in spring, summer, and fall, while agricultural areas showed the greatest diversity in winter. Across all land cover types, taxonomic diversity peaked in summer and reached its lowest levels in winter.

Global visitation patterns of iNaturalist contributors

For this analysis, we identified iNaturalist users who contributed at least once during winter or summer in Carinthia between 2015 and 2022, and retrieved the total number of countries they contributed to during this period (Figure 7). Users contributing in summer (mean = 4.29, median = 3) were active in a greater number of countries than those contributing in winter (mean = 3.57, median = 1). This indicates that winter contributors were more likely to be local, whereas summer contributors tended to be visitors who also submitted observations from other countries. During summer, which showed the highest level of international participation, the top three countries of contribution following Austria were Germany (230 users), Italy (194 users), and Croatia (121 users). In contrast, winter observations reflected lower international involvement, with most non-Austrian users originating from Germany (113 users), Italy (42 users), and the United States (39 users).
Figure 8 offers a complementary perspective on the international activity of iNaturalist users who contributed at least once to Carinthian observations. It displays the proportion of observations made in Austria relative to total user contributions, separated by season

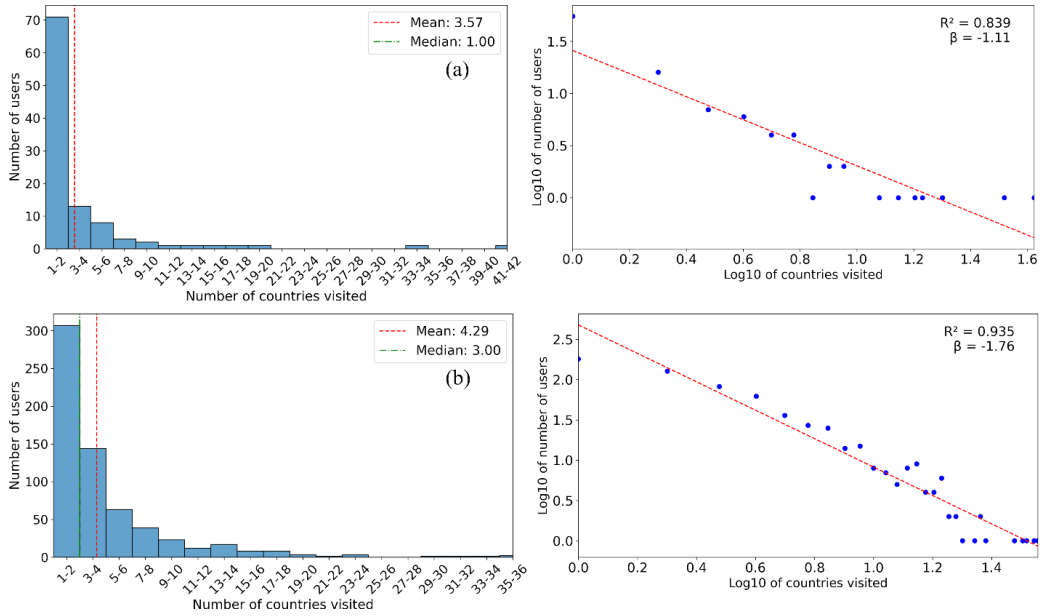


Fig. 7

Figure 7: Distribution of visited countries and corresponding log-log plots in winter (a) and summer (b)

Abbildung 7: *Statistische Verteilung von besuchten Ländern und entsprechende Punktdiagramme mit logarithmischer Achsenskalierung während des Winters (a) und des Sommers (b)*

and summarized over the study period. During summer, a substantial share of users (54.1%) recorded 90% or fewer of their observations in Austria, followed by spring (40.1%), indicating higher international mobility among contributors, likely reflecting visiting or traveling users. In contrast, the distributions for fall and winter suggest predominantly local (Austrian) contributors, with few users submitting observations from outside of Austria.

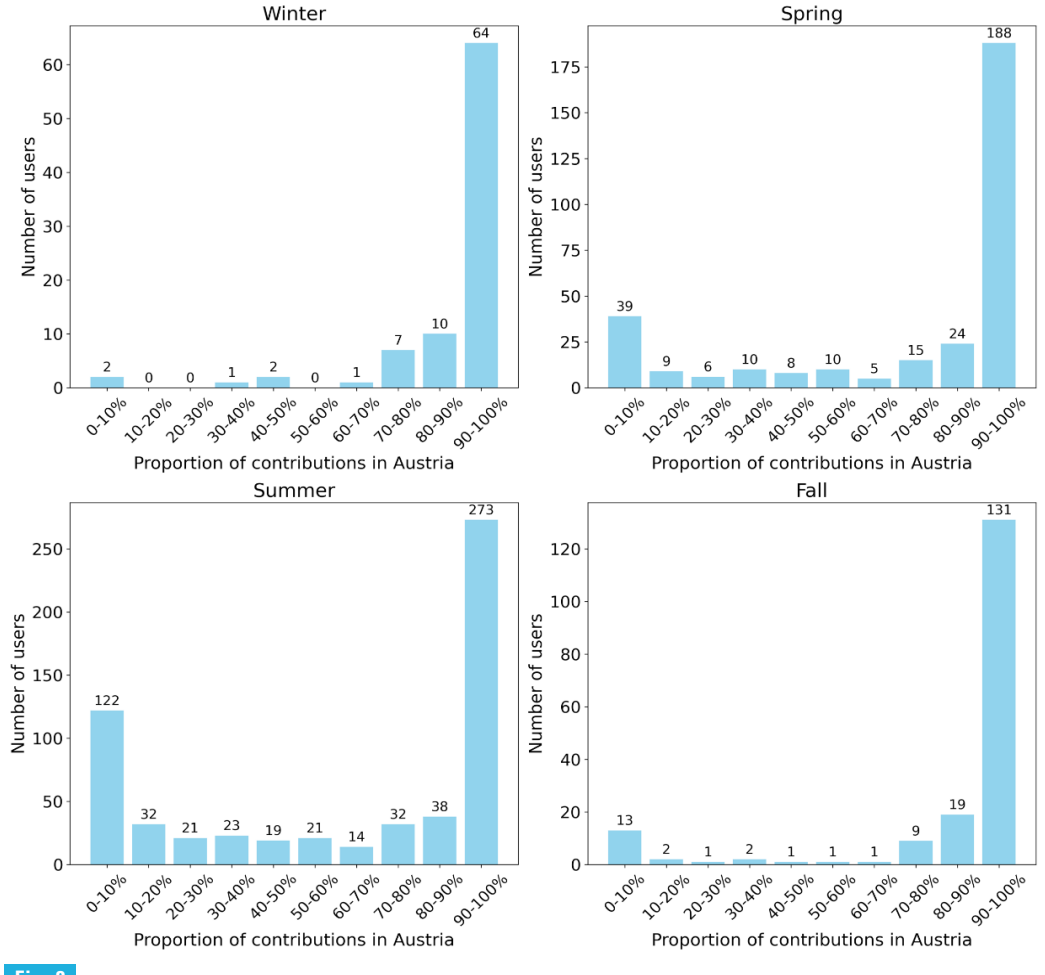


Fig. 8

Figure 8: Distribution of users contributing different proportions of observations to Austria by season

Abbildung 8: *Statistische Verteilung von Nutzern mit verschiedenen Anteilen von Beobachtungen in Österreich während der vier Jahreszeiten*

DISCUSSION

Land use cover and observation patterns

Although urban environments generally support fewer native plant and animal species [46], our results show a positive association between artificial surface land cover and observation density. This pattern reflects user contribution bias and supports previous findings that cities act as hotspots for biodiversity monitoring [47]. Some insect species frequently enter buildings during colder months, increasing their visibility to observers and leading to an overrepresentation of records from artificial surfaces [48]. Consequently, such observations may misrepresent the true outdoor distribution of these species. For example, in our dataset, 67.6% of annual observations of the Western conifer seed bug and the Asian lady beetle on artificial surfaces occurred in October and November alone, making them the most frequently recorded species in fall (compare Table 2). iNaturalist records lack an explicit indicator denoting whether an observation was made indoors, which constrains the ability to evaluate potential overrepresentation arising from insects that have entered buildings. Nonetheless, the iNaturalist *Never Home Alone: The Wild Life of Homes* project (https://www.inaturalist.org/projects/never-home-alone-the-wild-life-of-homes) provides relevant contextual information regarding data collection within indoor environments. As of September 2025, it had accumulated over 67,000 observations of more than 8,200 species worldwide, a negligible fraction compared to the hundreds of millions of total iNaturalist records. This pattern suggests that indoor observations are unlikely to introduce substantial bias.

Although not examined in this study, previous research found that the spatial bias of species occurrence records across multiple biodiversity databases has changed over time, varying among land use categories. Specifically, site visitation probability derived from crowd-sourced datasets increased more strongly in urban areas than in other land use types [49]. Therefore, when estimating long-term trends in species distributions from crowd-sourced data, analyses should account for temporal changes in spatial sampling bias.

The overall positive association of iNaturalist observations with water bodies observed in our study likely reflects both the ecological appeal of these habitats to wildlife and the attraction they hold for nature enthusiasts and the general public for recreational activities [50], which can lead to oversampling of freshwater organisms [51]. Individual user behavior can further amplify this observation bias. A striking example in our dataset is a single user who recorded 245 observations of Wels catfish in 2022, primarily using an underwater camera while diving at Millstätter See, making this species the most frequently observed in water bodies during summer (see Table 2). This user alone accounted for 82.5% of all fish records, demonstrating how specialized activities, such as diving or boating, can disproportionately influence species representation in certain environments. The behavior of "super users," who contribute exceptionally large numbers of observations, deviates from typical patterns linked to land cover or time of day, representing an outlier-driven user contribution bias that is distinct from other forms of sampling bias.

The negative relationship between iNaturalist contribution numbers and forested, semi-natural, and agricultural areas reflects the challenges of accessing remote locations, the additional time required to travel from urban centers, and the comparatively lower biodiversity of intensively farmed landscapes in Austria [52]. This insight highlights opportunities for education and outreach, suggesting that targeted initiatives could promote iNaturalist usage in agricultural and forested areas, thereby improving the spatial coverage of observations and providing a more comprehensive picture of

Carinthian biodiversity. Previous studies have shown that iNaturalist observations tend to cluster around tourist hotspots, particularly ecotourism sites rather than cultural sites [53], indicating that visits to cultural locations are generally less motivated by species observation than visits to natural sites. While the current study focused on the role of land cover types for biodiversity mapping, future work could analyze the role of different types of tourist and recreational sites for iNaturalist contribution behavior in Carinthia and explore its relationship with either official visitation counts or review counts from different online platforms, such as TripAdvisor, Yelp, or Google [54]. This could help to further disentangle the joint effect of phenology and user contribution bias in observed contribution patterns. Our dataset did not reveal a significant association between protected areas and iNaturalist mapping activities, representing a middle ground between previously reported patterns of either oversampling or undersampling in protected areas, which often vary depending on their location [55].

Temporal observation patterns

The temporal patterns in iNaturalist contributions show substantial seasonal and daily variation, influenced both by plant and animal phenology, as well as by observer schedules and daylight availability. Reduced activity in winter is expected due to shorter daylight hours, difficulties in spotting and photographing organisms under low-light conditions, and the decreased activity of many species, such as insects, small mammals, amphibians, and reptiles, which may hibernate [56], [57]. Previous studies reported strong seasonal trends in freshwater fish observations, with higher counts in summer as fish retreat to deeper waters during winter [58], consistent with the summer peak in fish observations seen in our dataset. Similarly, the autumn peak in fungal observations aligns partially with the fruiting season of edible mushrooms in Austria, which occurs in late summer and fall [59]. The low number of observations for Protozoa and Bacteria highlights the limitations of citizen science in capturing microscopic life forms [60], with records appearing only sporadically in summer and fall.

Our analysis reveals seasonal shifts in contribution bias, as measured by the distance between observation sites and the nearest city, with the magnitude of these changes varying by land cover type. For instance, the median distance for observations in forest and semi-natural areas increases from 14.3 km in winter to 18.9 km in summer, a rise of about 32%, whereas for artificial surfaces the increase is more pronounced, from 4.7 km to 8.9 km, or roughly 89%. This pattern indicates that the typical urban-centric overrepresentation is partially alleviated in summer, when human activities extend further into areas away from large urban settlements. Consequently, summer provides a more balanced and less biased dataset compared to winter.

The hourly distribution of user activity across seasons reveals a clear pattern of daytime-focused observations, with peak activity around 12:00 pm in summer, shifting to 1:00 pm in winter (see Figure 4). Similarly, analysis of eBird data [61] demonstrated that observation times closely track daylight hours across seasons. Previous research has also examined additional factors influencing observation bias, such as weekday, temperature, and precipitation. For example, one study assessed these effects using several tree species in the Iberian Peninsula, which retain a consistent appearance throughout the year [62]. While a similar approach could be applied in Carinthia, stronger seasonal variation in this region makes identifying species with year-round consistent appearance more challenging.

Limitations

Observations recorded exactly at midnight were excluded from the temporal analysis, as they likely represent data artifacts. Similar patterns have been noted in analyses of

eBird data, where default timestamps (12:00 a.m.) led to an overrepresentation of midnight observations [23]. A comparable data artifact, though occurring in the spatial domain, arises when latitude and longitude values are missing from point records, resulting in the appearance of a fictional "Null Island" located at 0° latitude and 0° longitude in the WGS 84 geographic coordinate system [63].

The identification of highly active contributors ("super users") led us to exclude some of their observation data from the spatial regression analysis, as their excessive numbers of contributions were unlikely to be explained by environmental factors and were more plausibly driven by personal motivations. Some super users may seek recognition by uploading numerous photos of the same individual organism each day, without an apparent intent to add genuine scientific value to the iNaturalist dataset. Others are (semi)professionals, such as members of local societies or participants in organized events like the City Nature Challenge or bioblitzes, who use the platform to document and manage their field data over multiple years. Their contributions often hold substantial scientific value, which can also result in repeated observations of the same species across time [10]. An examination of the top ten users in our dataset indeed reveals distinct contribution patterns. Some focus on a few taxa (for example, monitoring Lepidoptera or fungi at a single site throughout the year), whereas others document a broad range of species across many taxa and locations. Although both groups generate large volumes of data, the scientific value of their contributions cannot easily be inferred from their activity patterns alone. Regardless of motivation, including all data from these super users in the spatial regression analysis would give disproportionate influence to a small subset of individuals, potentially biasing the results. Their contributions, however, remain included in descriptive analyses to reflect the full spectrum of citizen science participation. Finally, examining anomalous activity patterns among individuals may still yield valuable insights into atypical participation behaviors among iNaturalist super users [64].

Land cover analyses relied on first- and second-level CORINE classifications derived from satellite imagery. While widely used, this approach can mask local conditions and functional differences within classes. For example, monoculture spruce plantations are typically classified as "forest and semi-natural areas," although their ecological and functional characteristics more closely resemble agricultural land. Similarly, the second-level "pasture" class may encompass both species-rich meadows and intensively managed grasslands for cattle, the latter being more akin to "heterogeneous agricultural areas." These limitations are inherent to the CORINE dataset but could be partially addressed by incorporating local land use data where available.

CONCLUSIONS AND FUTURE WORK

The analysis of iNaturalist data in Carinthia reveals several notable spatial and temporal patterns in data contributions. Some of these patterns likely reflect genuine ecological and phenological variation, such as fungi being most frequently observed in forest areas during the fall. Other patterns, however, may result from imbalanced sampling effort, including the overrepresentation of observations in densely populated areas. This study highlights user contribution biases that have received little attention in previous research, such as the influence of "super users" and the interaction of seasonality with proximity to cities and land use type. Future initiatives should aim to address spatial and temporal gaps in data collection to provide a more comprehensive and representative picture of Carinthian biodiversity [65]. To further investigate the complex relationships between environment and observation patterns, future research should apply additional analytical

approaches. Machine learning methods, such as random forests or gradient boosting, could help capture non-linear relationships and interactions among variables. Time series analyses would allow deeper exploration of temporal trends and seasonal effects. Furthermore, integrating data from multiple citizen science platforms or online review sources, and comparing these with professional biodiversity surveys, could provide a more comprehensive understanding of Carinthia's biodiversity and help identify priority areas for targeted citizen science efforts [60].

ACKNOWLEDGEMENTS

This research was supported by the Austrian Marshall Plan Foundation through a scholarship awarded to the first author.

REFERENCES

[1] T. J. Lloyd, R. A. Fuller, J. L. Oliver, A. I. Tulloch, M. Barnes, and R. Steven, "Estimating the spatial coverage of citizen science for monitoring threatened species," *Global Ecology and Conservation*, vol. 23, p. e01048, 2020, doi: 10.1016/j.gecco.2020.e01048

[2] R. Bonney, T. B. Phillips, H. L. Ballard, and J. W. Enck, "Can citizen science enhance public understanding of science?," *Public Understanding of Science*, vol. 25, no. 1, pp. 2-16, 2015, doi: 10.1177/0963662515607406

[3] J. C. Tourville, G. L. D. Murray, and S. J. Nelson, "Distinct latitudinal patterns of shifting spring phenology across the Appalachian Trail Corridor," *Ecology*, vol. 105, no. 10, p. e4403, 2024, doi: 10.1002/ecy.4403

[4] L. R. Forti, F. Hepp, J. M. de Souza, A. Protazio, and J. K. Szabo, "Climate drives anuran breeding phenology in a continental perspective as revealed by citizen-collected data," *Diversity and Distributions*, vol. 28, no. 10, pp. 2094-2109, 2022, doi: 10.1111/ddi.13610

[5] Wikipedia, "iNaturalist," 2024, https://en.wikipedia.org/wiki/INaturalist (accessed 2024-10-1)

[6] K. L. Prudic, K. P. McFarland, J. C. Oliver, R. A. Hutchinson, E. C. Long, J. T. Kerr, and M. Larrivée, "eButterfly: leveraging massive online citizen science for butterfly conservation, "*Insects*, vol. 8, no. 2, p. 53, 2017, doi: 10.3390/insects8020053

[7] D. Dalton, M. Jungmeier, K. Pascher, V. Berger, and K. Steinbauer, "Novel technologies and their application for protected area management: a supporting approach in biodiversity monitoring," in *Protected Area Management - Recent Advances*, M. N. Suratman (Ed.), London, UK: IntechOpen, 2021, pp. 269-292, doi: 10.5772/intechopen.99889

[8] L. Klemann-Junior, M. A. Villegas Vallejos, P. Scherer-Neto, and J. R. S. Vitule, "Traditional scientific data vs. uncoordinated citizen science effort: A review of the current status and comparison of data on avifauna in Southern Brazil," *PLOS One*, vol. 12, no. 12, p. e0188819, 2017, doi: 10.1371/journal.pone.0188819

[9] E. H. Boakes et al., "Patterns of contribution to citizen science biodiversity projects increase understanding of volunteers' recording behaviour," *Scientific Reports*, vol. 6, no. 1, p. 33051, 2016, doi: 10.1038/srep33051

[10] G. J. Di Cecco, V. Barve, M. W. Belitz, B. J. Stucky, R. P. Guralnick, and A. H. Hurlbert, "Observing the observers: how participants contribute data to iNaturalist and implications for biodiversity science," *BioScience*, vol. 71, no. 11, pp. 1179-1188, 2021, doi: 10.1093/biosci/biab093

[11] K. Kishimoto and H. Kobori, "COVID-19 pandemic drives changes in participation in citizen science project "City Nature Challenge" in Tokyo," *Biological Conservation*, vol. 255, p. 109001, 2021, doi: 10.1016/j.biocon.2021.109001

[12] J. Geldmann, J. Heilmann-Clausen, T. E. Holm, I. Levinsky, B. Markussen, K. Olsen, et al., "What determines spatial bias in citizen science? Exploring four recording schemes with different proficiency requirements," *Diversity and Distributions*, vol. 22, no. 11, pp. 1139-1149, 2016, doi: 10.1111/ddi.12477

[13] P. Tiago, A. Ceia-Hasse, T. A. Marques, C. Capinha, and H. M. Pereira, "Spatial distribution of citizen science casuistic observations for different taxonomic groups," *Scientific Reports*, vol. 7, no. 1, p. 12832, 2017, doi: 10.1038/s41598-017-13130-8

[14] L. Mair and A. Ruete, "Explaining spatial variation in the recording effort of citizen science data across multiple taxa," *PLOS ONE*, vol. 11, no. 1, p. e0147796, 2016, doi: 10.1371/journal.pone.0147796

[15] E. M. Geurts, J. D. Reynolds, and B. M. Starzomski, "Turning observations into biodiversity data: broadscale spatial biases in community science," *Ecosphere*, vol. 14, no. 6, p. e4582, 2023, doi: 10.1002/ecs2.4582

[16] J. Troudet, P. Grandcolas, A. Blin, R. Vignes-Lebbe, and F. Legendre, "Taxonomic bias in biodiversity data and societal preferences," *Scientific Reports*, vol. 7, no. 1, p. 9132, 2017, doi: 10.1038/s41598-017-09084-6

[17] A. I. T. Tulloch, H. P. Possingham, L. N. Joseph, J. Szabo, and T. G. Martin, "Realising the full potential of citizen science monitoring programs," *Biological Conservation*, vol. 165, pp. 128-138, 2013, doi: 10.1016/j.biocon.2013.05.025

[18] M. Dimson and T. W. Gillespie, "Who, where, when: observer behavior influences spatial and temporal patterns of iNaturalist participation," *Applied Geography*, vol. 153, p. 102916, 2023, doi: 10.1016/j.apgeog.2023.102916

[19] D. Bashan, A. Colléony, and A. Shwartz, "Urban versus rural? The effects of residential status on species identification skills and connection to nature," *People and Nature*, vol. 3, no. 2, pp. 347-358, 2021, doi: 10.1002/pan3.10176

[20] C. Randler and F. Heil, "Determinants of bird species literacy—activity/interest and specialization are more important than socio-demographic variables," *Animals*, vol. 11, no. 6, doi: 10.3390/ani11061595

[21] C. C. Rega-Brodsky et al., "Urban biodiversity: state of the science and future directions," *Urban Ecosystems*, vol. 25, no. 4, pp. 1083-1096, 2022, doi: 10.1007/s11252-022-01207-w

[22] J. Knape, S. J. Coulson, R. van der Wal, and D. Arlt, "Temporal trends in opportunistic citizen science reports across multiple taxa," *Ambio*, vol. 51, no. 1, pp. 183-198, 2022, doi: 10.1007/s13280-021-01550-w

[23] J. R. Courter, R. J. Johnson, C. M. Stuyck, B. A. Lang, and E. W. Kaiser, "Weekend bias in citizen science data reporting: implications for phenology studies," *International Journal of Biometeorology*, vol. 57, no. 5, pp. 715-720, 2013, doi: 10.1007/s00484-012-0598-7

[24] V. V. Barve, L. Brenskelle, D. Li, B. J. Stucky, N. V. Barve, M. M. Hantak, et al., "Methods for broad-scale plant phenology assessments using citizen scientists' photographs," *Applications in Plant Sciences*, vol. 8, no. 1, p. e11315, 2020, doi: 10.1002/aps3.11315

[25] Z. A. Panchen, J. Doubt, H. M. Kharouba, and M. O. Johnston, "Patterns and biases in an Arctic herbarium specimen collection: Implications for phenological research," *Applications in Plant Sciences*, vol. 7, no. 3, p. e01229, 2019, doi: 10.1002/aps3.1229

[26] N. E. Turley et al., "Bee monitoring by community scientists: comparing a collections-based program with iNaturalist," *Annals of the Entomological Society of America*, vol. 117, no. 4, pp. 220-233, 2024, doi: 10.1093/aesa/saae014

[27] C. T. Callaghan, A. G. B. Poore, M. Hofmann, C. J. Roberts, and H. M. Pereira, "Large-bodied birds are over-represented in unstructured citizen science data," *Scientific Reports*, vol. 11, no. 1, p. 19073, 2021, doi: 10.1038/s41598-021-98584-7

[28] H. H. Hochmair, R. H. Scheffrahn, M. Basille, and M. Boone, "Evaluating the data quality of iNaturalist termite records," *PLOS ONE*, vol. 15, no. 5, p. e0226534, 2020, doi: 10.1371/journal.pone.0226534

[29] S. Unger, M. Rollins, A. Tietz, and H. Dumais, "iNaturalist as an engaging tool for identifying organisms in outdoor activities," *Journal of Biological Education*, vol. 55, no. 5, pp. 537-547, 2021, doi: 10.1080/00219266.2020.1739114

[30] S. J. Hobbs and P. C. L. White, "Motivations and barriers in relation to community participation in biodiversity recording," *Journal for Nature Conservation*, vol. 20, no. 6, pp. 364-373, 2012, doi: 10.1016/j.jnc.2012.08.002

[31] S. J. Phillips, M. Dudík, J. Elith, C. H. Graham, A. Lehmann, J. Leathwick, et al., "Sample selection bias and presence-only distribution models: implications for background and pseudo-absence data," *Ecological Applications*, vol. 19, no. 1, pp. 181-197, 2009, doi: 10.1890/07-2153.1

[32] A. Shwartz, A. Turbé, L. Simon, and R. Julliard, "Enhancing urban biodiversity and its influence on city-dwellers: an experiment," *Biological Conservation*, vol. 171, pp. 82-90, 2014, doi: 10.1016/j.biocon.2014.01.009

[33] B. Hawelka, I. Sitko, E. Beinat, S. Sobolevsky, P. Kazakopoulos, and C. Ratti, "Geo-located Twitter as proxy for global mobility patterns," *Cartography and Geographic Information Science*, vol. 41, no. 3, pp. 260-271, 2014, doi: 10.1080/15230406.2014.890072

[34] J. Cao and H. H. Hochmair, "Use of iNaturalist biodiversity contribution data for modelling travel distances to parks across the United States," in *AGILE: GIScience Series*, Glasgow, UK, vol. 5: Copernicus Publications, p. 18, 2024, doi: 10.5194/agile-giss-5-18-2024

[35] A. F. A. Mutton, "Carinthia: A province of Austria's southern frontier," *Geography*, vol. 38, no. 2, pp. 83-93, 1953. Available: http://www.jstor.org/stable/40563404

[36] K. Christian, "Mountain biodiversity, its causes and function," *AMBIO: A Journal of the Human Environment*, vol. 33, no. sp13, pp. 11-17, 2004, doi: 10.1007/0044-7447-33.sp13.11

[37] D. Vanham, E. Fleischhacker, and W. Rauch, "Technical Note: Seasonality in alpine water resources management - a regional assessment," *Hydrology and Earth System Sciences*, vol. 12, no. 1, pp. 91-100, 2008, doi: 10.5194/hess-12-91-2008

[38] J. Beninde, T. W. Delaney, G. Gonzalez, and H. B. Shaffer, "Harnessing iNaturalist to quantify hotspots of urban biodiversity: the Los Angeles case study," *Frontiers in Ecology and Evolution*, vol. 11, p. 983371, 2023, doi: 10.3389/fevo.2023.983371

[39] Global Biodiversity Information Facility, "GBIF Occurrence Download," https://doi.org/10.15468/dl.kergb2

[40] J. M. Heberling and B. L. Isaac, "iNaturalist as a tool to expand the research value of museum specimens," *Applications in Plant Sciences*, vol. 6, no. 11, p. e01193, 2018, doi: 10.1002/aps3.1193

[41] A. Mitchell, The ESRI guide to GIS analysis. *Volume 2: Spatial measurements & statistics*. Redlands, California: ESRI Press, 2005

[42] M. V. Bishop, R. Ólafsdóttir, T. Michaud, and C. Metcalf, "Crowdsourced mapping of tourism distribution and dynamics in Iceland using Flickr," *Scandinavian Journal of Hospitality and Tourism*, vol. 24, no. 1, pp. 1-17, 2024, doi: 10.1080/15022250.2024.2355905

[43] M. Martins and A. Santos, "Exploring the potential of Flickr user–generated content for tourism research: insights from Portugal," *European Journal of Tourism, Hospitality and Recreation*, vol. 14, no. 2, pp. 258-272, 2024, doi: 10.2478/ejthr-2024-0019

[44] T. Fang, Y. Chen, H. Tan, J. Cao, J. Liao, and L. Huang, "Flood risk evaluation in the middle reaches of the Yangtze River based on eigenvector spatial filtering Poisson regression," *Water*, vol. 11, no. 10, p. 1969, 2019, doi: 10.3390/w11101969

[45] H. Leach and A. Leach, "Seasonal phenology and activity of spotted lanternfly (*Lycorma delicatula*) in eastern US vineyards," *Journal of Pest Science*, vol. 93, no. 4, pp. 1215-1224, 2020, doi: 10.1007/s10340-020-01233-7

[46] M. T. J. Johnson and J. Munshi-South, "Evolution of life in urban environments," *Science*, vol. 358, no. 6363, p. eaam8327, 2017, doi: 10.1126/science.aam8327

[47] D. M. Spear, G. B. Pauly, and K. Kaiser, "Citizen Science as a tool for augmenting museum collection data from urban areas," *Frontiers in Ecology and Evolution*, vol. 5, p. 86, 2017, doi: 10.3389/fevo.2017.00086

[48] M. Tamburini, G. Maresi, C. Salvadori, A. Battisti, F. Zottele, and F. Pedrazzoli, "Adaptation of the invasive western conifer seed bug *Leptoglossus occidentalis* to Trentino, an alpine region (Italy)," *Bulletin of Insectology*, vol. 65, no. 2, pp. 161-170, 2012, http://hdl.handle.net/10449/21533

[49] D. E. Bowler, C. T. Callaghan, N. Bhandari, K. Henle, M. B. Barth, C. Koppitz, et al., "Temporal trends in the spatial bias of species occurrence records," *Ecography*, vol. 2022, no. 8, p. e06219, 2022, doi: 10.1111/ecog.06219

[50] R. Ghimire, G. T. Green, K. P. Paudel, N. C. Poudyal, and H. K. Cordell, "Visitors' preferences for freshwater amenity characteristics: implications from the U.S. household survey," *Journal of Agricultural and Resource Economics*, vol. 42, no. 1, pp. 90-113, 2017, Available: http://www.jstor.org/stable/44131389

[51] S. R. Daniels, A. Barnes, N. Peer, V. T. Egan, R. Taylor, R. W. Taylor, and D. van der Colff, "iNaturalist is useful at enhancing biodiversity studies as evident from southern African freshwater crabs (Decapoda: Brachyura: Potamonautidae)," *Journal of Crustacean Biology*, vol. 42, no. 3, p. ruac042, 2022, doi: 10.1093/jcbiol/ruac042

[52] I. Schmitzberger, T. Wrbka, B. Steurer, G. Aschenbrenner, J. Peterseil, and H. G. Zechmeister, "How farming styles influence biodiversity maintenance in Austrian agricultural landscapes," *Agriculture, Ecosystems & Environment*, vol. 108, no. 3, pp. 274-290, 2005, doi: 10.1016/j.agee.2005.02.009

[53] H. Kwon, B. Seo, J. Kim, and H. Lee, "Crowdsourced indicators of flora and fauna species: comparisons between iNaturalist records and field observations," *Land*, vol. 14, no. 1, p. 169, 2025, doi: 10.3390/land14010169

[54] I. Owuor, H. H. Hochmair, and G. Paulus, "Use of social media data, online reviews and wikipedia page views to measure visitation patterns of outdoor attractions," *Journal of Outdoor Recreation and Tourism*, vol. 44, p. 100681, 2023, doi: 10.1016/j.jort.2023.100681

[55] L. J. Backstrom, C. T. Callaghan, H. Worthington, R. A. Fuller, and A. Johnston, "Estimating sampling biases in citizen science datasets," *Ibis*, vol. 167, no. 1, pp. 73-87, 2025, doi: 10.1111/ibi.13343

[56] P. A. Unterweger, J. Klammer, M. Unger, and O. Betz, "Insect hibernation on urban green land: a winter-adapted mowing regime as a management tool for insect conservation," *BioRisk*, vol. 13, pp. 1-29, 2018. [Online]. Available: https://doi.org/10.3897/biorisk.13.22316

[57] M. E. Lazzeroni, F. T. Burbrink, and N. B. Simmons, "Hibernation in bats (Mammalia: Chiroptera) did not evolve through positive selection of leptin," *Ecology and Evolution*, vol. 8, no. 24, pp. 12576-12596, 2018, doi: 10.1002/ece3.4674

[58] C. R. Penne and C. L. Pierce, "Seasonal distribution, aggregation, and habitat selection of common carp in Clear Lake, Iowa," *Transactions of the American Fisheries Society*, vol. 137, no. 4, pp. 1050-1062, 2008, doi: 10.1577/T07-112.1

[59] H. Maguire. "Schwammerl season: What is it and when does it start in Austria?" Available: https://www.thelocal.at/20220901/schwammerl-season-what-is-it-and-when-does-it-start-in-austria (accessed December 5, 2024)

[60] M. Chandler, L. See, K. Copas, A. M. Z. Bonde, B. Claramunt López, F. Danielsen, et al., "Contribution of citizen science towards international biodiversity monitoring," *Biological Conservation*, vol. 213, pp. 280-294, 2017, doi: 10.1016/j.biocon.2016.09.004

[61] A. Wiggins and Y. He, "Community-based data validation practices in citizen science," *Proceedings of the 19th ACM Conference on Computer-Supported Cooperative Work & Social Computing*, San Francisco, California, USA, 2016, doi: 10.1145/2818048.2820063

[62] I. T. Rosário, P. Tiago, S. Chozas, and C. Capinha, "When do citizen scientists record biodiversity? Non-random temporal patterns of recording effort and associated factors," *People and Nature*, vol. 7, no. 4, pp. 860-870, 2025, doi: 10.1002/pan3.70017

[63] L. Juhász and P. Mooney, ""I think I discovered a military base in the middle of the ocean"—Null Island, the most real of fictional places," *IEEE Access*, vol. 10, pp. 84147-84165, 2022, doi: 10.1109/ACCESS.2022.3197222

[64] G. Zhang, "A web-based geovisualization framework for exploratory analysis of individual VGI contributor's participation characteristics," *Cartography and Geographic Information Science*, vol. 52, no. 2, pp. 199-219, 2025, doi: 10.1080/15230406.2023.2293891

[65] M. A. S. Malik, S. A. Shah, and K. Zaman, "Tourism in Austria: biodiversity, environmental sustainability, and growth issues," *Environmental Science and Pollution Research*, vol. 23, pp. 24178-24194, 2016, doi: 10.1007/s11356-016-7609-x

ABOUT THE AUTHORS

Jiping Cao
School of Forest Fisheries, and Geomatics Sciences
Fort Lauderdale Research and Education Center
Geomatics Sciences
University of Florida
Davie, FL 33314, USA
jiping.cao@waikato.ac.nz

Hartwig Hochmair
School of Forest, Fisheries, and Geomatics Sciences, Fort Lauderdale Research and Education Center, Geomatics Sciences, University of Florida, Davie, FL 33314, USA

Gernot Paulus
Carinthia University of Applied Sciences, Engineering & IT, Spatial Informatics for ENvironmental Applications (SIENA), Villach, Austria

Corey T. Callaghan
Department of Wildlife Ecology and Conservation, Fort Lauderdale Research and Education Center, University of Florida, Davie, FL 33314, USA

BACK TO CONTENT

Applying a slime mold-inspired algorithm to network planning challenges in the Carinthian region

Kristina Wogatai, Emir Sinanović, Wilfried Elmenreich

ABSTRACT

This article presents the application of the slime mold-based algorithm *Simulation of Slime Molds* (SISMO) using case studies from the Carinthian region, demonstrating its applicability to various network structures. SISMO is inspired by the ability of the myxomycete *Physarum polycephalum* to process information and solve optimization tasks. The effectiveness of SISMO in network formation and finding shortest paths is first evaluated using parts of Carinthia's bus and railway infrastructure. Our results show that SISMO can create networks similar to the existing transportation network, consider obstacles, and replicate existing connections. These findings allow conclusions for the future optimization of further networks using bio-inspired approaches. Based on these insights, this paper presents an approach that uses SISMO to create a repair plan for the Carinthian power transmission network after a simulated electromagnetic pulse attack. The algorithm is applied to a corresponding graph model to identify the most critical areas to be repaired, analogous to the nutrient supply of the slime mold between food sources. SISMO was adapted for this grid planning task and fed with the positions of relevant power plants and substations of the Carinthian electricity transmission grid. This approach has significant potential for diverse applications, especially those where the algorithms are not limited by the physical or infrastructural constraints that shaped the original network topology. Further exploration of this approach could yield significant insights into various fields. Overall, the paper provides insights into the potential applications of bio-inspired algorithms, such as slime mold simulation, for solving network planning tasks and presents concrete case studies from the Carinthian region.

KEYWORDS

- bio-inspired algorithm
- slime molds
- network planning
- traffic networks
- transmission networks
- self-organization
- multi-agent simulation
- NetLogo
- Carinthian use-cases

Anwendung eines von Schleimpilzen inspirierten Algorithmus für Netzwerkplanungsherausforderungen in der Region Kärnten

ZUSAMMENFASSUNG

Dieser Artikel präsentiert die Anwendung des auf Schleimpilzen basierenden Algorithmus SISMO (Simulation of Slime Molds) anhand von Fallstudien aus der Kärntner Region und demonstriert dessen Anwendbarkeit auf verschiedene Netzwerkstrukturen. SISMO ist inspiriert von der Fähigkeit des Myxomyceten Physarum polycephalum, Informationen zu verarbeiten und Optimierungsaufgaben zu lösen. Die Effektivität von SISMO bei der Netzwerkbildung und der Ermittlung kürzester Wege wird zunächst anhand von Teilen der Bus- und Bahn-Infrastruktur Kärntens bewertet. Unsere Ergebnisse zeigen, dass SISMO in der Lage ist, Netzwerke zu erzeugen, die dem bestehenden Verkehrsnetz ähneln, Hindernisse zu berücksichtigen und bestehende Verbindungen nachzubilden. Diese Erkenntnisse ermöglichen Rückschlüsse auf die zukünftige Optimierung weiterer Netzwerke durch bioinspirierte Ansätze. Aufbauend auf diesen Einsichten stellt diese Arbeit einen Ansatz vor, bei dem SISMO zur Erstellung eines Reparaturplans für das Kärntner Stromübertragungsnetz nach einem simulierten elektromagnetischen-Impuls-Angriff (EMP) eingesetzt wird. Der Algorithmus wird auf ein entsprechendes Graphmodell angewandt, um die kritischsten Bereiche für Reparaturen zu identifizieren – analog zur Nährstoffversorgung des Schleimpilzes zwischen Nahrungsquellen. Für diese Aufgabe der Netzplanung wurde SISMO angepasst und mit den Standorten relevanter Kraftwerke und Umspannwerke des Kärntner Stromübertragungsnetzes gespeist. Dieser Ansatz birgt vielversprechendes Potenzial für eine Vielzahl von Anwendungen, bei denen Algorithmen nicht durch physische oder infrastrukturelle Einschränkungen limitiert sind, die das ursprüngliche Netzwerk beeinflusst haben könnten. Eine weiterführende Untersuchung dieses Ansatzes könnte wertvolle Erkenntnisse in unterschiedlichen Anwendungsfeldern liefern. Insgesamt bietet der Artikel Einblicke in das Potenzial bioinspirierter Algorithmen wie der Schleimpilz-Simulation zur Lösung von Aufgaben der Netzplanung und stellt konkrete Fallstudien aus der Region Kärnten vor.

INTRODUCTION

Motivation

Biological principles are increasingly being used in various disciplines to develop and optimize technical systems and products. One prominent example of these nature-inspired optimization algorithms is the Ant Colony Optimization algorithm (ACO), which is based on the foraging behavior of ants. Dorigo et al. first introduced the ACO algorithms in the early 1990s [1], [2], [3], and they have since been applied in various domains, including manufacturing and intralogistics route optimization, communication channel switching,

and transportation management. Similar research has been performed based on the myxomycete *Physarum polycephalum* (PP), with Nakagaki et al. demonstrating that these organisms are even capable of information processing [4], [5], [6]. PP is a unicellular organism that, during one phase of its unique life cycle, typically forms a multinucleated protoplasmic mass without internal cell walls, known as a plasmodium [7]. It consists of a single cell with billions of nuclei that can stimulate the formation of pseudopodia (false limbs) to facilitate movement. In addition to their mobility, these slime molds are particularly interesting in different research fields due to their chemosensory perception and spatial memory [8]. Their behavior can be leveraged to develop optimization algorithms.

Objectives

In this article, our objective is to answer the following questions:

- "To what extent does the SISMO algorithm replicate the network formation behavior of real slime molds under controlled conditions, including the presence of obstacles?" *We show that our algorithm can replicate the behavior of slime molds and thus can be assigned to network formation tasks.*
- "How accurately can SISMO model and reconstruct existing transportation and power transmission networks based on geographic and infrastructure data?" *Our results indicate that the algorithm would be able to partially reconstruct the Carinthian transmission network in the event of an electromagnetic pulse (EMP) attack.*
- *We further show that using layout preprocessing with Gephi's* [9] *layout algorithms, such as ForceAtlas, ForceAtlas2, or Yifan Hu, can improve the accuracy of SISMO in network environments where geographical proximity does not correspond to actual topological connectivity.*

This study does not include a comparison between SISMO and conventional planning methods, nor does it perform functional simulations (e.g., electrical simulations) of the resulting networks. The focus is on presenting a novel bio-inspired modeling approach.
Our team has developed the slime mold-inspired SISMO algorithm and evaluated its effectiveness in forming networks and determining the shortest paths between individual points within them. To test its applicability, sections of the Carinthian traffic network were chosen as examples. Initially, in vitro experiments were performed to determine whether slime molds cultivated in Petri dishes could build a network similar to the existing traffic network. Subsequently, the SISMO algorithm was tested on the same sections. The first experiment was to determine whether both the slime molds and SISMO could build a network similar to the existing traffic network. The second experiment evaluated whether SISMO mimicked the behavior of the natural model. This study aimed to demonstrate the potential of SISMO for application to all types of networks that can be modeled using slime mold-based planning. In a third, separate experiment, it was investigated how the algorithm behaved when obstacles were present. This third experiment was conducted using SISMO in NetLogo programming language. The results demonstrated that SISMO could achieve levels of accuracy similar to those of real slime molds when obstacles were incorporated into the simulation. In this context, accuracy refers to the number of pre-existing connections replicated by the algorithm. Furthermore, a performance update was conducted, revealing that the simulation approach, despite its computational intensity, exhibits significantly faster results compared to the in vitro experiments. By modeling natural barriers as obstacles within the simulation, a significant improvement in the accuracy of the results was observed. In addition, the scalability of the SISMO algorithm was evaluated. The scalability measurements indicate that the simulation time is mainly influenced by the number of network nodes present within the slime mold

network rather than by the number of points to find (food sources). As the effectiveness of SISMO has been successfully established, it can be expected to be applied in optimizing other networks in practical applications, such as power supply networks, communication networks, and supply chain networks.

After demonstrating that SISMO can achieve satisfactory results in the planning and reconstruction of transportation networks, the algorithm was tested for application to transmission networks. This work builds on Himmelstein's proposal [10] by applying a slime mold–inspired algorithm to restore a power transmission network after an EMP attack. The network is modeled as a graph, with substations as nodes and transmission lines as edges. SISMO identifies critical repair areas, enabling faster and more resource-efficient recovery. The goal of this work was to develop an approach for reconstructing the power grid to ensure the protection of critical infrastructure.

The Carinthian transmission network was originally designed with geomorphological and infrastructural conditions in mind. In such networks, it often occurs that the geographical location of the nodes does not correspond to their actual connections. In the first and second experiments, this discrepancy often led SISMO to create edges between geographically close points that do not exist. We attempted to solve this problem by using the layout algorithms in the software Gephi [9] to adjust the network layout based on the existing connections. Through this preprocessing, we aim to improve the accuracy and usability of the simulation results.

Background

Slime Molds

Slime molds show characteristics of animals and fungi, but do not belong to either of these groups. Rather, they form their own taxon and have over 1000 different species distributed all over the world, roughly divided into the three groups Myxomycetes, Dictyostelia, and Protostelia. PP belongs to the Myxomycetes, characterized by the formation of plasmodia, a multinucleated plasma mass in one of its unique life phases. The cell nuclei can stimulate the formation of pseudopodia, which serve the organism for locomotion. PP is mainly found on rotting wood and on fruiting bodies of fungi, but occasionally also grows on living plants (Figure 1). Due to its easy handling, cultivability and cell size, it is often used as a model organism in research. SISMO simulates the behavior of the PP in the plasmodium stage. In this stage, the slime mold grows as long as it has food available. It doubles the number of its cell nuclei approximately every eight hours. A plasmodium feeds on organic material such as bacteria, algae, fungal spores or fungi. While feeding, the plasmodial mass moves around the food source, ingesting digestible material and excreting indigestible material. In doing so, the slime mold leaves a trail which, together with a kind of chemosensory perception, is used in the search for food [11].



Fig. 1

Figure 1: Plasmodium of *Fuligo septica* found in the Carinthian Woods (Photo by W. Marcher). Source: Figure 2.2, [16]

Abbildung 1: *Plasmodium von Fuligo septica, gefunden in den Kärntner Wäldern (Foto: W. Marcher). Quelle: Abbildung 2.2, [16]*

The locomotion of the slime mold is made possible by a cytoskeleton of actin filaments and the protein myosin. Contractions in a slime mold follow the same principle as muscle contractions. The two protein filament structures are also responsible for the plasma currents that promote locomotion. Organisms capable of locomotion generally use sensory mechanisms that allow them to sense changes in environmental conditions and move toward better conditions. The plasmodium of PP uses specific signal transduction mechanisms to respond to changes in the chemoreceptor conformation with motor chemotaxis responses. Chemotaxis is the movement of cells toward attracting substances (positive chemotaxis) or away from repelling substances (negative chemotaxis) [11].

PP is not only capable of movement and sensing chemical stimuli, but also has a remarkable ability to remember the location of food for future use. Although spatial memory is typically associated with the brain of an organism, PP, like all slime mold species, does not have a brain [8]. However, it is able to avoid previously explored areas while foraging, enabling it to solve complex optimization problems. This ability cannot be solely attributed to its chemosensory perception, indicating that slime molds possess a type of memory. Memory refers to the retention and retrieval of information related to previous events [12]. Some ant species employ external memory by leaving pheromone trails to mark the route between the nest and the food source. This enables indirect route communication without individual memory retention [8]. The plasmodium of PP consists of many small oscillating units that oscillate at a frequency determined by their environment and interaction with neighboring oscillators [13]. Positive chemotaxis increases the oscillatory frequency near the food source, causing plasma to flow in that direction. In contrast, negative chemotaxis decreases the oscillatory frequency [14]. The collective behavior of the many oscillating units leads to the movement of the organism. As it moves, the plasmodium leaves behind a specific protein-based extracellular slime (Figure 2). In their research, Reid et al. [8] suggest that the plasmodium avoids areas with this slime when foraging, but this behavior ceases when there are no unexplored areas left. Based on this observation, Reid et al. inferred the existence of an externalized spatial memory system in the plasmodium of PP.



Fig. 2

Figure 2: Plasmodium of *Physarum polycephalum* cultivated in a Petri dish. Source: own image

Abbildung 2: *Plasmodium von Physarum polycephalum, kultiviert in einer Petrischale. Quelle: eigenes Bild*

SISMO

The first version of SISMO was developed as part of two master's theses at the University of Klagenfurt [15], [16]. NetLogo was used to implement the SISMO algorithm. Developed by Uri Wilensky in 1999, NetLogo is a free, open-source modelling environment for simulating complex natural and social systems. It enables independent mobile agents, known as *turtles* and stationary *patches* to interact and form networks or graphs, making it ideal for multi-agent simulations. It is well-suited to model slime mold behavior, effectively capturing movement and chemical responses. Advantages include scalability, flexibility and ease of programming, enabling the detailed study of decentralized, emergent behaviors in complex systems. Figure 3 illustrates how our algorithm operates within the NetLogo framework. It details how the slime mold network locates, searches for, and spreads to food sources, and how it forms the shortest possible path. SISMO is primarily based on the first three phases of the slime mold algorithm (SMA) [17] foraging process, namely searching food, approaching food, and wrapping food. In the SMA, pseudopods balance exploration and exploitation by first randomly searching for food sources and then reinforcing efficient paths once found. This ensures the algorithm avoids local optima while gradually identifying the shortest or most effective routes. SISMO applies this principle to optimize network restoration by focusing on critical connections without overlooking alternative paths. The SMA uses parameters LB and UB, where LB and UB denote the lower and upper limits, to set the search range bounds that define the area in which the slime mold can move. In contrast, the simulation of SISMO in NetLogo defines these boundaries by the size of the world model settings. Once a pseudopod finds a food source, it moves toward it during the foraging phase, following the NetLogo propagation pattern, known as the wiggle function, which is different from the arbitrary

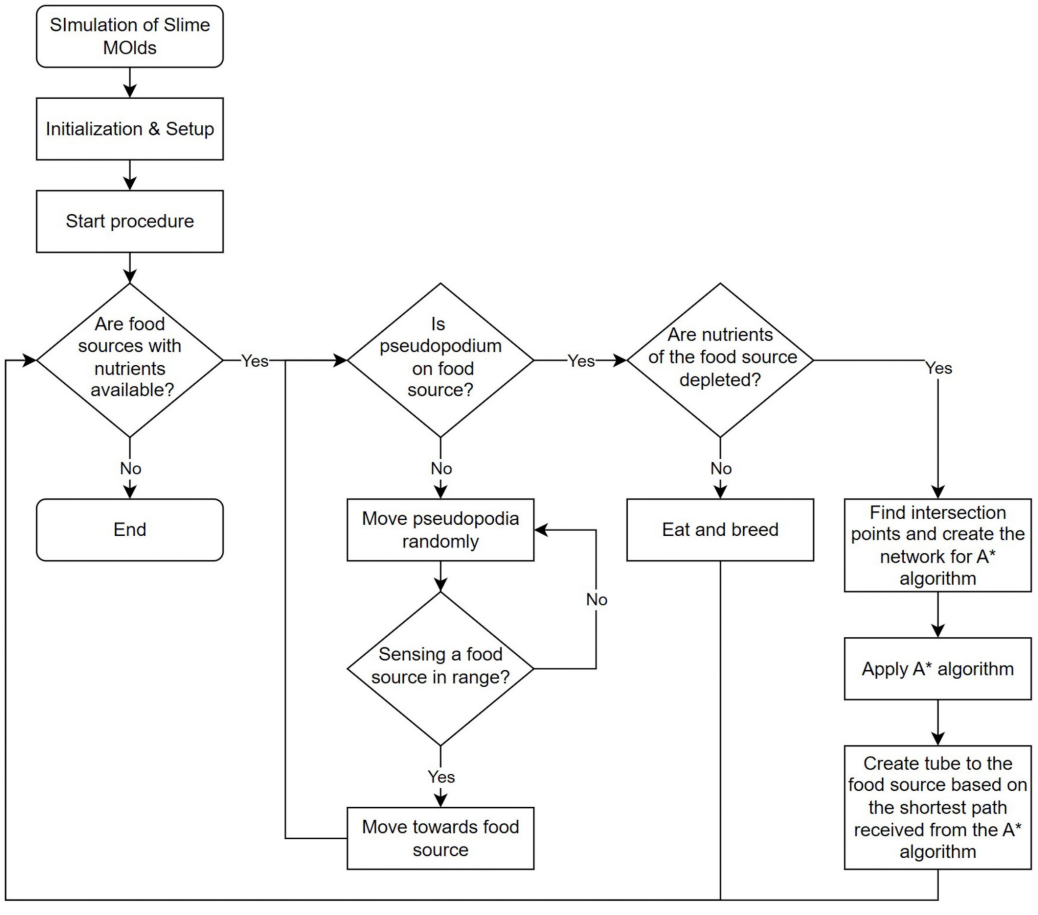


Fig. 3

Figure 3: NetLogo SISMO algorithm workflow. Source: own image

Abbildung 3: *Arbeitsablauf des NetLogo-SISMO-Algorithmus. Quelle: eigenes Bild*

pseudopodia alternating positions in SMA. The wiggle command causes a turtle, in this case a pseudopodium, to perform a random rotation at a specified angle. The pseudopod considers the food source as a point during the food approach phase [15], [16]. The simulation terminates when there are no more food sources for the simulated slime mold to explore. This condition is based on global knowledge that would not be available for a natural slime mold and is not part of the core algorithm.

SISMO is available as open source on GitHub under a Creative Commons license [18]. To run simulations with SISMO, NetLogo version 6.2.2 is recommended. Clicking on the SETUP button will create the plasmodium, the selected number of food sources, and the selected number of initial pseudopodia. The slider AMOUNTPSEUDOPODIA can be used to set the number of initial pseudopodia. The AMOUNT-FOODSOURCES slider sets the number of food sources. The SHOW-NUTRIENT-VALUE switch determines whether or not to display the number of nutrients from the food sources. The SHOW-NETWORK switch determines whether the created network needed for the A* algorithm should be displayed or not. The SHOW-INTERSECTION-POINTS switch defines whether the calculated intersection points should be displayed or not. The simulation is started with the GO button.

Prior to initiating SISMO, various simulation parameters can be established and configured using the NetLogo graphical user interface (GUI).

- AMOUNT-PSEUDOPODIA Defines the number of pseudopodia.
- AMOUNT-FOODSOURCES Defines the number of food sources.
- SHOW-NUTRIENT-VALUE Defines whether the nutrient value of the food sources should be displayed.
- SHOW-NETWORK Defines whether the network for the A* algorithm should be displayed.
- SHOW-INTERSECTION-POINTS Defines whether the intersection points should be displayed.

During initialization, all agent types (breeds) are created with their required properties and values. Users can choose certain values, such as the number of pseudopods and food sources, through the GUI.

The simulation uses six different breeds:

- Plasmodium
  The plasmodium forms the core of the slime mold. From it, the pseudopodia spread out. In addition, the plasmodium serves as a starting point for calculating the shortest path using the A* algorithm.
- Pseudopodia
  The pseudopodia are responsible for foraging. They spread randomly and form new pseudopodia when a food source is found.
- Tubes
  Tubes are responsible for the visualization of the shortest path. The pseudopodia also form tubes, but in the separately created breed, the shortest path is thicker and visualized differently.
- Foods
  This breed acts as food sources for the slime mold.
- Networkpoints
  This breed is used for the network points in the A* algorithm.
- Searchers
  In the A* algorithm searchers are used to calculate the shortest path.

During the setup phase, all pre-defined breeds are generated along with their respective attributes. The procedure involves creating each breed, defining their properties, assigning values to their traits, and ultimately displaying the plasmodium, pseudopodia, and food sources.

The SISMO algorithm's primary element is the simulation process, which comprises four main components: movement, feeding and breeding, network construction, and pathfinding. Agents (pseudopodia) move left or right at random and then move forward one step. If this is not possible, the agent rotates 180 degrees. During the movement, the agents cannot leave the specified map boundaries and bounce off the edge if encountered. After performing the movement, the *x* and *y* coordinates of the new position of the pseudopodium are stored in a list. When a pseudopodium reaches a food source during its propagation, it picks up nutrients from that source as long as they are present. A random number (ξ*)* between zero and one is generated. This random number determines whether a plasmodium will divide or not. The value of 15% for the hatching probability was chosen after several test runs, as it gives the best results in terms of performance and visualization. If this random number is less than or equal to 0.15, a new pseudopodium is generated. It inherits all the properties of its parent except its ID. A new path list is created for the newly created pseudopodium, with the values for ξ set to 1. This means that the entries in the new path list are a copy of the entries in the path list of the respective parent. For further movement, ξ is set to 0, since the new plasmodium will move independently of the parent from this point. In the construction of the network, all paths traveled by all pseudopodia must be considered. These paths are stored in the path lists of each pseudopod. As each path list is compared to itself and the others, the system searches for intersection points. The position of an intersection point found is entered into the path list. If no intersection point is found, a node is created. The graphical output of a

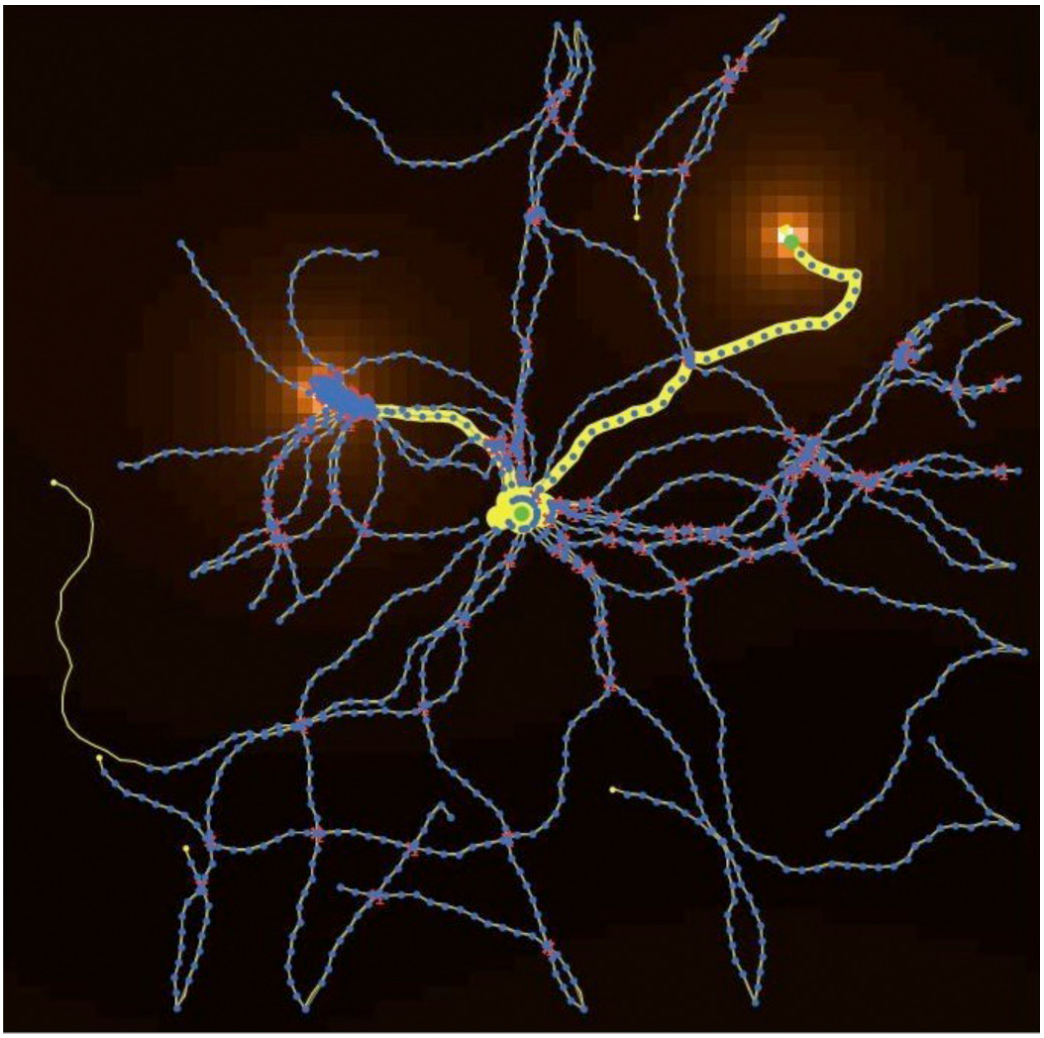


Fig.4

Figure 4:
SISMO Algorithm: Simulation with Shortest Path, Network Nodes, and Intersection Points. Source: Figure 5.12, [16]

Abbildung 4:
SISMO-Algorithmus: Simulation mit kürzesten Wegen, Netzwerkknoten und Schnittpunkten. Quelle: Abbildung 5.12, [16]

SISMO simulation in NetLogo is depicted in Figure 4. The blue points represent the created network nodes. The crossing points are represented as red crosses. The A* algorithm is used to find the shortest path within the network. The thick yellow path represents the shortest routes between the core and the food sources.

To emulate the behavior of the slime mold in finding the shortest path in the network on which the mold is located [19], the simulation implements an A* algorithm to find the shortest path. To build the network for the A* algorithm, all pseudopodia paths must be considered and stored in a list of path lists. When there are multiple pseudopodia, the first path list is compared to the other path lists, including itself to prevent overlapping. The first element in the path list is compared with all other elements. Subsequently, the second element of the path list is compared to all others except the first to avoid unnecessary iterations. Checking for overlap is critical in constructing a network similar to that of a real slime mold. To achieve this, intersection points in the paths are identified except in specific situations where no intersection check is necessary. After constructing the mesh, the A* algorithm is utilized to calculate the shortest path. The implementation of the A* algorithm used for this project is built upon Caparrini's *General A* Solver in NetLogo* [20]. However, it has been modified to include a graphical display of the shortest path. Once the A* algorithm is applied, a new path is created using the coordinates of the shortest path, which is then represented as a thicker yellow line. This approach is inspired by the behavior of slime molds in nature, where paths through which the most nutrients flow are more pronounced. The thicker yellow line serves to highlight the most optimal path found by the algorithm and provides a visual representation of the efficiency of the A* algorithm in finding the shortest path.

METHODS

This section presents several tests performed to verify and assess the functionality of SISMO. When developing SISMO, it was important for the algorithm to behave as similarly as possible to its model in nature. The first two experiments, therefore, aimed to test how closely the results of simulations with SISMO resemble the spread of slime molds in Petri dishes. For this purpose, the plasmodium in the Petri dish and the simulation tool were provided with the same information. Another series of experiments considered obstacles such as lakes and mountains in the planning of the traffic network. SISMO showed promising results in all the transportation network planning experiments conducted. With some modifications, SISMO can also be applied to various other types of networks. A series of tests on the planning and reconstruction of the Carinthian distribution network is presented here. In the first use case, SISMO was applied to the original network of KNG-Kärnten Netz GmbH. Then, SISMO was applied on different networks in which the layout was adjusted based on the existing connections.

Evaluation Metrics

1) *Accuracy:* The primary metric used to evaluate the performance of network reconstruction methods is accuracy, defined as the ratio of the number of connections identified by the method—whether simulated or biologically grown—to the total number of actual existing connections in the built network. This metric quantifies how closely the reconstructed network aligns with real-world infrastructure.
2) *Performance Metrics for SISMO:* The effectiveness of the SISMO algorithm is assessed using several performance metrics. Simulation time measures the computational effort required to find food sources or complete the network reconstruction, including scalability relative to the number of nodes.

To evaluate the simulation's ability to identify connections, the following terms are defined: True positives (TP) represent connections correctly predicted by the simulation that exist in the real network. False positives (FP) are connections predicted by the simulation that do not exist in reality, while false negatives (FN) are actual connections in the real network that were missed by the simulation. True negatives (TN), though less relevant in this context, refer to non-existent connections correctly not predicted by the simulation.

Precision measures the proportion of correctly predicted connections among all predicted connections:

$$Precision = \frac{\mathrm{TP}}{\mathrm{TP} + \mathrm{FP}}$$

Recall quantifies the proportion of correctly identified connections among all actual connections:

$$Recall = \frac{TP}{TP + FN}$$

The F1 score combines precision and recall as a harmonic mean, providing a balanced assessment of the simulation's performance:

$$F1\ Score = 2x\ \frac{Precision \cdot Recall}{Precision + Recall}$$

The F1 score ranges between 0 and 1, where a value of 1 denotes an ideal classifier with perfect precision and recall, and a value of 0 indicates a classifier with no predictive capability.

These metrics collectively enable a comprehensive evaluation of the SISMO algorithm's ability to accurately reconstruct and optimize network structures.

Experimental Analysis of Living Slime Molds

This set of experiments was part of a master's thesis at the University of Klagenfurt in 2022 [16]. The slime molds for the experiments were ordered partly via Amazon from the company KREZUS in France and partly via the online store Pro Formica (https://pro-formica.de/).

A hygiene protocol was followed to prevent mold growth on the test objects. Before use, the Petri dishes and all other utensils (pipettes, tweezers) were sterilized by treatment with boiling water. Agar-agar was mixed and distributed in the Petri dishes as a culture medium before the slime mold, in its dried form of the sclerotium, was placed in it. In this dry form, the plasmodium survives even if the necessary conditions (temperature, humidity, pH value, etc.) are not given. To return the plasmodium to its viscous form, a few drops of distilled water were added.

Experiment 1: ÖBB Railroad Network Carinthia

To prepare for the in vitro experiment, the chosen map section was printed, resized, and affixed to the bottom of the Petri dish. The Klagenfurt main station (point one) was chosen as the starting point for the experiment. At this point, the sclerotium of PP was placed in the Petri dish. From there, the slime mold spread across the map. Both the starting point and the selected stations were marked with oatmeal flakes, which served as food sources for the slime mold. An overview of the selected stations is available in Supplementary Table 1. The setup of this experiment and the setup of the simulation is shown in Figure 5.

Experiment 2: KMG Bus Line to University Klagenfurt

For the second experiment, bus line C of Klagenfurt Mobil GmbH (KMG) was chosen. Line C connects the Klagenfurt main station with the University of Klagenfurt and Lakeside



Figure 5:
Setup ÖBB Experiment 1. Source: adapted from [16]

Abbildung 5:
Aufbau des ÖBB-Experiments 1. Quelle: angepasst nach [16]

Fig. 5

Park every ten minutes. Here, too, the slime mold in the Petri dish and the slime mold simulated with SISMO was tested on the same route section. The selected stations are listed in Supplementary Table 2. The experimental setup of the in vitro experiment and the setup of the simulation are shown in Figure 6.



Figure 6:
Setup KMG Experiment 2. Source: adapted from [16]

Abbildung 6:
Aufbau des KMG-Experiments 2. Quelle: angepasst nach [16]

Fig. 6

In the first experiment, the slime mold mimicked part of Carinthia's rail network. After 16 days, it created a structure largely similar to the real network, especially from St. Veit an der Glan. Deviations may have been due to too few or suboptimal stations or deformation of the Petri dish. In the second experiment, the slime mold replicated parts of Klagenfurt's bus line C within nine days. Several sections closely matched the actual route, while others differed, likely for the same reasons as in the first experiment.

Simulations of Experiments 1 and 2: Verifying the Behavior of SISMO

To test whether the behavior of the simulated slime mold in SISMO corresponded to the natural behavior, experiments 1 and 2 were carried out using in vitro experiments in parallel to the simulation tool. For the simulation with SISMO in NetLogo, the same background as printed and affixed on the Petri dishes was inserted as an image, and the same points were selected for the starting point and the food sources. The setup is shown together with the experimental design of the in vitro experiments in Figure 5 and Figure 6. In the first experiment, the slime mold in the Petri dish and SISMO had the task to plan a part of the railroad network of Carinthia based on some given stops. Both were able to plan a network that at least in places corresponded to the real network. The slime mold in the Petri dish took 16 days to solve this task. The simulation with SISMO needed six days for the same task.

In the second experiment, the in-vitro slime mold and SISMO had the task to plan a part of the KMG Klagenfurt bus network. For this purpose, a part of bus line C was chosen, covering the route from Heiligengeistplatz to the University of Klagenfurt and Lakeside Park. Also in this experiment, both the simulation and the natural slime mold were able to

plan a network that at least in places matched the real network. Figure 8 shows the results of the second in-vitro experiment and its simulation with SISMO. For the comparison, the eighth and thus penultimate day of the experiment with the slime mold in the Petri dish was used, since the tubes formed can be seen best here. In this experiment, the slime mold took nine days to reach all the desired stops in the map section and establish a network between them. The SISMO algorithm took four days to simulate the same scenario, considerably faster than the in-vitro experiment.

SISMO simulations showed greater deviations from real networks than the in-vitro slime mold experiments. These differences may result from limited food sources, historical network evolution, or ignored real-world constraints. In both experiments, the in vitro slime mold was slightly more accurate, though SISMO was faster in the second case. Better stop selection could improve both methods.

Table 1 presents a comparison between in vitro experiments and SISMO simulations, the accuracy value reflecting the degree to which the planned network sections correspond to the actual bus and rail networks. Concretely, the first value indicates the number of connections found by the method, while the second value represents the total number of actual existing connections.

Tab. 1

ÖBB Experiment	Duration	Accuracy
Slime Mold	16 days	4/6
SISMO	16 days	2/6

KMG Experiment	Duration	Accuracy
Slime Mold	9 days	4/7
SISMO	4 days	3/7

Table 1:
Comparison of real slime mold and SISMO [16]

Tabelle 1:
Vergleich von echtem Schleimpilz und SISMO

After the two series of experiments showed promising results with regard to the similarity of the behavior of the simulation and the slime mold in the Petri dishes, further series of simulations were carried out with SISMO. A comparison of the results of the in-vitro tests and the simulations is shown in Figure 7 and Figure 8.

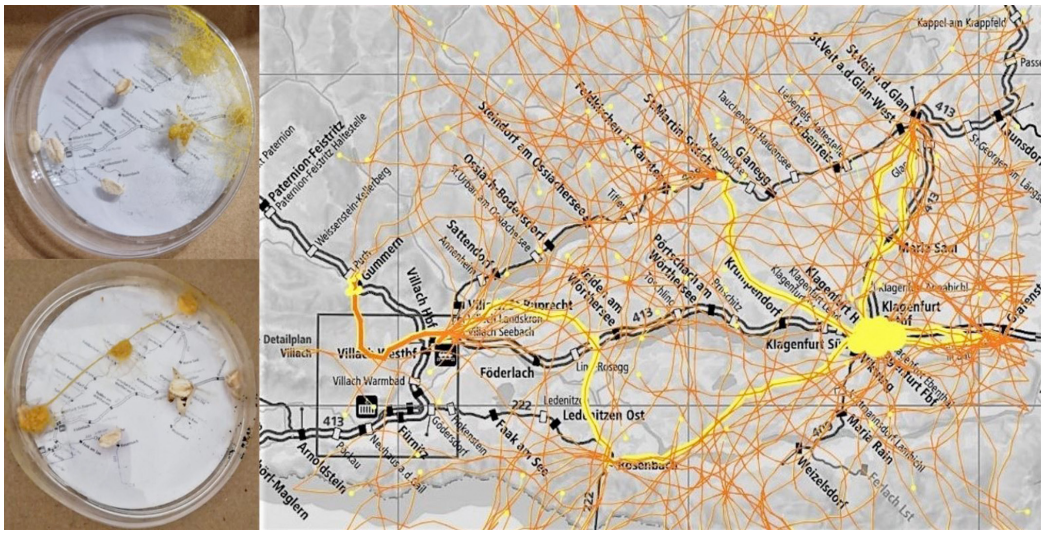


Fig. 7

Figure 7:
Comparison of the ÖBB in-vitro experiment 1 with SISMO. Source: adapted from [16]

Abbildung 7:
Vergleich des ÖBB-In-vitro-Experiments 1 mit SISMO. Quelle: angepasst nach [16]

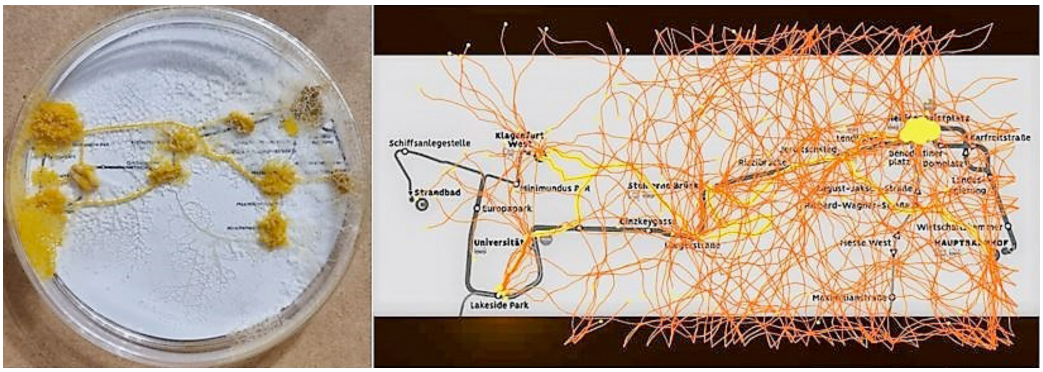


Fig. 8

Figure 8:
Comparison of the KMG in-vitro experiment 2 with SISMO. Source: adapted from [16]

Abbildung 8:
Vergleich des KMG-In-vitro-Experiments 2 mit SISMO. Quelle: angepasst nach [16]

Experiment 3: Inclusion of Obstacles and Performance Improvement

To simulate obstacles, the SISMO code was not only adapted, but also optimized for performance, which is also important for scalability. In this simulation, the background image used as the map was adjusted. Non-accessible areas were colored green and blue, with blue representing lakes. Specifically, the simulation included the Ossiacher See to the north of the green area and the Wörthersee to the south. The green area itself represented insurmountable obstacles, such as mountains or areas that are legally required to stay free of transportation lines, such as protected areas.

To enhance performance, code optimization was implemented in two areas. The first optimization pertained to the mesh creation for the A* algorithm. Previously, the mesh created during the first food source search was retained, resulting in all coordinates in a large list being checked for existing mesh points during future mesh calculations and extensions. To reduce runtime, the entire mesh was discarded and recreated after each A* algorithm run, for instance, by omitting the search for existing entries in a list containing several thousand items. For the first pseudopodium coordinate list, the runtime was significantly reduced. The second optimization related to the A* algorithm itself. Previously, the algorithm didn't consider whether a searcher was already on a network point, which led to multiple unnecessary runs for already checked routes with multiple searchers on the same point. By avoiding unnecessary redundancy in this way, performance was enhanced.

For implementation of the simulation considering obstacles, the task of the first in vitro experiment (replication of the network of ÖBB) was used. The same route section was simulated with the obstacles using the optimized implementation in NetLogo [15].

Figure 9 presents a comparison between two simulation results for the ÖBB network map. The left side of the figure displays the simulation result without obstacles, while the right side shows the result with obstacles. The simulations were evaluated based on their ability to replicate existing connections between various stops. The comparison reveals that both simulations performed well in replicating the connection between Klagenfurt and Grafenstein. The connection from Klagenfurt to St. Veit also showed similar results in both simulations, with the first difference appearing in the connection to St. Martin Sittich. In the simulation without obstacles, the connection was created cross-country, while the other result showed a much better approximation to the existing route of the ÖBB due to the obstacle. The connection from Klagenfurt to Rosenbach showed similar results in the south of the map in both simulations, with neither simulation creating anything close to a similar connection to the existing network. However, the simulation with obstacles approximated the existing connection between Klagenfurt and Villach much better than the simulation without obstacles, which had a deviation from the existing network. The connection from

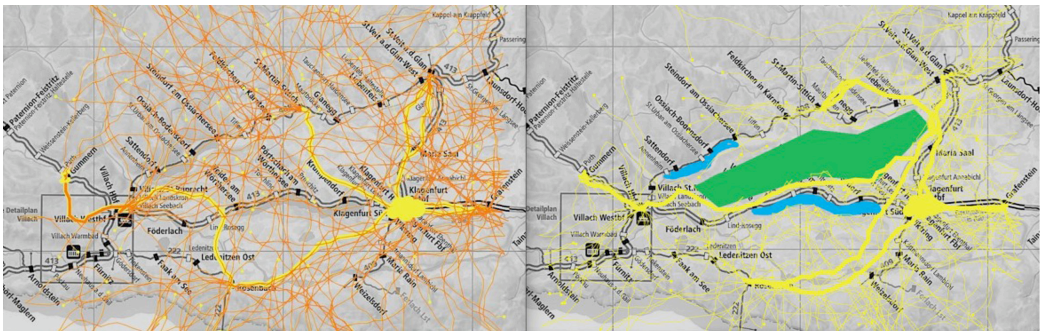


Fig. 9

Figure 9: ÖBB experiment 1 SISMO Simulation Comparison. Source: Fig. 6.48 [15]

Abbildung 9: *Vergleich des ÖBB-Experiments 1 mit der SISMO-Simulation.*

Villach to Gummern was well approximated by the simulation with obstacles, but not by the other simulation. Notably, neither simulation created the connection from St. Martin Sittich to Villach. Overall, the simulation with obstacles achieved better results by more accurately approximating the network map of the ÖBB.

Scalability

The results presented in this section were measured with the optimized code. In Table 2, an overview of various measurements conducted with SISMO is presented. The table compares the time taken by SISMO to locate a specific number of food sources, where *FS* in the table denotes the amount of food sources. The time is measured in minutes. It should be noted that some food sources may have a higher nutritional value than others, giving the pseudopodia more time to search for additional food sources. Meanwhile, if other pseudopodia have already found a food source, the calculation of the next shortest path is likely to occur almost immediately. Additionally, if fewer pseudopodia have hatched, fewer paths need to be examined for reticulation. The results show that the calculation for the last food source always takes the most time. As the experiment with only two food sources shows, the calculation for the second food source takes considerably longer than the calculation for the second food source in the following experiments with more than two food sources, which is shown in the second column of Table 2. As previously mentioned, the last iteration always takes the longest due to the behavior of the SISMO algorithm. The food sources have a certain number of nutrients, and only when the total number of nutrients is exhausted, the A* algorithm calculates the shortest path. While the nutrients are being depleted, other pseudopodia can continue to move and new pseudopodia can be hatched, resulting in the final iteration taking more time [15].

Tab. 2

# FS	1 found	2 found	3 found	4 found	5 found	6 found	7 found	8 found
1	0.35	-	-	-	-	-	-	-
2	0.08	2.95	-	-	-	-	-	-
3	0.05	1.40	4.19	-	-	-	-	-
4	0.04	0.70	4.44	33.83	-	-	-	-
5	0.05	0.93	3.06	7.86	51.90	-	-	-
6	0.05	0.09	0.67	4.68	22.55	146.97	-	-
7	0.07	0.23	1.50	4.51	20.46	46.94	131.02	-
8	0.04	0.14	0.24	0.44	4.47	20.30	120.83	236.6
Average	0.09	0.92	2.35	10.26	24.85	71.40	125.93	236.6

Table 2: Number of food sources (FS) to be found and time taken (minutes) to find all of them [15]

Tabelle 2: *Anzahl der zu findenden Nahrungsquellen (FS) und dafür benötigte Zeit (Minuten) [15]*

To optimize the simulation of shortest paths in a network, it is helpful to take into account the number of network nodes in each simulation step. Table 3 shows the time SISMO takes per node depending on the number of food sources. In this table, the time required to calculate the shortest path to the food source is indicated by the abbreviation STIS (Simulation Time In Seconds). The value represents the simulation time required for the number of nodes specified in NON (Number Of Nodes). Therefore, STIS/NON (S/N) indicates the value of how many seconds per node are needed. As the network size increases, this value increases as well. This is due to the fact that the list of nodes in the network becomes larger during creation, so it takes longer to check whether a node already exists to avoid creating unnecessary nodes.

Tab. 3

# FS			S/N		S/N		S/N		S/N		S/N		S/N		S/N		S/N
1	STIS	21	0.02	-	-	-	-	-	-	-	-	-	-	-	-	-	-
	NON	1041		-	-	-	-	-	-	-	-	-	-	-	-	-	-
2	STIS	4.8	0.01	177	0.09	-	-	-	-	-	-	-	-	-	-	-	-
	NON	622		1915		-	-	-	-	-	-	-	-	-	-	-	-
3	STIS	3	0.01	84	0.06	251	0.16	-	-	-	-	-	-	-	-	-	-
	NON	522		1427		1609		-	-	-	-	-	-	-	-	-	-
4	STIS	2.4	0.01	42	0.04	266	0.14	2030	0.54	-	-	-	-	-	-	-	-
	NON	463		1162		1902		3741		-	-	-	-	-	-	-	-
5	STIS	3	0.01	55.8	0.04	184	0.12	472	0.23	3114	0.64	-	-	-	-	-	-
	NON	534		1250		1507		2063		4888		-	-	-	-	-	-
6	STIS	3	0.01	5.4	0.01	40.2	0.03	281	0.12	1353	0.4	8818	1.52	-	-	-	-
	NON	475		490		1257		2359		3419		5793				-	-
7	STIS	4.2	0.01	13.8	0.02	90	0.06	271	0.16	1228	0.41	2816	0.88	7861	1.57	-	-
	NON	586		616		1419		1700		2967		3216		5016			
8	STIS	2.4	0.005	8.4	0.01	14.4	0.02	26.4	0.03	268	0.12	1218	0.34	7250	1.25	14196	2.14
	NON	498		675		676		860		2276		3570		5801		6629	
Sum			0.06		0.28		0.53		1.08		1.56		2.74		2.82		2.14
Average			0.01		0.04		0.09		0.22		0.39		0.91		1.41		2.14

Table 3:
Time for SISMO needed per network point [15]

Tabelle 3:
Für SISMO benötigte Zeit pro Netzwerkknoten [15]

Use Case: Repair Plan for the Carinthian Transmission Grid

In [21], we have presented an approach in which a repair plan for the Carinthian power transmission network after an EMP attack is developed using SISMO. In summary, SISMO is applied to a graph model to identify critical areas for repair. For this purpose, the algorithm was adapted and provided with the positions of the relevant power plants and substations in the Carinthian power transmission network. The locations of the 63 considered power plants and substations were taken from an overview by the *Landesrechnungshof Kärnten* (Supplementary Table 3) [22], and their coordinates were converted into a format compatible with NetLogo using a custom-developed program. Since the simulation results sometimes contained disconnected networks or introduced non-existent connections, graph visualization algorithms were proposed for preprocessing. Specifically, the layout was improved using Force Atlas, Force Atlas2 and Yifan Hu Proportional algorithms provided within the Gephi software [9]. Graph-layout-algorithms rearrange the nodes in a network without altering the nodes or edges themselves. Some of these algorithms align node positions based on their connectivity, placing connected nodes closer together and unconnected nodes further apart. This preprocessing step improves the accuracy and significance of the simulation results.

A total of eight simulations were performed using the original network before rearranging it with graph layout algorithms. The average duration of the simulations was 50 minutes and 5 seconds. Figure 10 (upper left) shows the result of one simulation based on Carinthia's power transmission network. The plasmodium is visualized as a yellow cloud in the center, while food sources, placed at the coordinates of substations and power plants are marked as black dots with orange frames.

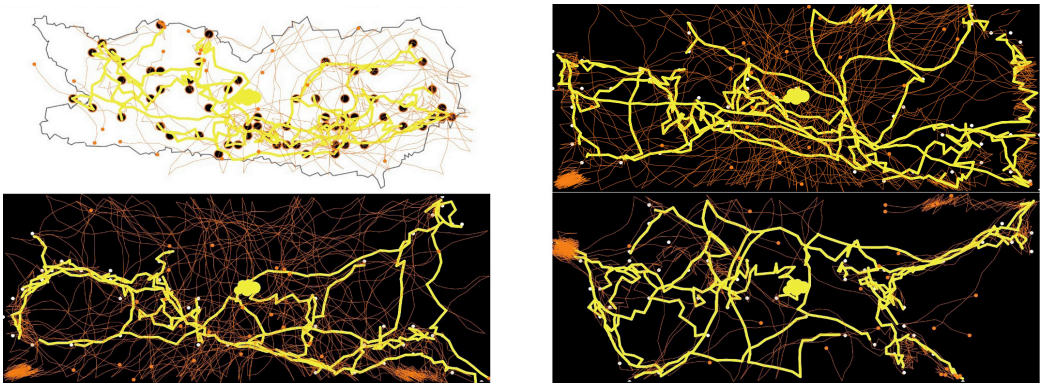


Fig. 10

Figure 10:
Simulation Results: Original Model (upper left), Force Atlas (upper right), Force Atlas2 (lower left) and Yifan Hu (lower right).
Source: own image

Abbildung 10:
Simulationsergebnisse: Originalmodell (oben links), Force Atlas (oben rechts), Force Atlas2 (unten links) und Yifan Hu (unten rechts).
Quelle: eigenes Bild

Orange lines represent the paths taken by the pseudopodia, and the shortest connections are highlighted with thicker yellow lines. In terms of performance metrics, the simulation achieved 29 TP, 1821 TN, 60 FP, and 43 FN. The precision was 0.33, the recall was 0.4, and the F1 score was 0.36. These results indicate that while the simulation successfully identified some actual connections, there is still room for improvement in accuracy.

A setup with Force Atlas node layout was simulated using the same settings, with an average runtime of 7 hours and 18 minutes each. The simulation achieved 34 TP, 1821 TN, 60 FP, and 38 FN, resulting in a precision of 0.36, recall of 0.47, and an F1 score of 0.41.

Ten simulations of the optimized network using Force Atlas2 were conducted with the same settings and initial values, averaging 1 hour and 42 minutes each. The simulations resulted in 33 TP, 1815 TN, 66 FP, and 39 FN, yielding a precision of 0.33, a recall of 0.46, and an F1 score of 0.39.

The Yifan Hu Proportional algorithm was used to optimize the network layout, keeping all other settings consistent with previous simulations. Ten simulations were conducted, averaging 5 hours, 14 minutes, and 13 seconds each. The simulations achieved 37 TP, 1818 TN, 63 FP, and 35 FN. The precision was 0.37, the recall 0.51, and the F1 score 0.43. While a higher F1 score is generally better, some FN can be acceptable as they indicate network thinning, potentially reducing repair efforts. Notably, the original network layout performed worse than the optimized models in this regard.

Table 4 provides an overview of the values for TP, TN, FP, FN, as well as the derived metrics precision, recall, and F1 score of all simulations conducted. A comparison of the F1 scores indicates that all simulations based on the rearranged graph models outperformed the simulation using the original network. Notably, the Yifan Hu model achieved the highest F1 score of 0.43, reflecting the most balanced trade-off between precision and recall.

Tab. 4

	Avg. Duration	TP	TN	FP	FN	Precision	Recall	F1 Score
Original network	00:50:05	29	1821	60	43	0.33	0.4	0.36
Yifan Hu	05:14:13	37	1818	63	35	0.37	0.51	0.43
Force Atlas 1	07:18:46	34	1821	60	38	0.36	0.47	0.41
Force Atlas 2	01:42:04	33	1815	66	39	0.33	0.46	0.39

Table 4:
Comparison of the simulation results [22]

Tabelle 4:
Vergleich der Simulationsergebnisse [22]

Overall, this series of simulations used SISMO to implement Himmelstein's slime mold-inspired method [10] for energy network repair. However, the results often produced fragmented or unrealistic connections, limiting its practical use. To improve outcomes, we applied graph layout algorithms (Force Atlas, Force Atlas2, Yifan Hu Proportional), which reduced false links by reorganizing the network structure—though at the cost of longer computation times. While slime mold approaches may benefit complex network design, simpler methods like minimum spanning trees may be more suitable for targeted repair tasks. Our study is, to the best of our knowledge, the first to combine slime mold simulations with graph layouts, opening new possibilities for future research.

RESULTS

The accuracy of network reconstruction was assessed using precision, recall, and the F1 score. Among the tested models, the Yifan Hu layout achieved the highest F1 score of 0.43, followed by ForceAtlas with 0.41 and ForceAtlas2 with 0.39. The original network performed the worst, reaching only 0.36. Incorporating obstacles such as lakes and mountains improved the realism of the reconstructed networks. For example, the connection between Klagenfurt and Villach was more accurately represented in the model that included obstacles compared to the one without them. The scalability of the SISMO algorithm was evaluated by analyzing simulation times. Results showed that runtime increased with the number of food sources.

SISMO was able to identify critical areas for repair following a simulated EMP attack. The integration of graph layout algorithms, such as ForceAtlas and Yifan Hu, improved the accuracy of the repair planning, although this came at the expense of longer runtimes. Among the tested methods, the Yifan Hu model achieved the best balance, with a precision of 0.37 and a recall of 0.51. The performance metrics further illustrate the differences between models. The original network achieved 29 TP, 1821 TN, 60 FP, and 43 FN. The Yifan Hu model performed best, with 37 TP, 1818 TN, 63 FP, and 35 FN. ForceAtlas yielded 34 TP, 1821 TN, 60 FP, and 38 FN, while ForceAtlas2 resulted in 33 TP, 1815 TN, 66 FP, and 39 FN.

Compared to the in vitro slime mold experiments, SISMO proved to be considerably faster—for instance, requiring only four days instead of nine days for reconstructing the KMG bus line—but was less accurate. The application of graph layout algorithms improved accuracy but also increased computational effort. Overall, SISMO demonstrates potential for network optimization and repair planning, particularly when natural obstacles are considered.

DISCUSSION

We have shown through experiments that the slime mold *P. polycephalum* and our simulation implementation SISMO can form and reconstruct networks by placing food sources as network nodes. Both the in vitro and simulation experiments validated this approach using Carinthian electricity transmission networks as well as public transportation systems in Carinthia and its regional cities. Results demonstrated that SISMO achieves comparable accuracy in transportation network reconstruction while providing significantly faster computational performance than in vitro experiments. The application of SISMO to Carinthian railway and bus networks highlights its potential for bio-inspired network optimization, particularly when incorporating natural obstacles such as lakes and mountains to improve path accuracy. Furthermore, our findings show that preprocessing network layouts with graph visualization algorithms such as ForceAtlas2 and Yifan Hu Proportional substantially improves SISMO's performance in network

recreation, especially in power transmission scenarios, with the Yifan Hu model achieving the highest F1 score of 0.43. The successful adaptation of SISMO for power grid repair planning after EMP attacks underlines the algorithm's versatility beyond transportation networks, offering a novel approach to critical infrastructure restoration that accounts for both geographical and topological constraints. While in some cases SISMO shows greater deviations from real networks than natural slime molds, its ability to account for obstacles and generate alternative configurations provides valuable insights for optimization scenarios unconstrained by existing infrastructure limitations. Integrating NetLogo's multi-agent simulation environment with bio-inspired algorithms thus proves effective for network planning research, enabling rapid prototyping and testing of diverse network scenarios with customizable parameters.

In comparison to other *Physarum*-inspired approaches, such as the work of Tero et al. [23] on the Tokyo railway system, SISMO offers a more flexible and computationally efficient solution. Tero demonstrated through biological experiments that *P. polycephalum* can reconstruct efficient, fault-tolerant networks and complemented these findings with a mathematical flow-based model, in which tubular conductance is reinforced or weakened depending on flux to achieve robust structures [23]. SISMO builds on these principles but translates them into a multi-agent simulation framework that operates significantly faster, allows stochastic exploration by independent agents, and provides greater adaptability. Unlike biological and purely mathematical approaches, SISMO can explicitly account for geographical obstacles and topological constraints, improve accuracy through network layout preprocessing, and extend beyond transportation to applications such as power grid restoration. Thus, SISMO represents a practical advancement over existing *Physarum*-inspired methods, providing concrete tools for network planning, optimization, and recovery.

FUTURE WORK

To expand the applicability of SISMO beyond network formation, future work will investigate how information could be transmitted within the simulated networks. This includes modeling communication or energy flow and analyzing how the network topology affects the efficiency and resilience of information propagation. Although SISMO has demonstrated promising results, further optimization of the algorithm is necessary to improve performance and scalability. This includes enhancing computational efficiency and reducing simulation time. To facilitate agent-based experimentation and integration with other models, the implementation of SISMO within the Python-based MESA framework is planned. This will allow for greater flexibility in testing, improved visualization capabilities, and easier comparison with other agent-based algorithms. At the application level, it is planned to test the SISMO algorithm as part of a method for Maximum Power Point Tracking, known as MPPT, in photovoltaic systems. The aim is to evaluate whether bio-inspired network formation can contribute to optimizing energy yield, particularly under dynamic environmental conditions.

References

[1] M. Dorigo, "Optimization, Learning and Natural Algorithms," Dissertation. Politecnico di Milano, Milan, 1992.

[2] M. Dorigo, V. Maniezzo, and A. Colorni, "The ant system: an autocatalytic optimizing process," Milan: Politecnico di Milano, Milan, 1991.

[3] M. Dorigo, V. Maniezzo, and A. Colorni, "Ant system: optimization by a colony of cooperating agents," In *IEEE transactions on systems, man, and cybernetics. Part B, Cybernetics: a publication of the IEEE Systems, Man, and Cybernetics Society* 26 (1), pp. 29–41, 1996, doi: https://doi.org/10.1109/3477.484436.

[4] T. Nakagaki, "Smart behavior of true slime mold in a labyrinth," *Res. Microbiol.* 152 (9), pp. 767–770, 2001, doi: https://doi.org/10.1016/S0923-2508(01)01259-1.

[5] T. Nakagaki, R. Kobayashi, Y. Nishiura, and T. Ueda, "Obtaining multiple separate food sources: Behavioural intelligence in the *Physarum* plasmodium," *Proc. Biol. Sci.* 271 (1554), pp. 2305–2310, 2004, doi: https://doi.org/10.1098/rspb.2004.2856.

[6] T. Nakagaki, H. Yamada, and A. Tóth, "Maze-solving by an amoeboid organism," *Nature* 407 (6803), p. 470, 2000, doi: https://doi.org/10.1038/35035159.

[7] C. Gao, C. Liu, D. Schenz, X. Li, Z. Zhang, M. Jusup, et al., "Does being multi-headed make you better at solving problems? A survey of *Physarum*-based models and computations," *Phys. Life Rev.* 29, pp. 1–26, 2019, doi: https://doi.org/10.1016/j.plrev.2018.05.002.

[8] C. R. Reid, T. Latty, A. Dussutour, and M. Beekman, "Slime mold uses an externalized spatial "memory" to navigate in complex environments," *Proc. Natl. Acad. Sci.* USA, 109 (43), pp. 17490–17494, 2012, doi: https://doi.org/10.1073/pnas.1215037109.

[9] M. Bastian, S. Heymann, and M. Jacomy, "Gephi: An Open Source Software for Exploring and Manipulating Networks," *ICWSM* 3 (1), pp. 361–362, 2009, doi: https://doi.org/10.1609/icwsm.v3i1.13937.

[10] D. Himmelstein, "Biologically inspired designs for restoring power transmission after an electromagnetic pulse attack," Online: https://figshare.com/articles/journal_contribution/Biologically_inspired_designs_for_restoring_power_transmission_after_an_electromagnetic_pulseattack/1488841?file=2182796

[11] A. Awad, W. Pang, D. Lusseau, and G. M. Coghill, "A survey on physarum polycephalum intelligent foraging behaviour and bio-inspired applications," *Artif. Intell. Rev.* 56 (1), pp. 1–26, 2023, doi: https://doi.org/10.1007/s10462-021-10112-1.

[12] J. D. Sweatt, Mechanisms of memory, 2nd ed. Amsterdam: Academic Press, 2010, Online: https://ebookcentral.proquest.com/lib/kxp/detail.action?docID=583431.

[13] C. Durham and E. B. Ridgway, "Control of chemotaxis in *Physarum polycephalum*," *J. Cell Biol.* 69 (1), pp. 218–223, 1976, doi: https://doi.org/10.1083/jcb.69.1.218.

[14] T. Latty and M. Beekman, "Irrational decision-making in an amoeboid organism: transitivity and context-dependent preferences," *Proc. Biol. Sci.* 278 (1703), pp. 307–312, 2011, doi: https://doi.org/10.1098/rspb.2010.1045.

[15] E. Sinanović, "Simulation and mobility planning with a slime mold based algorithm," Master Thesis. Alpen Adria University of Klagenfurt, Klagenfurt am Wörthersee, 2022, Online: https://netlibrary.aau.at/obvuklhs/download/pdf/8504854, checked on 10/9/2025.

[16] K. Wogatai, "SISMO (SImulation of Slime MOlds): a slime mold based algorithm and its application in traffic management," Master Thesis. Alpen Adria University of Klagenfurt, Klagenfurt am Wörthersee, 2022, Online: https://netlibrary.aau.at/obvuklhs/download/pdf/8440422, checked on 10/9/2025.

[17] S. Li, H. Chen, M. Wang, A. A. Heidari, and S. Mirjalili, "Slime mould algorithm: A new method for stochastic optimization," *Future Gener. Comput. Syst.* 111, pp. 300–323, 2020, doi: https://doi.org/10.1016/j.future.2020.03.055.

[18] E. Sinanović and K. Wogatai, "SISMO," Klagenfurt am Wörthersee: GitHub, Online: https://github.com/barlum15/SISMO, checked on 10/9/2025.

[19] V. Bonifaci, K. Mehlhorn, and G. Varma, "Physarum can compute shortest paths," *J. Theor. Biol.* 309, pp. 121–133, 2012, doi: https://doi.org/10.1016/j.jtbi.2012.06.017.

[20] F. S. Caparrini, "A General A* Solver in NetLogo," University of Seville, Seville, 2018, Online: https://www.cs.us.es/~fsancho/Blog/posts/General_A_Solver_NetLogo.md.html, checked on 10/9/2025.

[21] K. Wogatai, J. Winkler, and W. Elmenreich, "A Graph-Based Approach for Applying Biologically-Inspired Slime Mold Algorithms for Repairing a Power Transmission Network after an Electromagnetic Pulse Attack," In: *2023 2nd International Conference on Power Systems and Electrical Technology (PSET)*, Milan, Italy, 2023, pp. 163–172. doi: https://doi.org/10.1109/PSET59452.2023.10346595.

[22] Landes Rechnungshof Kärnten, "Kärnten Netz - Stromnetztarife und Herausforderungen. Landes Rechnungshof Kärnten," Klagenfurt am Wörthersee, 2020, Online: https://lrh-ktn.at/berichte/kaernten-netz/, checked on 10/9/2025.

[23] Tero, S. Takagi, T. Saigusa, K. Ito, D. P. Bebber, M. D. Fricker, et al., "Rules for biologically inspired adaptive network design," *Science* 327 (5964), pp. 439–442, 2022, doi: https://doi.org/10.1126/science.1177894.

ABOUT THE AUTHORS

Kristina Wogatai
Networked and Embedded Systems
University of Klagenfurt, Austria kristina.wogatai@aau.at

Emir Sinanović
Networked and Embedded Systems
University of Klagenfurt
Austria

Wilfried Elmenreich
Networked and Embedded Systems
University of Klagenfurt
Austria

BACK TO CONTENT

Supplementary Material

Supplementary Tab. 1

No.	Location
1	Klagenfurt main station
2	Grafenstein
3	St. Veit a.d. Glan
4	St. Martin-Sittich
5	Gummern
6	Villach main station
7	Rosenbach

Supplementary Tab. 2

No.	Location
1	Heiligengeistplatz
2	Hauptbahnhof
3	Jergitschsteg
4	Steinerne Brücke
5	Luegerstraße
6	Universität Klagenfurt
7	Lakeside Park
8	Klagenfurt West

Supplementary Tab. 3

No.	Location	No.	Location
1	KUSW Außerfragant	33	USW Kirchengasse Klagenfurt
2	KUSW Feistritz	34	USW Klagenfurt Nord
3	KUSW Freibach	35	USW Klagenfurt Ost
4	KUSW Innerfragant	36	USW Klagenfurt West
5	KUSW Koralpe	37	USW Kleinkirchheim
6	KUSW Lavamünd	38	USW Landskron
7	KUSW Malta Hauptstufe	39	USW Lassendorf
8	KUSW Malta Unterstufe	40	USW Lienz
9	KUSW Schwabeck	41	USW Lieserhofen
10	KUSW Zirknitz	42	USW Oberdrauburg
11	KW Annabrücke	43	USW Obersielach
12	KW Edling	44	USW Radenthein
13	KW Feldsee	45	USW Rennweg
14	KW Forstsee	46	USW Seebach
15	KW Malta Oberstufe	47	USW Spittal
16	KW Reißeck	48	USW St. Andrä
17	KW Rosegg	49	USW St. Leonhard
18	KW Wölla	50	USW St. Margarethen
19	USW Auen	51	USW St. Martin
20	USW Bleiburg	52	USW St. Veit
21	USW Brückl	53	USW Steinfeld
22	USW Ettendorf	54	USW Treibach
23	USW Feldkirchen	55	USW Tröpolach
24	USW Ferlach	56	USW Villach Süd
25	USW Fürnitz	57	USW Vorderberg
26	USW Gallitz	58	USW Völkermarkt
27	USW Gmünd	59	USW Warmbad
28	USW Greuth	60	USW Wietersdorf
29	USW Gummern	61	USW Windischbach
30	USW Gurk	62	USW Wolfsberg
31	USW Hermagor	63	USW Würmlach
32	USW Kamering		

SUPPLEMENTARY TABLE 1
List of selected Stations of ÖBB.
Source: adapted from Table 6.1 [16]

Ergänzende Tabelle 1:
Liste der ausgewählten Stationen der ÖBB. Quelle: angepasst nach Tabelle 6.1 [16]

SUPPLEMENTARY TABLE 2
List of selected Stations of KMG Bus Line
Source: adapted from Table 6.2 [16]

Ergänzende Tabelle 2:
Liste der ausgewählten Stationen der KMG-Buslinie C. Quelle: angepasst nach Tabelle 6.2 [16]

SUPPLEMENTARY TABLE 3
List of relevant Power Plants and Substations of the Carinthian Transmission Network. Adapted from [22]

Ergänzende Tabelle 3:
Liste der relevanten Kraftwerke und Umspannwerke des Kärntner Übertragungsnetzes. Angepasst nach [22]

Short Articles

Predictive maintenance in infrastructure: Utilizing 3D point clouds for efficient damage detection

Christina Petschnigg, Alexander Pamler, Kazim Onur Arisan, Jan Morten Loës, Torsten Ullrich

ABSTRACT

Growing urbanization is driving the demand for infrastructure such as parking lots, roads, and bicycle lanes. While green spaces and trees are often integrated into these development projects to mitigate negative climate impacts, they can cause root-related damage that poses safety risks and requires costly monitoring. Public road networks are typically inspected with advanced but expensive surveillance vehicles that are too costly for private applications, leaving private infrastructure such as parking lots, private roads, and storage areas without comparable solutions. Thus, this paper presents a methodology for detecting and classifying damage areas in 3D point clouds of parking lots, distinguishing root-related damage from construction joints using a combination of deep learning and classical statistics. The approach is evaluated on data from Vienna International Airport and validated against manually labeled ground truth data. Results show that accurate localization and classification of damage is feasible using only a single laser scanner, providing a cost-effective alternative to conventional monitoring. Moreover, the method facilitates predictive maintenance by automatically detecting damage and enabling integration into Building Information Modeling software.

Vorausschauende Instandhaltung von Infrastruktur: Effiziente Schadensdetektion mithilfe von 3D-Punktwolken

ZUSAMMENFASSUNG

Die wachsende Urbanisierung erhöht die Nachfrage nach Infrastruktur wie Parkplätzen, Straßen und Radwegen. Grünflächen und Bäume werden häufig in diese Entwicklungsprojekte integriert, um negative Effekte des Klimawandels abzumildern. Allerdings können diese wurzelbedingte Schäden verursachen, die Sicherheitsrisiken bergen und eine kostenintensive Überwachung erfordern. Das öffentliche Straßennetz wird in der Regel mit fortschrittlichen, jedoch teuren Überwachungsfahrzeugen inspiziert, die für private Infrastruktur wie Parkplätze, Privatstraßen und Lagerflächen zu kostspielig sind. Daher wird in diesem Paper eine Methodik zur Erkennung und Klassifizierung von Schäden in 3D Punktwolken von Parkplätzen vorgestellt, bei der wurzelbedingte Schäden mithilfe einer Kombination aus Deep Learning und klassischer Statistik von Baufugen unterschieden werden. Der Ansatz wird anhand von Daten des Flughafens Wien evaluiert und mit manuell annotierten Ground-Truth-Daten validiert. Die Ergebnisse zeigen, dass eine präzise Lokalisierung und Klassifizierung von Schäden mit einem einzelnen Laserscanner möglich ist, was eine kostengünstige Alternative zu herkömmlichen Monitoringverfahren darstellt. Darüber hinaus unterstützt die vorgeschlagene Methode Predictive-Maintenance-Maßnahmen, indem Schäden automatisch erkannt und in Building Information Modeling-Software integriert werden können.

KEYWORDS

- 3D point cloud
- tree roots
- predictive maintenance
- damage detection

INTRODUCTION

Since 2008, more than half of the global population lives in urban areas, a proportion that is expected to increase to 68% by 2050 [1]. While urbanization drives economic and social progress, it also increases soil sealing, impacting the environment and society [2]. The expansion of impervious surfaces – such as roads, buildings, and parking lots – at the expense of green and open spaces is a global trend with profound environmental consequences. It exacerbates the effects of heavy rainfall by contributing to flooding and also intensifies the urban heat island effect. A common strategy to mitigate these effects is incorporating green spaces, especially trees, into sealed areas, as they promote cooling [3], water evaporation, air purification [4], and hydrological protection [5]. While essential for addressing climate change-related challenges, plant and root growth can damage infrastructure, causing cracks or bulges in surfaces. Consequently, systematic infrastructure monitoring and inspection are essential for early damage detection and predictive maintenance, enabling cost-effective repairs, reducing accident risks, extending infrastructure lifespan, and enhancing public safety. However, these monitoring and inspection efforts demand substantial time and financial resources from infrastructure operators.

 https://doi.org/10.71911/cii-p3-nt-2025223

A significant portion of infrastructure, including parking lots, roads, and bike lanes, is publicly owned and is monitored using expensive surveillance vehicles. While effective for inspections, their high cost makes them inaccessible to private sector organizations, businesses, and operators of commercial or private infrastructure who are responsible for managing and maintaining private roads, parking lots, and other outdoor spaces. Consequently, inspecting infrastructure in these settings presents a more significant challenge. Recent studies on low-cost road and infrastructure inspections mainly utilize two-dimensional (2D) images, as they are cost-effective and easily captured with readily available devices such as smartphones [6]. However, 2D imagery lacks depth information, which limits its ability to capture detailed geometric characteristics of surface conditions. In contrast, three-dimensional (3D) point clouds provide rich geometric and color information, enabling a more comprehensive analysis, which not only improves the detection and classification of surface anomalies but also allows for a more accurate assessment of their extent. Consequently, 3D data support more informed decision-making by enabling the prioritization of maintenance tasks based on the geometric severity of the detected damage. For instance, pavement damage inspection using 3D point clouds is described in [7] and [8].

Against this background, our paper presents a cost-effective methodology for detecting and classifying damage to parking infrastructure using 3D point cloud data, acquired using a terrestrial laser scanner instead of a full surveillance vehicle. The proposed approach combines deep learning with classical statistical techniques to distinguish between damage caused by root growth and construction joints. Specifically, a PointNet-based [9] neural network is applied to segment the parking lot into relevant and non-relevant points. Damage is then identified at the relevant points through the geometric approximation of the ground surface and the classification and directional analysis of damage. Since the damage detection takes place within a georeferenced 3D point cloud, the results can be integrated directly into Building Information Modeling (BIM) systems, enabling efficient planning and management of maintenance activities. In summary, our contributions are:

- **Framework**: We propose a common framework for detecting, documenting, and classifying infrastructure damage using georeferenced 3D point cloud data. The framework segments relevant surface points and distinguishes damage caused by root growth from construction joints. This offers a more cost-efficient solution compared to the use of surveillance vehicles and delivers greater accuracy than conventional 2D image-based monitoring methods.
- **Experiment:** We assess the accuracy and completeness of damage detection by comparing the model's output with manually annotated ground truth data, using a real-world parking lot at Vienna International Airport as a test site.

MATERIALS AND METHODS

Data Collection and Pre-Processing

The study was conducted in Parking Lot D at Vienna International Airport, which spans an area of approximately 13,000 m² and is depicted in Figure 1. Data acquisition was performed using the terrestrial laser scanner VZ-400i (Riegl International GmbH, Vienna, Austria). For accurate georeferencing, existing control points in the surrounding area were additionally captured. In total, 98 scan positions were recorded and subsequently processed using RiSCAN PRO software (RIEGL Deutschland Vertriebsgesellschaft mbH, Gilching bei München, Germany) . The raw point cloud data were filtered to exclude points with reflectivity values below -25 dB or above 5 dB, as well as those with a deviation value exceeding 15. Low reflectivity often results from weak signal returns on dark or absorbent

surfaces, whereas high reflectivity may indicate sensor artifacts. Elevated deviation values typically reflect measurement noise. Filtering these outliers improves geometric accuracy for subsequent analysis and reliability. The individual scan positions were then registered relative to each other to align and merge them into a unified coordinate system. The resulting point cloud was colorized using RGB values extracted from images taken by the scanner's internal camera. Movable objects, such as vehicles and pedestrians, were removed by the software, while residual noise was manually eliminated using the Terrain Filter tool.

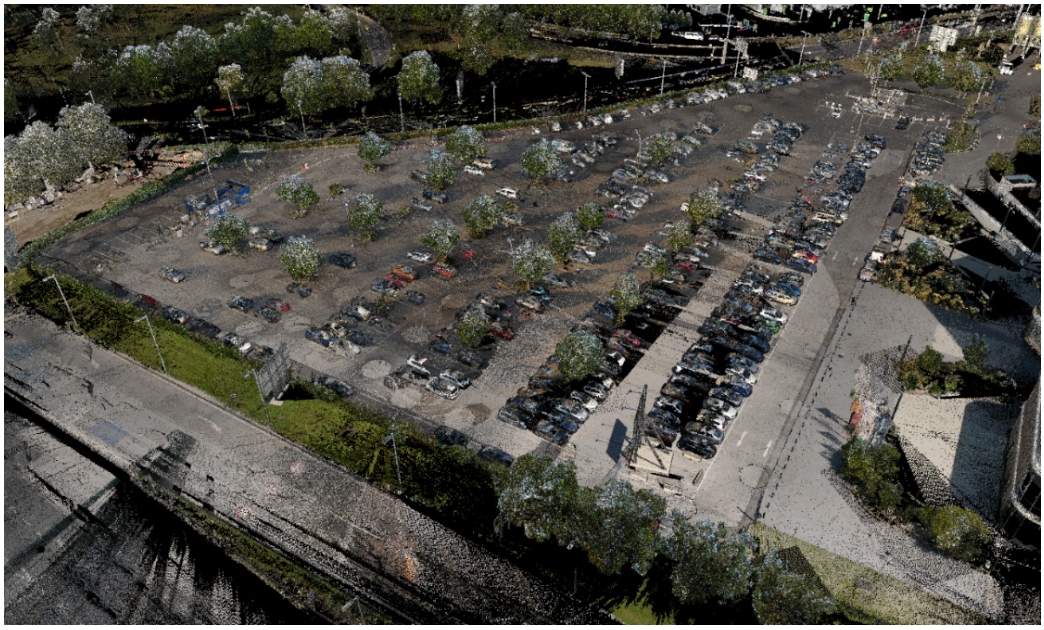


Fig. 1

Figure 1: Parking Lot D at Vienna International Airport. Source: own figure.

Abbildung 1: *Parkplatz D am Flughafen Wien. Quelle: eigene Abbildung.*

The consolidated point cloud with a resolution of 1 cm was imported into the software program CloudCompare [10] for further refinement. Statistical outlier removal was conducted to further eliminate noise points that compromise the integrity of the dataset. Subsequently, the point cloud was manually annotated to assign each point to one of the classes: ground, tree, low vegetation, and car. Figure 2 presents the point cloud of the test site at Vienna International Airport in two formats: one representing the cleaned data and the other depicting the class labels.

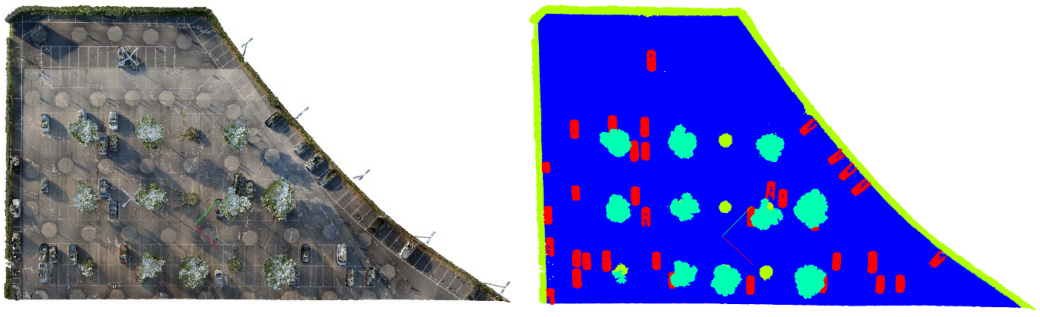


Fig. 2

Figure 2: Cleaned (left) and labeled (right) point cloud of the test site at the Vienna International Airport. Source: own figure.

Abbildung 2: *Gesäuberte (links) und klassifizierte (rechts) Punktwolke des Testgeländes am Flughafen Wien. Quelle: eigene Abbildung.*

Model Implementation and Training

Our methodology comprises three primary steps: 1) segmentation of the point cloud to identify relevant features (such as ground, vegetation, and trees) for further analysis, while excluding irrelevant points (such as vehicles); 2) tree documentation and damage detection, which leverages geometric features such as positive and negative protrusions

to identify surface anomalies; and 3) classification and documentation of the identified areas of damage, distinguishing between those caused by root growth and construction joints. Future research will extend this analysis to include additional damage types, such as those induced by heavy usage or freeze-thaw cycles, including potholes and subsidence.

Segmentation

In the first step, we employ deep learning techniques for automatic point cloud segmentation. Specifically, we adopt a PointNet-based approach [9], which processes raw point cloud data directly [11], eliminating the need for intermediate steps like voxelization [12] or 2D image conversion [13]. To improve computational efficiency, the point cloud is first down-sampled using uniform grid sampling and then split into training (≈70%), validation (≈20%), and testing (≈10%) sets. The PointNet-based model is implemented using Python's PyTorch framework [14] and is trained for 100 epochs on a GeForce RTX 3090 GPU (NVIDIA Corporation, Santa Clara, CA, USA) for parameter optimization. Post-inference inaccuracies, which primarily result from limited training data and labeling noise, are reduced using a multi-step refinement of car and vegetation detection. Initially, the inference results are projected onto a 2D bird's-eye view of the scene, where the respective objects are delineated through density-based clustering. The boundaries of these regions are subsequently refined, and the corrected segmentations are reprojected into the 3D point cloud to enhance spatial accuracy. Subsequently, all detected vehicles are removed from the dataset, as they are not relevant for assessing ground surface damage.

Damage Detection

In the second step, tree positions are extracted from the segmented "tree" point cloud. Individual trees are identified and isolated using density-based clustering. The position of each tree is defined as the ground-level coordinate located at the center of the tree stem. This georeferenced information can be directly integrated into a BIM system, which is increasingly important in a smart facility planning context, where accurate, up-to-date models of both built and natural assets are essential. Such integration helps in assessing risks related to root intrusion, visibility obstructions, and vulnerability to storms.

The segmented point clouds corresponding to the "ground" and "vegetation" classes are further analyzed. The ground point clouds are divided into disjoint square regions for ground plane approximation. Within each subdivision, a fourth-degree polynomial regression model is applied to capture nonlinearities in the data, such as surface irregularities. To ensure robustness against outliers, a RANSAC (Random Sample Consensus) regressor is employed. This process generates a fourth-degree polynomial function for each square segment of the ground, which models its complex and uneven surface. The resulting surfaces are then connected using bicubic interpolation, providing a smooth and continuous approximation of the entire ground surface. This approximation facilitates the identification of damage, with root-induced defects manifesting as positive protrusions and construction joints corresponding to either positive or negative protrusions. These deviations are identified by comparing the point cloud data to the approximated ground surface.

Damage Classification

In the third step, we differentiate whether the identified areas of damage are caused by tree root growth or construction. This involves a detailed analysis of the damage structure. Initially, individual damage areas are delineated from one another. The point

cloud is then converted into a graph representation using a k-d tree, which is a data structure optimized for efficient nearest-neighbor searches and partitioning of points in k-dimensional spaces. Each connected component in the point cloud is initially assigned to a single area of damage. However, due to the inherent incompleteness of point clouds, collinear areas of damage are merged, as missing points often cause discontinuities that actually represent one single contiguous area of damage. After this merging process, areas of damage are classified based on their geometric properties. Root-induced damage tends to be curved and aligns with the direction of the recorded tree positions, distinguishing them from linear construction joints, which are typically straight. Other damage types, such as potholes, were not present in the test data.

RESULTS

As outlined in the previous section, the proposed infrastructure monitoring framework consists of three main stages: segmentation of the point cloud, documentation of trees and detection of damage, and subsequent damage classification. To ensure a comprehensive evaluation of the framework's effectiveness, each stage is assessed independently. As previously mentioned, the evaluation is conducted on Parking Lot D at Vienna International Airport.

Segmentation Results

Training and optimizing the PointNet-based neural network over 100 epochs on the training set—which includes approximately two rows of the parking area—yielded a point-wise accuracy of 97.16% on the training data and 95.32% on the validation data. Evaluation of the unseen test area, which corresponds to a short parking row, resulted in a point-wise accuracy of 92.61%. Table 1 summarizes the corresponding per-class accuracies and the mean Intersection over Union (mIoU) for each class. Qualitative visualization of the segmentation results is provided in Figure 3. The model demonstrated a strong ability to distinguish between the predefined classes, with particularly high separability observed for the "ground" and "tree" classes. However, due to the limited extent of the training data and some labeling noise in the "vegetation" and "ground" classes, the segmentation exhibited inaccuracies at class boundaries, especially between the classes "car", "ground", and "vegetation". These boundary ambiguities were subsequently mitigated by incorporating geometric features of the point cloud, as described in the previous section, resulting in the refined segmentation illustrated in Figure 4 and yielding an overall classification accuracy of 97.74% on the test set.

Tab. 1

	After Segmentation		After refinement	
Class	**Class Accuracy**	**IoU**	**Class Accuracy**	**IoU**
Ground	0.944	0.925	0.999	0.978
Tree	0.943	0.921	0.989	0.963
Vegetation	0.726	0.644	0.739	0.704
Car	0.824	0.602	0.917	0.916

Table 1: Class accuracy and class IoU after segmentation and refinement.

Tabelle 1: *Class Accuracies und Class IoU nach der Segmentierung und Verfeinerung.*

Damage Detection

As tree detection is performed through straightforward density-based clustering on a clearly distinguishable point cloud class, it was considered a trivial task in this context

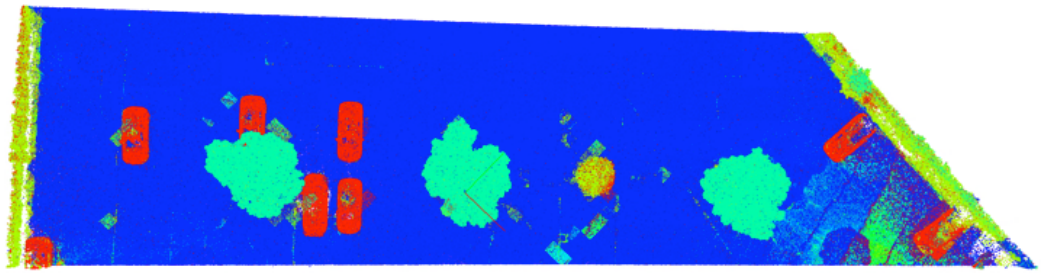


Fig. 3

Figure 3: Qualitative segmentation results on the test data set. Source: own figure.

Abbildung 3: *Qualitative Segmentierungsergebnisse auf dem Testdatensatz. Quelle: eigene Abbildung.*

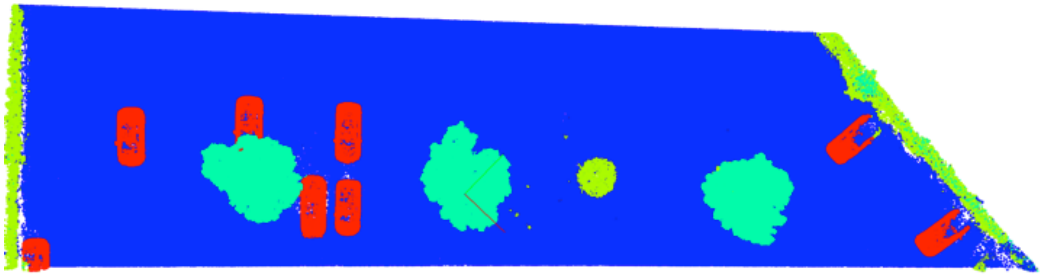


Fig.4

Figure 4: Qualitative segmentation results on the test data set after refinement. Source: own figure.

Abbildung 4: *Qualitative Segmentierungsergebnisse auf dem Testdatensatz nach der Verfeinerung. Quelle: eigene Abbildung.*

and therefore not subject to quantitative evaluation.

The previously described method, which detects damage by analyzing deviations between the point cloud and the approximated ground surface, effectively localized damaged regions, achieving a mutual overlap of 95.9% with manually annotated ground truth data. The overlap was calculated by measuring nearest-neighbor distances between points in both point clouds, with overlap defined as points within a distance threshold set at 1% of the bounding box diagonal. The mutual overlap ratio was computed by averaging the directional overlaps from each cloud to the other. Figure 5 presents a comparison between manually labeled damage and examples of damage identified by the system. Overlapping points are shown in green, while red and blue points represent those unique to the ground truth and system output, respectively. Although the overall overlap was high, our method occasionally failed to detect fine construction joints characterized by subtle negative surface deviations. In contrast, it demonstrated high sensitivity to positive protrusions, detecting root-induced damage with high accuracy.

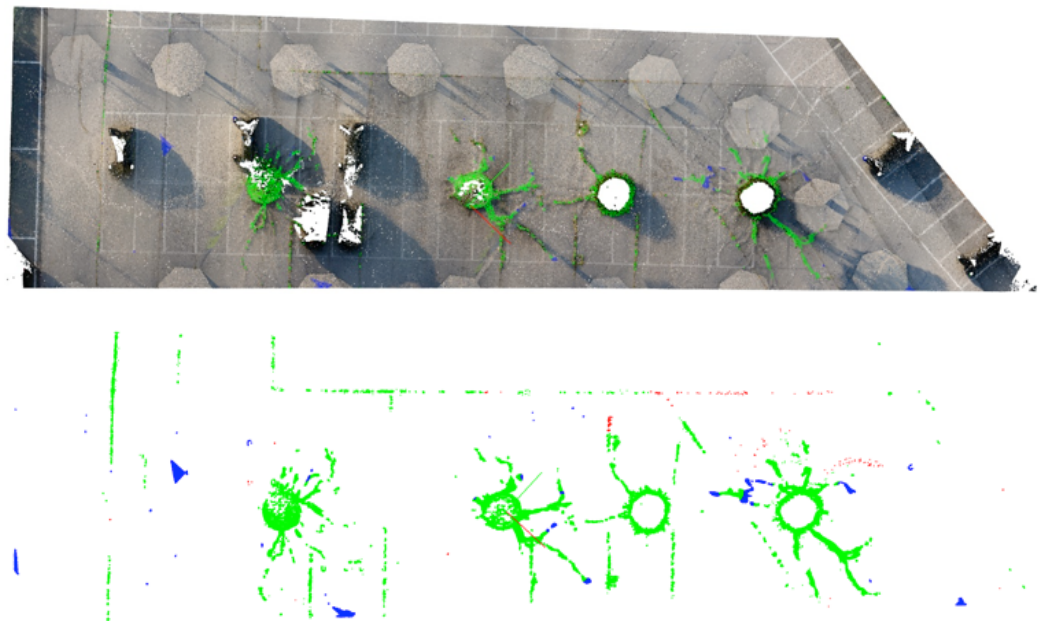


Fig. 5

Figure 5: Comparison of ground truth and detected damage. Overlapping points are shown in green, while red and blue indicate points unique to the ground truth and system output, respectively. Full point cloud (top), damage only (bottom). Source: own figure.

Abbildung 5: *Vergleich von manuell erkannten und automatisch detektierten Schadstellen. Überlappende Punkte sind in Grün dargestellt, Rot und Blau zeigen jeweils Punkte, die ausschließlich in der Ground Truth bzw. in der Auswertung enthalten sind. Gesamte Punktwolke (oben), nur Schäden (unten). Quelle: eigene Abbildung.*

Damage Classification

Subsequently, individual areas of damage were classified based on their geometric characteristics to differentiate between curved, root-induced damage and the typically linear patterns associated with construction-related damage. Figure 6 illustrates the qualitative results of the classified damage, where root-induced damage is visualized in red and construction joints in green. The overall classification achieved an accuracy of 95.15%. The accuracy was determined by establishing spatial correspondence between the predicted and ground truth point clouds. This was achieved by identifying the nearest neighbor in the ground truth for each point in the predicted dataset using a k-d tree. Since the point clouds differed in sampling density and exhibited spatial deviations between predictions and annotations, they also differed in the number of points, making one-to-one correspondence infeasible. Consequently, the nearest-neighbor approach offered a robust solution for establishing spatial correspondence and evaluating geometric overlap between the two datasets.

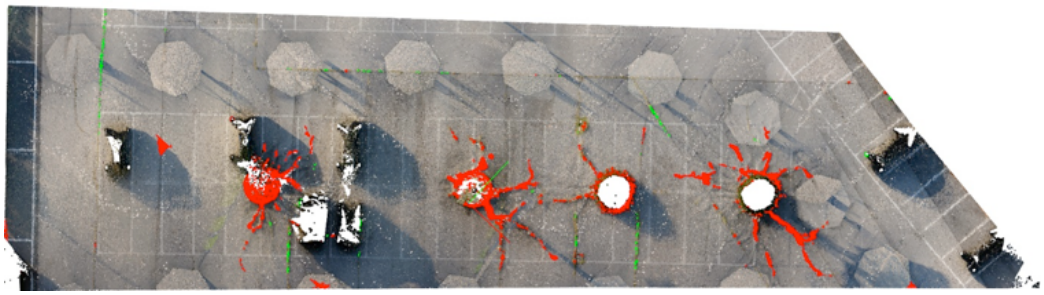


Fig. 6

Figure 6: Qualitative results of damage classification. Root-induced damage is depicted in red, while construction joints are shown in green. Source: own figure.

Abbildung 6: *Qualitative Ergebnisse der Schadensklassifikation. Wurzelschäden sind in Rot dargestellt, während Baufugen in Grün dargestellt werden. Quelle: eigene Abbildung.*

DISCUSSION AND CONCLUSION

This study presents a low-cost and scalable methodology for detecting and classifying surface-level infrastructure damage using 3D point cloud data. Our framework represents a significant advancement in making infrastructure monitoring more accessible. By eliminating the need for expensive surveillance vehicles and relying instead on terrestrial laser scanners and point cloud processing, it enables smaller organizations and private entities to conduct reliable, automated inspections. This has the potential to improve predictive and preventive maintenance efforts as well as safety, especially in private parking lots, campuses, and commercial zones. Moreover, preliminary estimates indicate that surveying with terrestrial laser scanning is significantly more cost-efficient per square meter than vehicle-based systems, while simultaneously providing richer geometric information than low-cost 2D imaging methods.

The segmentation results demonstrated high accuracy (>92%) even in unseen test areas, affirming the effectiveness of the neural network approach in extracting relevant infrastructure features from raw point cloud data. However, challenges remain—particularly at the boundaries of segmented classes—where label ambiguity and point cloud noise can impair performance. The subsequent damage detection and classification processes effectively differentiated between root-induced and construction-related damage, achieving high detection overlap (95.9%) and classification accuracy (95.15%).

The results presented in the paper demonstrate that the proposed method achieves high accuracy in damage detection in the test area, particularly in detecting root-induced damage. Another notable aspect is the integration of the methodology with BIM systems, which supports more effective predictive maintenance planning. By classifying and documenting both root-induced surface damage and construction joints, the approach

facilitates the development of a holistic digital representation of a facility, including maintenance-relevant information for outdoor infrastructure. Overall, the findings suggest that the proposed methodology constitutes a promising and cost-effective solution for infrastructure monitoring.

Nonetheless, there remains potential for improvement, especially in refining the segmentation of complex surfaces, improving the detection of subtle construction-related damage, and extending the framework to accommodate a broader range of damage types. Despite the high overall accuracy, the segmentation process exhibited limitations, particularly in handling ambiguities at class boundaries—most notably between the classes "car", "ground", and "vegetation". These issues are expected to be mitigated in future work through an expanded and more diverse dataset, which will provide the deep learning model with increased variability and improved generalization. Additional improvements will focus on extending the framework's capabilities to include further damage types, such as those resulting from heavy mechanical wear or environmental effects like freeze-thaw cycles—an effort that will also benefit from a larger dataset. Furthermore, the damage detection component showed reduced sensitivity to subtle construction joints, including fine cracks and slight surface depressions, which the current approach struggles to detect. To address this, future developments will incorporate additional data types, such as image data, into the analysis pipeline. The inclusion of visual information is expected to enhance the detection and validation of fine cracks. Additionally, the current method of data collection—terrestrial laser scanning—is time-consuming. The substitution of terrestrial scanners with drone-based surveys offers a promising alternative to reduce acquisition time and increase coverage; however, it may introduce additional sources of error like motion artifacts or positional inaccuracies that must be considered. Moreover, the application of semi-supervised learning techniques can help alleviate the annotation workload and enable better generalization across diverse surface types and environmental conditions.

While the Vienna International Airport parking lot provided a controlled environment for testing, the applicability of the proposed method to more safety-critical areas of airport infrastructure—particularly runways and taxiways, where surface integrity is essential for safe aircraft operations—remains a subject for future investigation. Beyond the aviation domain, the methodology can be adapted for a wide range of outdoor infrastructure applications, including bridges, building exteriors, and industrial sites. This versatility, in combination with the system's cost-efficiency, positions the framework as a valuable instrument for proactive infrastructure monitoring and maintenance.

ACKNOWLEDGEMENTS

The research was funded by the Austrian Research Promotion Agency (FFG) within the project "AMAzE 2.0" (#897833).

REFERENCES

[1] United Nations Department of Economic and Social Affairs, "2018 Revision of World Urbanization Prospects," United Nations, Department of Economic and Social Affairs, 2019

[2] R. Scalenghe and F. A. Marsan, "The anthropogenic sealing of soils in urban areas," *Landscape and Urban Planning*, vol. 90, no. 1-2, p. 1–10, 2009, doi: 10.1016/j.landurbplan.2008.10.011

[3] Z. Ring, D. Damyanovic and F. Reinwald, "Green and open space factor Vienna: A steering and evaluation tool for urban green infrastructure," *Urban Forestry & Urban Greening*, vol. 62, p. 127131, 2021, doi: 10.1016/j.ufug.2021.127131

[4] S. Jaafari, A. Shabani, M. Moeinaddini, A. Danehkar and Y. Sakieh, "Applying landscape metrics and structural equation modeling to predict the effect of urban green space on air pollution and respiratory mortality in Tehran," *Environmental Monitoring and Assessment*, vol. 192, no. 412, 15 p., 2020, doi: 10.1007/s10661-020-08377-0

[5] L. Sturiale and A. Scuderi, "The role of green infrastructures in urban planning for climate change adaptation," *Climate*, vol. 7, no. 10, p. 119, 2019, doi: 10.3390/cli7100119

[6] H. Maeda, Y. Sekimoto, T. Seto, T. Kashiyama and H. Omata, "Road damage detection and classification using deep neural networks with smartphone images," *Computer-Aided Civil and Infrastructure Engineering*, vol. 33, no. 12, p. 1127–1141, 2018, doi: 10.1111/mice.12387

[7] M. E. Mohammadi, D. P. Watson and R. L. Wood, "Deep learning-based damage detection from aerial SfM point clouds," *Drones*, vol. 3, no. 3, p. 68, 2019, doi: 10.3390/drones3030068

[8] Z. Feng, A. El Issaoui, M. Lehtomäki, M. Ingman, H. Kaartinen, A. Kukko, et al., "Pavement distress detection using terrestrial laser scanning point clouds – Accuracy evaluation and algorithm comparison," *ISPRS Open Journal of Photogrammetry and Remote Sensing*, vol. 3, p. 100010, 2022, doi: 10.1016/j.ophoto.2021.100010

[9] C. Petschnigg, M. Spitzner, L. Weitzendorf and J. Pilz, "From a point cloud to a simulation model—Bayesian segmentation and entropy based uncertainty estimation for 3D modelling," *Entropy*, vol. 23, no. 3, p. 301, 2021, doi: 10.3390/e23030301

[10] CloudCompare, version 2.14, CloudCompare, available: https://www.cloudcompare.org/release/, 2025

[11] R. Q. Charles, H. Su, M. Kaichun, and L. J. Guibas, "PointNet: deep learning on point sets for 3D classification and segmentation," in *2017 IEEE Conference on Computer Vision and Pattern Recognition (CVPR)*, pp. 77-85, 2017, doi: 10.1109/CVPR.2017.16

[12] C. Choy, J. Gwak, and S. Savarese, "4D spatio-temporal convnets: Minkowski convolutional neural networks," in *2019 IEEE/CVF Conference on Computer Vision and Pattern Recognition (CVPR)*, pp. 3070-3079, 2019, doi: 10.1109/CVPR.2019.00319

[13] J. Deng, W. Zhou, Y. Zhang and H. Li, "From multi-view to hollow-3D: hallucinated hollow-3D R-CNN for 3D object detection," *IEEE Transactions on Circuits and Systems for Video Technology*, vol. 31, no. 12, p. 4722–4734, 2021, doi: 10.1109/tcsvt.2021.3100848

[14] A. Paszke, S. Gross, F. Massa, A. Lerer, J. Bradbury, G. Chanan, et al., "PyTorch: An imperative style, high-performance deep learning library," in *33rd Conference on Neural Information Processing Systems*, 12 p., 2019, doi: 10.48550/arXiv.1912.01703

ABOUT THE AUTHORS

Christina Petschnigg
Fraunhofer Austria Research GmbH, Klagenfurt
E-Mail: christina.petschnigg@fraunhofer.at

Alexander Pamler
Fraunhofer Austria Research GmbH, Graz

Kazim Onur Arisan
VIE Build GmbH, Vienna

Jan Morten Loës
VIE Build GmbH, Vienna

Torsten Ullrich
Fraunhofer Austria Research GmbH, Graz

BACK TO CONTENT

Assessing forest structure with LiDAR: A method benchmark in the Rohrach Natural Forest Reserve

Larissa Posch, Hanns Kirchmeir, Klaus Steinbauer, Markus Hollaus

ABSTRACT

The Rohrach Natural Forest Reserve, located in the northern foothills of the Alps, serves as a long-term reference area for preserving and studying natural forest development. In this study, three methods for assessing forest structure—classical field-based inventory, terrestrial laser scanning (TLS), and drone-based LiDAR (UAV-LS)—were systematically compared. Building on an initial survey conducted in 1996, 44 sample plots were revisited and supplemented with high-resolution 3D measurements.

The results show that TLS provides highly accurate volume estimates that closely match those obtained through the classical inventory. The UAV-based approach enabled a comprehensive, area-wide survey of the 48-ha study site and yielded average growing stock values of 547 m³/ha—almost identical to those from the classical inventory (549 m³/ha). However, automated detection of lying deadwood using UAV data underestimated the volume by up to 50% compared to the line intersect method. Whether this discrepancy is due to the line intersect method's assumption of randomly distributed logs being unsuitable for this site, or whether UAV-LS underestimates deadwood due to canopy shadowing or algorithmic omission of fine structures, requires further investigation.

The study also highlights persistent challenges in tree segmentation within steep or densely vegetated areas: overlapping crowns often result in misclassifications or undetected stems. While TLS continues to offer the highest geometric accuracy, UAV-LS provides the advantage of rapid, large-scale data acquisition with minimal disturbance to sensitive environments.

These findings underscore the importance of integrated methodological approaches for effective long-term monitoring in natural forest ecosystems.

KEYWORDS

- forest structure analysis
- Rohrach Natural Forest Reserve
- method benchmarking
- TLS
- LiDAR
- UAV
- Deadwood
- large woody debris
- growing stocks
- beech forest

Einsatz von LiDAR in der Waldstrukturanalyse: Methodenbenchmark im Naturwaldreservat Rohrach

ZUSAMMENFASSUNG

Das Naturwaldreservat Rohrach im nördlichen Alpenvorland dient als langfristiges Referenzgebiet zur Untersuchung der natürlichen Waldentwicklung. In dieser Studie wurden drei Methoden zur Erfassung der Waldstruktur – klassische terrestrische Inventur, terrestrisches Laserscanning (TLS) und drohnenbasiertes LiDAR (UAV-LS) – systematisch verglichen. Aufbauend auf einer Ersterhebung aus dem Jahr 1996 wurden 44 Stichprobeflächen erneut untersucht und durch hochauflösende 3D-Messungen ergänzt.

Die Ergebnisse zeigen, dass TLS sehr präzise Volumenschätzungen liefert, die mit der klassischen Inventur nahezu übereinstimmen. Die UAV-gestützte Methode wiederum ermöglichte eine vollständige flächenhafte Erhebung des 48 Hektar großen Untersuchungsgebiets und ergab mit durchschnittlich 547 m³/ha nahezu identische Vorratswerte wie die klassische Erhebung (549 m³/ha). Die automatische Erfassung von liegendem Totholz mittels UAV unterschätzte jedoch das Volumen um bis zu 50 % gegenüber der Line-Intersect-Methode. Ob die Line-Intersect-Methode, die von einer zufälligen Verteilung der Baumstämme ausgeht, für dieses Gebiet ungeeignet ist, oder ob die UAV-LS-Auswertung das Totholz aufgrund von Abschattungen unter dichten Kronendächern bzw. algorithmisch bedingten Auslassungen feiner Strukturen systematisch unterschätzt, muss in einer weiterführenden Untersuchung geklärt werden.

Zudem wird deutlich, dass Baumsegmentierungen in steilen oder dichten Beständen problematisch bleiben: Überlappende Kronenbereiche führen zu Fehlklassifikationen und übersehenen Stämmen. Während TLS nach wie vor die höchste geometrische Genauigkeit bietet, hat die UAV-LS Methode den Vorteil der flächendeckend, zeitsparenden Erfassung und der geringeren Störung empfindlicher Standorte.

Die Ergebnisse betonen die Bedeutung integrierter Methodenansätze für ein effektives Langzeitmonitoring in Naturwäldern.

INTRODUCTION

The 47.5-ha Rohrach Natural Forest Reserve (Figure 1) was established in 1992 and represents a characteristic forest ecosystem of the flysch-dominated Molasse zone in the northern fringe of the Alps. As a long-term unmanaged forest, it serves as an important ecological reference site – both for observing natural forest development processes

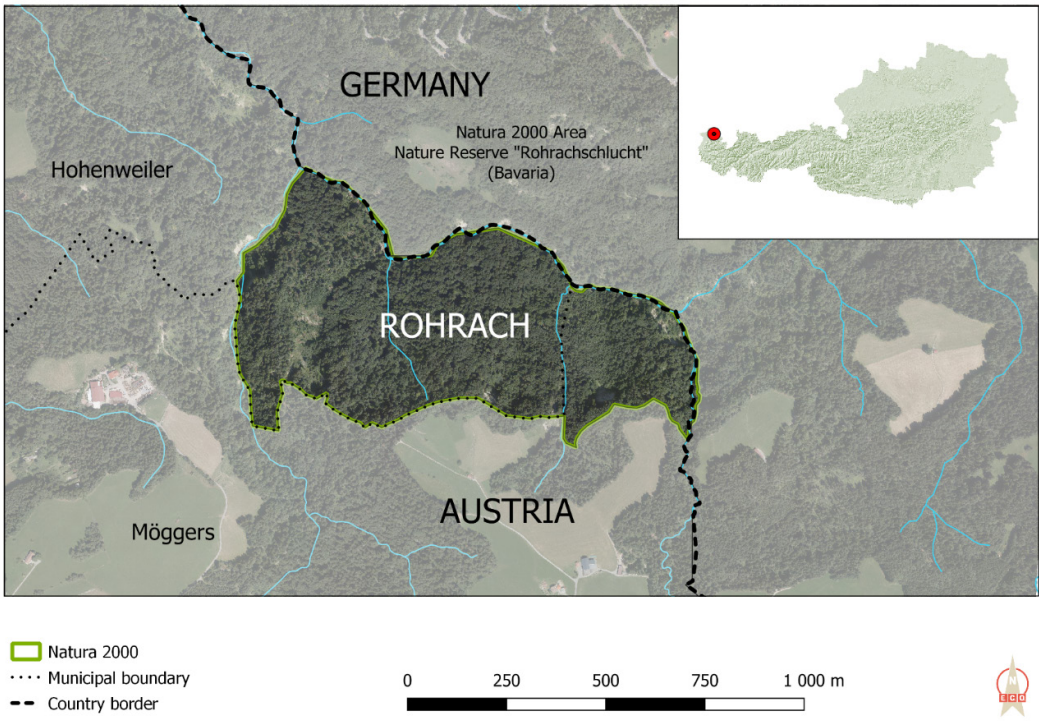


Fig. 1

Figure 1: Study area: Rohrach Natural Forest Reserve

Abbildung 1: *Untersuchungsgebiet Naturwaldreservat Rohrach*

and for deriving potential transformation pathways for managed production forests on comparable site types.

In recent years, the ecological and societal relevance of such natural forests has gained increasing attention. Against the backdrop of the global climate crisis and accelerating biodiversity loss, forests are recognized as multifunctional ecosystems of critical importance [1], [2], [3], [4], [5]. The EU Biodiversity Strategy highlights the need to exclude natural forests from utilization to secure their functions as biodiversity hotspots, carbon sinks, and long-term reference areas. Particularly in the context of the Paris Climate Agreement, forest's role in carbon sequestration and storage has become a key variable in achieving emission reduction targets.

One increasingly important concept in this context is "proforestation" – the deliberate promotion of natural forest development to maximize carbon storage, biodiversity, and other ecosystem services [6], [7]. A central question for policymakers and forest managers is how the structural transformation from managed forests to natural forests affects carbon stocks and other ecosystem functions such as recreation, protection, water retention, and biodiversity [8], [9].

In 1996, an extensive structural and geobotanical baseline survey was conducted in the Rohrach Natural Forest Reserve under the direction of Grabherr et al. [10]. The study included transect-based vegetation surveys as well as a systematic forest structure inventory on a 100 × 100 m grid, documenting tree species, deadwood, and rejuvenation. This dataset laid a solid foundation for long-term scientific monitoring of forest development following cessation of management.

In 2022, this baseline was revisited through a joint research initiative by E.C.O. Institute of Ecology and TU Wien [11]. The objective was to evaluate the performance and applicability of modern forest structure analysis methods by directly comparing them with classical inventory techniques. In addition to traditional field-based sampling, two digital technologies were tested: terrestrial laser scanning (TLS) at sample plots and high-resolution drone-based LiDAR (UAV-LS) for airborne 3D data acquisition. These

technologies enable highly detailed structural mapping of above-ground biomass, including canopy architecture, stem volume, and branch mass – particularly valuable for assessing carbon stocks in broadleaved forests [12], [13], [14], [15], [16].

Combining long-term baseline data with state-of-the-art 3D scanning techniques opens new opportunities for tracking structural and biomass changes in short monitoring cycles of 3 to 5 years. This positions the Rohrach Natural Forest Reserve not only as a reference area for natural forest dynamics, but also as a European model site for carbon stock monitoring in unmanaged forests – with a significant temporal advantage over newly designated reference areas.

METHODS

As outlined in the introduction, the forest structure survey originally conducted by Grabherr et al. [10] in 1995-96 was repeated in 2022. In the course of the follow-up study, three different methods were applied and systematically compared. These methods were:

1. classical field-based forest inventory,
2. TLS conducted within the forest, and
3. drone-based laser scanning.

In the classical field-based approach, a 100 × 100 m grid was overlaid across the entire area of the forest reserve. At each grid intersection, a sample plot was established, resulting in a total of 44 sampling locations. The center of each plot was originally marked in 1995-96 by a wooden post. In about 2/3 of the plots, this post was found again. When no post was found, GPS coordinates were used to identify the plot location.

TLS was conducted in 18 of the 44 sample plots. Due to the steep and slippery terrain in parts of the reserve, it was not feasible to transport and operate the approximately 17-kg TLS device in all locations. The complete sampling grid is shown in Figure 2. Sample plots where TLS data were successfully collected are highlighted in yellow. UAV-LS was carried out across the entire area of the reference site.

Classical field-based forest inventory

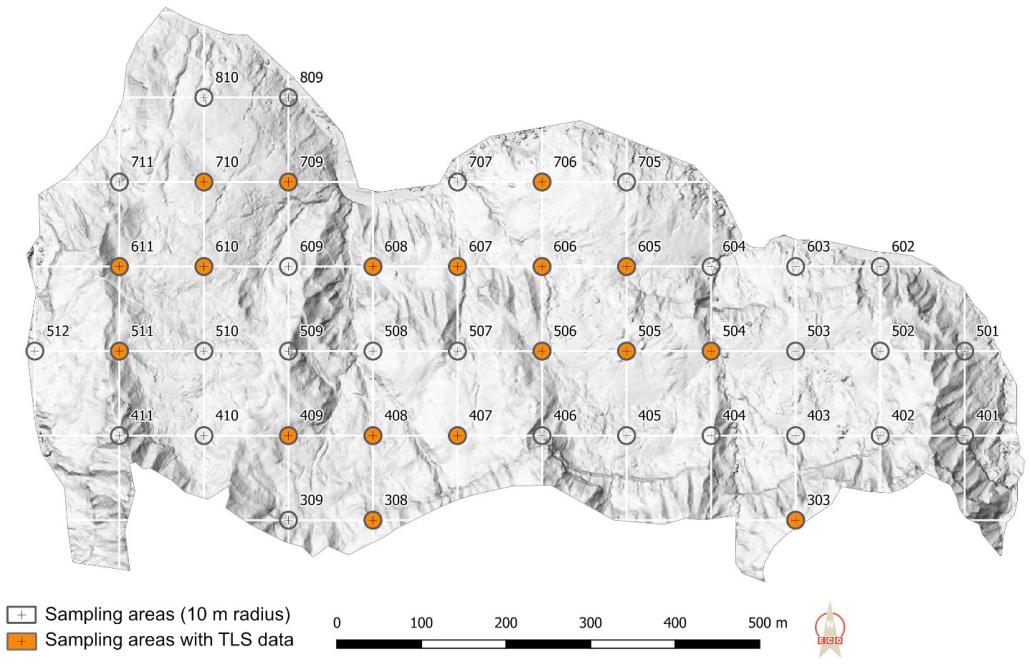


Fig. 2

Figure 2: Sampling Areas, Source: sampling grid by Grabherr et al. [10]

Abbildung 2: *Testgebiete, Quelle: Stichprobenraster übernommen von Grabherr et al. [10]*

In the classical field-based approach at each of the 44 sample areas, all trees within a 10-meter radius of the plot center were recorded. The collected data included the relative position of each tree position (angle and distance to the center of the sample), tree species, vitality status (alive or dead), and diameter at breast height (DBH). Tree height was not recorded in the field, as height measurements were later derived from TLS data. This decision was made because TLS provides significantly more accurate height estimates compared to measurements taken with a conventional forestry laser rangefinder [17].

Based on the collected field data (DBH and TLS-derived tree height), tree volume was estimated using the Denzin formula, a forestry-specific approach that incorporates height, diameter, and species-dependent form factors. This formula is used to estimate merchantable trunk volume, rather than total tree biomass. This includes timber with a diameter larger than 7 cm.

To improve height estimates for plots without TLS data, linear regression models were developed using measurements from the 18 TLS-scanned plots. The models describe the relationship between DBH and tree height using the Peterson transformation, which stabilizes variance and improves linear fit. The transformed variables were defined as:

$$x = 1/DBH \quad \text{and} \quad y = \frac{1}{\sqrt{Height - 1{,}3}}$$

Species were grouped to ensure sufficient sample sizes for regression analysis. After removing outliers caused by TLS errors or structural tree damage, regression models of the form:

$$y = b * x + a$$

were used to predict tree heights in the remaining 26 plots. These estimated heights, along with measured DBH, were then used in the Denzin formula (Table 1):

$$Vol = \left(\frac{DBH^2}{1000}\right) + \frac{DBH^2}{1000} * (Height\ - Hnorm) * Vol_Corr$$

Vol = volume in m³ of timber > 7cm diameter
DBH = Diameter at breast height in cm
Height = height of sample tree in m
Hnorm = Norm height calculated based on the tree species and the DBH

Tab. 1

Tree species	Hnorm (m)	Vol_Corr
spruce (*Picea abies*)	19+2*DBH (dm)	4%
larch (*Larix decidua*)	17+3*DBH (dm)	5%
fir (*Abies alba*)	21+DBH (dm)	4%
pine (*Pinus sylvestris*)	28	3%
beech (*Fagus sylvatica*)	25	3%
All other deciduous trees	25	3%

Table 1: Parameters to calculate norm height and correction factors for tree species

Tabelle 1: *Parameter zur Berechnung der Norm-Höhe und des Korrekturfaktors.*

In addition to recording standing live trees, the field inventory also included an assessment of lying deadwood. To quantify this, the line intersect sampling method was applied. Originally developed in North America to evaluate the fire hazard of forest floor fuels [18], this method records any piece of downed deadwood that intersects a transect line and meets or exceeds a defined minimum diameter at the point of intersection—regardless

of the piece's total length. The method has already been implemented in European forest inventories, e.g., [19].

Importantly, deadwood pieces do not need to be in contact with the ground to be recorded. Fragments that cross the transect several meters above ground, such as branches from a recently fallen crown, are also included. Additionally, dead trees leaning more than 45° from the vertical axis are classified as downed and are recorded if they intersect the transect. If a single piece of wood intersects the transect line multiple times (or intersects more than one line), each crossing is counted. Trunks that run exactly along a transect (i.e., their longitudinal axis aligns with the line) or merely touch it without intersecting the centerline are not recorded—though these cases are rare.

In this study, two 40-meter transect lines were established per plot. The transects were arranged perpendicularly and intersected at the plot center, forming a cross-shaped layout with a total sampling length of 80 meters, as recommended by Fraver et al. [20]. On sloped terrain (slope > 5%), one transect was aligned parallel to the contour lines, while the other followed the slope line (upslope and downslope). In flat terrain (slope < 5%), the transects were oriented along cardinal directions: north–south and east–west.

In our fieldwork, it proved practical to work with true distances (slope distances) measured in whole meters. Thus, four transect segments of 20 meters each were laid out from the center point in the four cardinal directions (Figure 3). For horizontally aligned segments, the slope distance corresponded to the projected horizontal length. For upslope and downslope segments, slope was taken into account to correct for horizontal projection (using the cosine of the inclination angle), meaning that the effective transect length was reduced to ensure that volume estimates per hectare of horizontal surface area remained accurate.

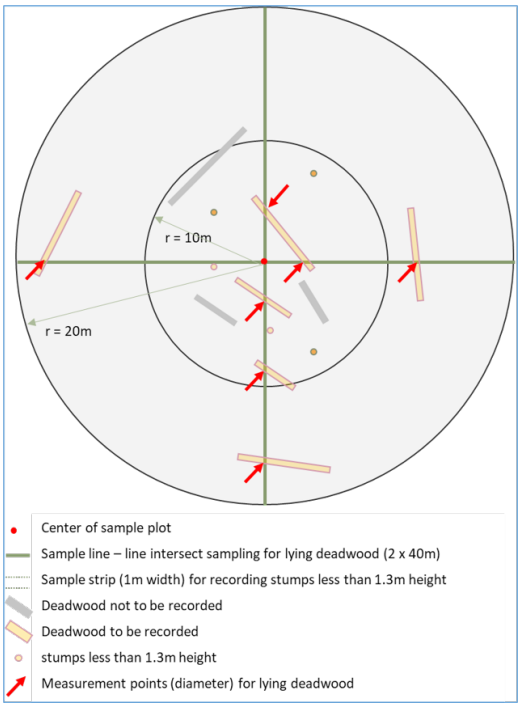


Fig. 3

Figure 3: Line intersect method, Source: E.C.O. according to [18]

Abbildung 3: *Line-intersect Methode, Quelle: E.C.O. nach [18]*

All downed woody fragments with a diameter ≥10 cm at the point where their imaginary centerline intersects the transect were recorded. The following attributes were measured:

- Diameter (in cm) at the intersection point (measured perpendicular to the stem axis)
- Tree species (in advanced decay stages categorized as coniferous, broadleaved, or unidentified)
- Decay class (five-stage classification)
- Origin: cut, broken, or windthrown

Windthrow was identified by the presence of a root plate or exposed roots. In addition, all stumps and cut stems under 130 cm in height within a 20-meter radius from the plot center were recorded. For each, the following parameters were documented: diameter, tree species, and decay class.

The following formula was used to calculate the biomass [18]:

$$V_{LG} = \frac{\pi^2 \sum_{l=1}^{i} d_L^2}{8L}$$

V_{LG} = Volume of lying deadwood
d_L = diameter in cm of the cross-sectional area of the i-th lying tree trunk l with a central diameter > 10 cm

Terrestrial laser scanning

To estimate standing tree volume using TLS, 18 of the 44 sample plots were scanned. Due to steep and inaccessible terrain, TLS data collection was not feasible at all locations. Each of the selected plots was scanned using a VZ-400i terrestrial laser scanner (RIEGL Deutschland Vertriebsgesellschaft mbH, Gilching bei München, Germany). The instrument provides a ranging accuracy of approximately 5 mm and a precision of about 3 mm (1σ at 100 m under standard manufacturer test conditions), which ensures highly reliable distance measurements even in complex field environments. From approximately 10 to 20 scan positions per plot, a full 3D point cloud of all trees and the shrub layer within a 30-meter radius of the plot center was captured, allowing for detailed structural documentation.

The processing and analysis of the TLS point clouds were conducted by Forest Design SRL (Brașov, Romania). For each individual tree, quantitative structure models (QSMs) were generated by fitting cylindrical elements to the tree's point cloud (Figure 4). Based on these models, the stem volume of each tree was calculated. Subsequently, plot-level volume values were scaled to a per-hectare basis to allow for direct comparison with other inventory methods.

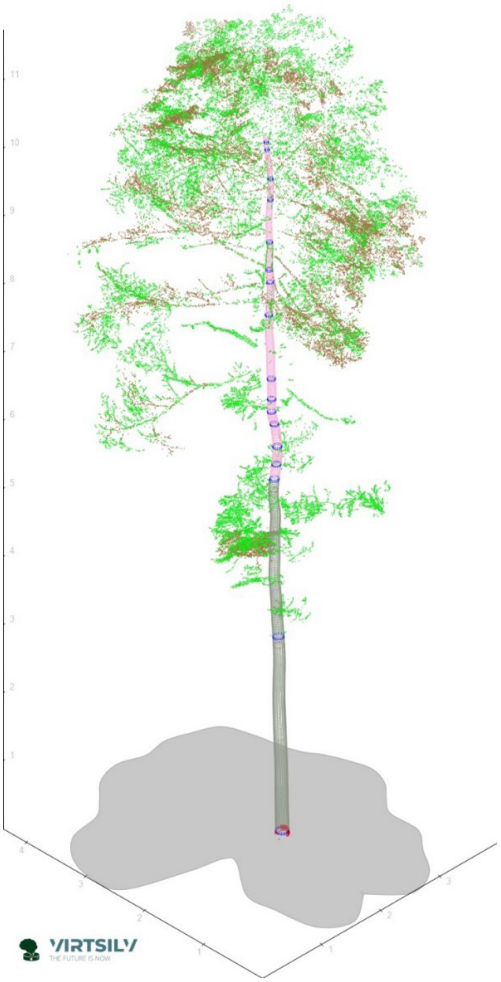


Fig.4

Figure 4:
Fitting cylinders in the trunk to determine the volume, Source: Forest Design SRL

Abbildung 4:
Einpassen von Zylinder in den Stamm zur Volumen-Ermittlung, Quelle: Forest Design SRL

Drone-based laser scanning

The entire study area, covering 48 ha, was surveyed using a drone-mounted LiDAR system combined with a high-resolution camera. The system consisted of a VUX-120 laser scanner (RIEGL Deutschland Vertriebsgesellschaft mbH, Gilching bei München, Germany) and an iXM100 camera (Phase One A/S, Frederiksberg, Denmark), both mounted on a LasCO 2 multicopter (Soleon GmbH, Varna, Italy). The VUX-120 provides a ranging accuracy of approximately 10 mm and a precision of about 5 mm (1σ at 100 m under standard manufacturer test conditions). The aerial survey was conducted by Alto Drones (South Tyrol, Italy) in April 2022 under leaf-off conditions to ensure optimal visibility of ground and understory structures, and TLS took place under similar conditions. The

average point density of the laser scan flight exceeded 4,200 points per square meter. The resulting 3D point clouds were processed in the ETRS89 / UTM Zone 32 coordinate system with orthometric heights, calculated using the official geoid model provided by the Austrian Federal Office of Metrology and Surveying (BEV). To ensure accurate georeferencing, the area was flown in overlapping parallel flight lines with additional cross-strip flights, improving spatial consistency and coverage (Figure 5).

At TU Wien, the total aboveground biomass for the entire study area was estimated using an approach analogous to the TLS-based method. Cylindrical models were fitted to the tree trunks within the UAV-derived 3D point cloud to reconstruct individual tree volumes.

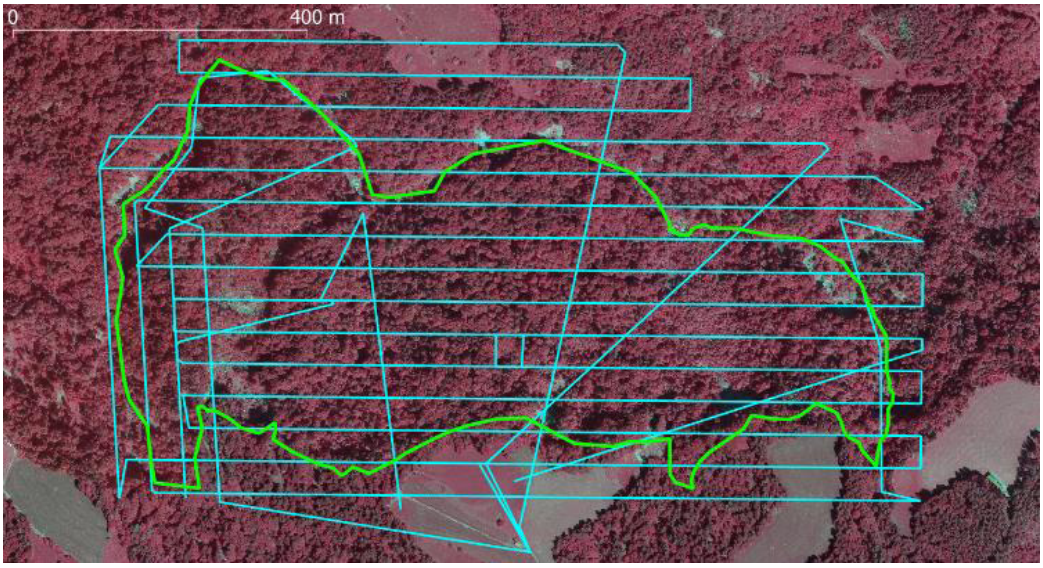


Fig. 5

Figure 5:
Flight trajectories, Source: TU Wien (Markus Hollaus)

Abbildung 5:
Flugtrajektorien, Quelle: TU Wien (Markus Hollaus)

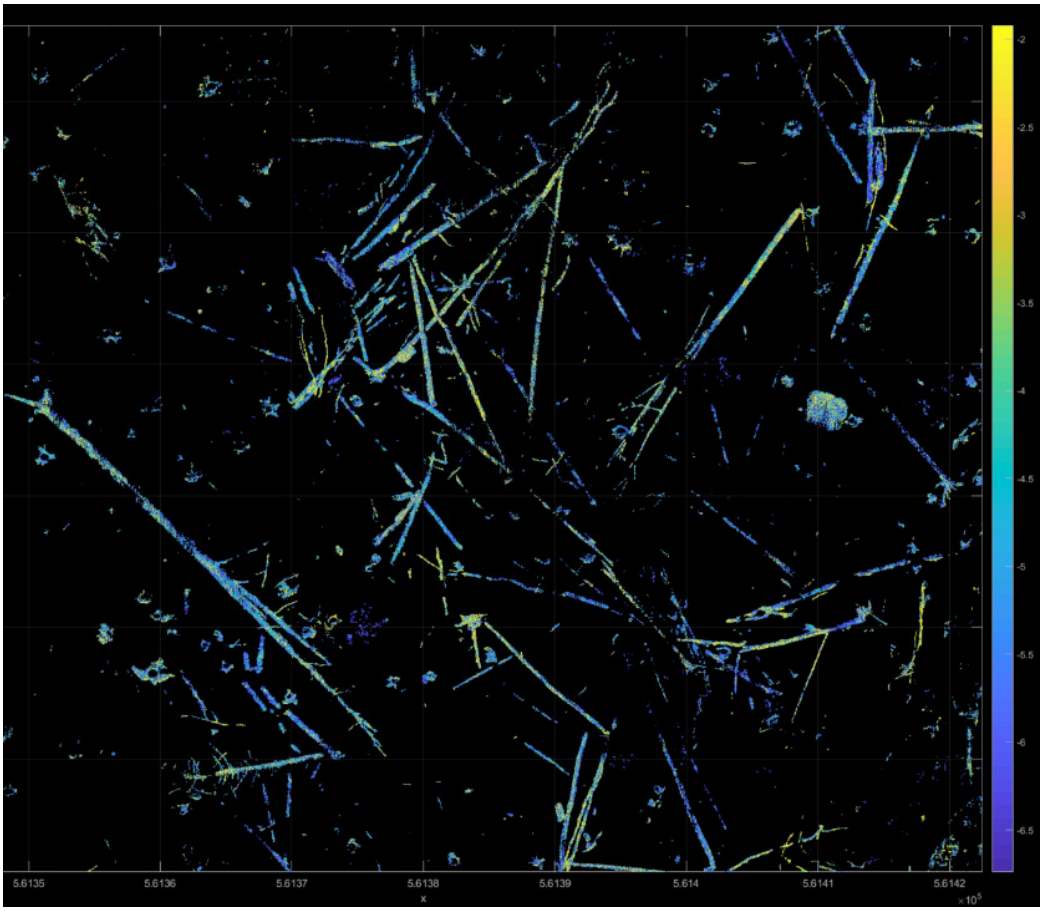


Fig. 6

Figure 6:
UAV-LS – Lying deadwood detection, Source: TU Wien (Markus Hollaus)

Abbildung 6:
UAV-Laserscanning – Detektion des liegenden Totholzes, Quelle: TU Wien (Markus Hollaus)

In addition, an automated analysis of lying deadwood was carried out (Figure 6). Detection was based on a knowledge-based decision tree, applied to the normalized point cloud. The algorithm incorporated both geometric and radiometric properties of the LiDAR points to distinguish deadwood elements from other structures. The analysis focused on near-ground deadwood segments located up to 5 meters above ground level. Once identified, the volume of lying deadwood was estimated using a voxel-based approach with a voxel resolution of 5 × 5 × 5 cm³.

Some limitations were noted in areas with overlapping trunks or gaps in the point cloud, for example due to occlusions or shadowing effects during scanning. In the case of several vertically overlapping lying stems only the top-most stem is considered for the deadwood volume estimation. Furthermore, this method only considers horizontal distances, which may lead to an underestimation of deadwood volume if the stems are lying on steep terrain.

RESULTS

Standing stock volume

The calculation of standing volume per hectare (including live and dead wood) based on TLS data from 10-meter-radius plots yielded results closely aligned with those derived from the classical field-based inventory (Table 2). The difference between the two methods was only 24 m³/ha. In some cases, there are significant discrepancies between individual plots when comparing the results of traditional inventory methods with TLS analysis (e.g., Plot 511, Plot 710). One possible cause could be insufficient spatial accuracy in plot positioning. A slight displacement of the plot center (different center depending on the method), and thus the entire plot, can lead to the inclusion of different trees. If these trees have a large DBH, this can consequently impact volume estimates.

Tab. 2

Plot Nr.	m³/ha Classic inventory sampling in the field (10 m radius)	m³/ha TLS (10 m radius)	m³/ha TLS (20 m radius)
303	416	476	590
308	1321	1149	759
407	826	795	791
408	124	150	491
409	464	416	656
504	687	669	748
505	1066	845	740
506	731	893	588
511	790	289	351
605	715	1060	816
606	357	651	728
607	668	676	845
608	824	758	753
610	119	194	172
611	635	844	665
706	1612	1462	874
709	786	745	543
710	397	43	755
Average volume/ha	**697**	**673**	**659**

Table 2: Comparison of field sampling and TLS methods: Volume (m³) of standing (living and dead) trees per hectare across 18 forest inventory points

Tabelle 2: *Vergleich Klassische Stichprobeninventur im Gelände und TLS: Volumen stehender (lebender und toter) Bäume pro Hektar in 18 Waldinventurpunkten Norm-Höhe und des Korrekturfaktors.*

Additionally, Plot 710 represents an open forest area with few trees within the 10-meter radius. However, as the radius increases, several large tree trunks become part of the sample. When looking at all plots collectively, these spatial accuracy deviations appear to balance out across the dataset.

When all 44 classical inventory plots are considered, the total average volume is slightly lower—549.27 m³/ha - compared to 697 m³/ha in the 18 TLS-sampled plots (standing living and dead). This approximately 27% higher value in the TLS subset is primarily due to the fact that TLS data were collected in fully stocked forest areas, whereas the full dataset includes plots on landslide zones dominated by pioneer forests with lower biomass.

To assess the effect of sample area size, standing volume per hectare was also calculated using 20-meter-radius TLS plots, thus quadrupling the sampled area. Interestingly, this larger sampling area resulted in a mean volume per hectare that differed by only 2 % compared to the 10-meter plots. This indicates that the 10-meter-radius plots provide a representative estimate of forest volume for the study area.

In addition to the TLS-based assessment, TU Wien also calculated standing live and deadwood volume using drone-based LiDAR data. This approach covered the entire 48-ha area of the natural forest reserve, including fully stocked forests, pioneer forests on landslides, and open landslide areas.

The mean volume per hectare derived from the UAV-LiDAR data was **547.42 m³/ha,** which matches closely with the **549.27 m³/ha** (standing living and dead) obtained from the 44 manually recorded inventory plots. This strong agreement underscores the reliability of UAV-LiDAR for large-scale forest volume assessments.

Deadwood estimation

One major advantage of UAV-based deadwood analysis is the ability to automatically and operationally detect deadwood, even in areas where it is barely visible from above. Despite the presence of classification artifacts—such as outlines of rocks or terrain features mistakenly identified as deadwood—the average volume of lying deadwood derived from the UAV analysis was nearly 50% lower than the estimate obtained using the line intersect method (Table 3).

Tab. 3

	Average lying deadwood (m³/ha)		
Type	**Field survey**	**UAV in relation to total area of the Rohrach Natural Forest Reserve (47.5 ha)**	**UAV related to the 10 m radius plots**
Lying deadwood	99.6	55.9	45.8
Standing deadwood	39.97	N/A	N/A

Table 3: Comparison of deadwood classic sample inventory and UAV evaluation

Tabelle 3: *Vergleich liegendes Totholz klassische Stichprobeninventur und UAV-Auswertung*

Time resources

Additionally, the study also evaluated the time resources required for each inventory method (Table 4). A significant advantage of laser scanning technologies—particularly UAV-LS—is the ability to collect data remotely, without the need for extensive on-site fieldwork.

Tab. 4

Method	Time (in the field)	Sample Size
Classical field-based forest inventory (44 plots)	170 h (field work)	All trees within a 10 m radius of the sample center
TLS (18 plots)	25 h (including moving from one plot to the next)	All trees within a 30 m radius of the sample center
UAV	16 h (2 people, one day)	Full test area

Table 4: Comparison the time resources required for each inventory method

Tabelle 4: *Vergleich der Zeitressourcen je nach Erhebungsmethode*

While traditional field-based inventories are labor-intensive and time-consuming—requiring physical access to each plot and manual measurements for every tree—UAV-LS enables rapid data acquisition over large and inaccessible areas. A single drone flight can cover the entire study area in a fraction of the time, often producing results of equal or even higher precision compared to manual measurements.
This reduction in field effort not only improves operational efficiency, but it also minimizes disturbance to sensitive natural habitats—making UAV-LS a compelling option for modern forest monitoring.

DISCUSSION

Structural Characteristics and Biomass Dynamics of the Rohrach Natural Forest Reserve

From 1996 to 2022, the living growing stock increased from 426 m³/ha [10, p. 55] to 509 m³/ha (traditional method, 44 plots, standing living trees only) in 2022. It is likely that the forest stands in Rohrach had not yet reached an equilibrium in 1996 like in a natural forest ecosystem. This is underpinned by the fact that the deadwood volume increased over the same interval from 49 m³/ha (1996) to 141 m³/ha (2022, standing and lying). The volume of living and dead biomass is higher than in most natural beech forest habitats in the Kalkalpen National Park of Austria (247 m³/ha living, 25 m³/ha deadwood) [21] but less than in the comparable primeval beech forests Uholka-Shyrokyi Luh in Ukraine (582 m³/ha living, 163 m³/ha deadwood) [22]. The forest reserve in Rohrach is characterized by extensive landslides, which leads to a significant portion of areas (12%) that are not covered by forests. The soft shist, marl and flysch bedrock increase the likelihood of windthrow, which, together with the landslides, might be an explanation of the exceptionally high deadwood volumes.
A standing timber volume of 547.42 m³/ha, or 549.27 m³/ha based on UAV analysis, is characteristic of an undisturbed natural forest. This large volume indicates a dense, structurally complex, and highly productive forest ecosystem. The forest stands in the Rohrach Natural Forest Reserve are notable for their high proportion of standing deadwood, massive old trees, and multilayered canopy structure.

Current challenges in methodologies for the assessment of standing biomass

The comparison of the three methods confirmed findings from previous studies [23], highlighting that among all terrestrial point cloud techniques, TLS still provides the highest data quality in terms of geometric accuracy and level of detail. However, a consistent challenge for all terrestrial point cloud data is the occlusion in the upper canopy layers.

UAV-based laser scanning offers a promising alternative by potentially combining the advantages of both above- and below-canopy measurements. As demonstrated by Liang et al. [24], UAV-LS point clouds can perform comparably to terrestrial methods under favorable stand conditions. While the geometric precision of UAV-LS (particularly in the stem region) does not yet match that of TLS, the method's high mobility and rapid data acquisition make it a highly attractive option for forest inventories [24].

In the study by Pitkänen et al. [25], it is pointed out that stem volume estimates derived from automated cylinder or circle fitting are often compromised by registration errors and occlusions—i.e., parts of the stem that are only partially visible.

In our study, occlusions also occurred, such as branches, leaves from lower vegetation, or other obstacles that partially obscured parts of the trunk. As a result, the automatic fitting process generated incomplete data, which could lead to an underestimation of the volume. Conversely, if the leaves were mistakenly counted as part of the trunk, the volume could be overestimated.

These issues frequently led to poorly fitted geometries and difficulties in accurately identifying the treetop. To address this, the study incorporated additional field measurements to improve the fitting process and reduce major errors in stem volume prediction. The findings demonstrate that combining TLS point clouds with simple field measurements can significantly enhance the accuracy of stem volume estimation compared to using TLS data alone [25].

In the study by Wang et al. [26], the number of trees that could be manually detected in terrestrial and airborne point clouds was assessed. The results showed that the denser the forest stand, the fewer stems could be detected. At the plot level (fixed plots of 32 m × 32 m), TLS with five scan positions captured approximately 97% of individual trees in low-density stands (about 700 stems/ha), 93% in medium-density stands (about 900 stems/ha), and 75% in high-density stands (about 2,200 stems/ha). Using UAV-LS with a point density of around 450 points/m², 87%, 69%, and 55% of the individual trees were detected low-, medium-, and high-density stand types, respectively. The study of Wang et al. [26] highlights the potential of a combined approach: using manually measured DBH values from TLS together with tree heights derived from UAV-LS proves to be particularly promising [26].

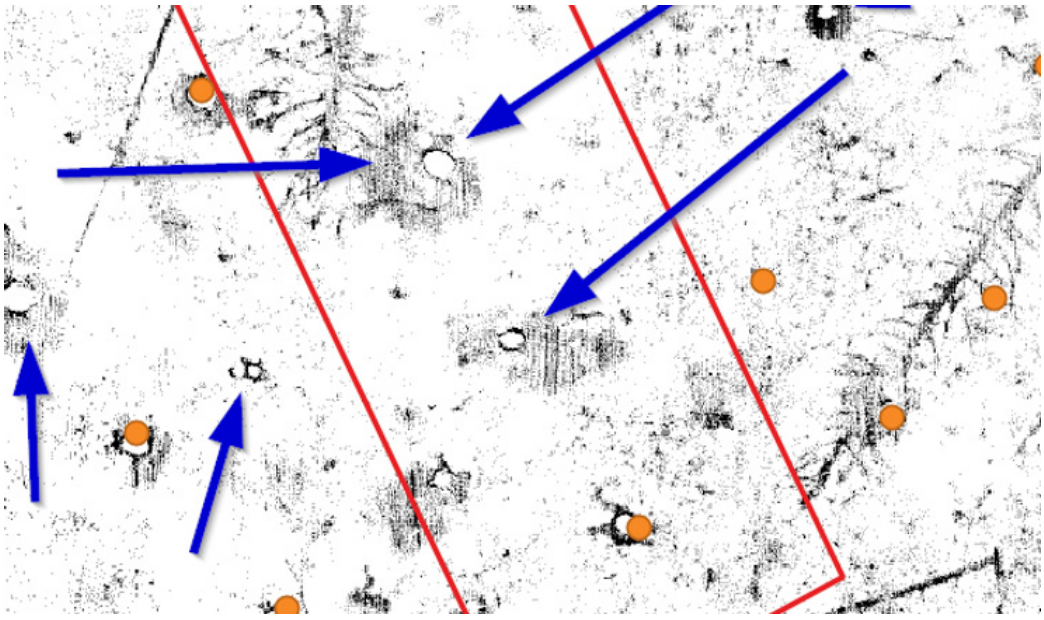


Fig. 7

Figure 7:
Example of missed tree stems in single tree detection

Abbildung 7:
Beispiel für fehlende Baumstämme in der Einzelbaumdetektion

Figure 7 illustrates a representative example from our study. While the yellow dots indicate the positions of detected individual trees from the UAV-LS data, the underlying point density map suggests that several stems were missed during the detection process.

Our study also revealed that individual tree segmentation based on laser scanning data (both TLS and UAV-LS) shows inaccuracies, despite the high level of detail in the data, particularly in very steep or densely vegetated areas. Segmenting individual trees from laser scanning data has long been a major challenge in forest remote sensing. When determining above-ground biomass based on laser scanning data, not only the volume of the trunk, but also the volume of the branches, is taken into account. While the estimation of stem biomass is relatively straightforward, capturing the tree crown using TLS is significantly more complex due to overlapping branches [27]. In our study, this led to several cases where two neighboring trees were erroneously segmented as a single tree, especially in the upper canopy layers captured with UAV-LS data (Figure 8).

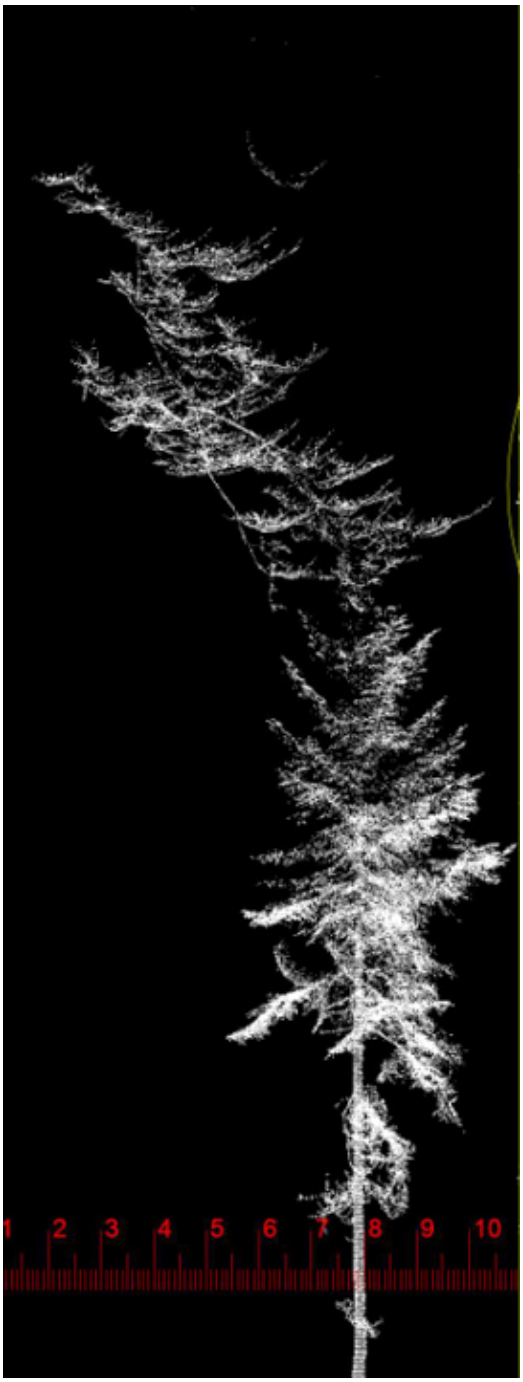


Fig. 8

Figure 8:
Incorrect individual tree segmentation due to overlapping branches

Abbildung 8:
Fehlerhafte Einzelbaum Segmentierung aufgrund überlappender Äste

While numerous algorithms for tree segmentation are available, comparative studies remain scarce due to the difficulty of obtaining reliable reference data. The need to evaluate tree segmentation algorithms directly using benchmark datasets, rather than relying on indirect comparisons through forest metrics such as biomass, or the number and size distribution of trees, is emphasized in the literature [28].

In the study by Abegg et al. [29], it was found that volume estimates derived from point clouds are systematically biased—by around 25% for small trees and only a few percent for larger ones. In particular, small tree components with diameters under 7 cm cannot be estimated with sufficient accuracy. For small trees with a DBH of 12 cm, the volume of these components is overestimated by an average of 110%, with high variability. In contrast, for large trees (DBH ≥ 75 cm), the same components are underestimated by an average of 50% [29].

Given the benefits of integrating multiple remote sensing platforms, it is not surprising that various studies have already explored the combination of UAV, TLS, and airborne laser scanning (ALS) data. However, most of these approaches remain resource-intensive and often involve downsampling or aggregation, which leads to a reduction in point density or

spatial resolution compared to the original capabilities of the sensors [12]. In this context, Calders et al. [12] raise a critical but still insufficiently addressed question: to what extent do such processing steps result in the loss of valuable structural information — and does this loss actually impact the accuracy or relevance of specific ecological applications?

Challenges in detecting lying deadwood

Detecting lying deadwood remains challenging, as overstory canopy, dense understory vegetation, and ground obstructions like rocks often interfere with reliable identification. Recent methods apply object-based image analysis or clustering techniques on point cloud data, but their effectiveness is typically limited to larger logs with DBH exceeding 25–30 cm [30].

Our study reached similar conclusions. The results showed that reference data collected using the line intersect method yielded nearly twice the amount of deadwood biomass compared to the automated drone-based analysis.

The line intersect method assumes that deadwood is randomly distributed across the sampling area, without directional bias. However, this assumption may not hold true in the Natural Forest Reserve Rohrach, where deadwood distribution could be influenced by slope processes, windthrow direction, or past disturbances. But this bias has been largely mitigated by the perpendicular orientation of the two transects within each plot.

Additionally, the UAV-LS based method may underestimate deadwood volume in dense canopy areas, where fallen trunks beneath the crown cover remain undetected by the aerial laser scan. These factors likely contributed to the lower deadwood estimates obtained from the UAV-based approach.

To determine whether the line intersect method may be unsuitable in this context—due to its assumption of a random distribution of logs—or whether the UAV-based approach systematically fails to detect a significant number of logs, a complete census of deadwood on a test plot would be required.

OUTLOOK AND LIMITATIONS OF THE STUDY

The findings of this study provide a valuable foundation for subsequent research. The collected data offer substantial potential for additional analyses and extended applications. At the same time, certain methodological and evaluative limitations must be acknowledged. This section therefore outlines the most relevant limitations of the present study and highlights potential directions for further analyses and future research.

This study compared three methods for determining above-ground biomass (field-based forest inventory, TLS, and UAV-LS), but the sample size varied. The field-based forest inventory used 44 sample areas, while TLS only considered 18 of the areas (due to inaccessible terrain). UAV-LS was performed across the entire area.

Moreover, the three methods were not applied in complete methodological isolation. Tree height, for instance, was not measured during the field inventory but subsequently derived from TLS data and then incorporated into the field dataset. This approach was chosen because field-based height measurements are prone to substantial inaccuracies, whereas TLS provides more reliable estimates. Field measurements are more sensitive to stand density, crown classes, and tree species than ALS and TLS measurements. Overall, field-based measurements tend to overestimate the height of tall trees, particularly the largest individuals. In dense stands, field-measured heights of smaller trees also exhibit considerable uncertainty [17]. Nevertheless, for a rigorous comparison of the three approaches, such cross-use of information should ideally be avoided.

In this study, only UAV-derived estimates were compared with the field-based line intersect method for lying deadwood. This comparison yielded markedly different results (see Discussion, Section 3). For the sake of completeness and to strengthen the overall analysis, it would also be valuable to derive deadwood estimates from the TLS data.

To estimate above-ground biomass from the UAV and TLS laser scanning data, QSM models were applied in this study. Nevertheless, numerous alternative approaches for biomass estimation from LiDAR data exist, and a comparison of these methods would be of considerable interest. The same consideration applies to deadwood assessment. In this study, a voxel-based approach was employed, although various other methods are also available.

Beyond QSM models and voxel-based techniques, allometric models, machine learning approaches, and advanced deep learning frameworks such as 3D-CNNs could be explored, either individually or in combination, to further improve biomass and deadwood estimation.

REFERENCES

[1] P. J. Verkerk, P. Delacote, E. Hurmekoski, J. Kunttu, R. Matthews, R. Mäkipää, et al., "Forest-based climate change mitigation and adaptation in Europe," European Forest Institute, *From Science to Policy*, vol. 14, 2022, doi: 10.36333/fs14

[2] F. M. Sabatini, W. S. Keaton, M. Lindner, M. Svoboda, P. J. Verkerk, J. Bauhus, et al., "Protection gaps and restoration opportunities for primary forests in Europe," *Diversity and Distributions*, vol. 26, no. 12, pp. 1646–1662, 2020, doi: 10.1111/ddi.13158

[3] H. B. Smith, N. E. Vaughan, and J. Forster, "Long-term national climate strategies bet on forests and soils to reach net-zero," *Commun Earth Environ*, vol. 3, no. 305, 12 p., 2022, doi: 10.1038/s43247-022-00636-x

[4] L. Wang, F. Wei, T. Tagesson, Z. Fang, and J.-C. Svenning, "Transforming forest management through rewilding: enhancing biodiversity, resilience, and biosphere sustainability under global change," *One Earth*, vol. 8, no. 3, p. 101195, 2025, doi: 10.1016/j.oneear.2025.101195

[5] European Commission, "Communication from the Commission to the European Parliament, the Council, The European Economic and Social Committee and the Committee of the Regions," in EU Biodiversity Strategy for 2030 Bringing nature back into our lives, 2020, available: https://eur-lex.europa.eu/legal-content/EN/TXT/?uri=celex:52020DC0380

[6] B. Law and W. Moomaw, "The best carbon capture technology? Leaving forests alone," Trellis Group, Available: https://www.greenbiz.com/article/best-carbon-capture-technology-leaving-forests-alone

[7] W. R. Moomaw, S. A. Masino, and E. K. Faison, "Intact forests in the United States: proforestation mitigates climate change and serves the greatest good," *Front. For. Glob. Change*, vol. 2, no. 27, 2019, doi: 10.3389/ffgc.2019.00027

[8] G. Winkel et al., "Governing Europe's forests for multiple ecosystem services: opportunities, challenges, and policy options," *Forest Policy and Economics*, vol. 145, p. 102849, 2022, doi: 10.1016/j.forpol.2022.102849

[9] IPCC, "Climate Change 2021: the physical science basis. Contribution of Working Group I to the Sixth Assessment Report of the Intergovernmental Panel on Climate Change," Cambridge University Press, UK, 2021, available: https://www.ipcc.ch/report/ar6/wg1/downloads/report/IPCC_AR6_WGI_Full_Report.pdf

[10] G. Grabherr, C. Peter, J. Enzenhofer, V. Pfefferkorn-Dellali, K. Pfeifer, E. Ritter, et al., "Ein Wald im Aufbruch: das Naturwaldreservat Rohrach (Vorarlberg, Österreich)" in *Bristol-Schriftenreihe*, no. 7. Teufen: Flück-Wirth, 224 p., ISBN 9783905209068, 1999

[11] H. Kirchmeir et al., "Digitale Bestanderfassung und Entwicklungsanalyse für das Naturwaldreservat Rohrach," E.C.O. Institute of Ecology and TU Wien, Department of Geodesy and Geoinformation, Klagenfurt, Bericht im Auftrag der Nationalpark Gesäuse GmbH, Fachbereich Naturschutz und Naturraum, 2024

[12] K. Calders, J. Adams, J. Armstrong, H. Bartholomeus, S. Bauwens, L. P. Bentley, et al., "Terrestrial laser scanning in forest ecology: expanding the horizon," *Remote Sensing of Environment*, vol. 251, p. 112102, 2020, doi: 10.1016/j.rse.2020.112102

[13] M. Demol, P. Wilkes, S. M. Krishna Moorthy, K. Calders, B. Gielen, et al., "Volumetric overestimation of small branches in 3D reconstructions of *Fraxinus excelsior*," *Silva Fenn.*, vol. 56, no. 1, 2022, doi: 10.14214/sf.10550

[14] F. Tupinambá-Simões, A. Pascual, J. Guerra-Hernández, C. Ordóñez, S. Barreiro, and F. Bravo, "Combining hand-held and drone-based lidar for forest carbon monitoring: insights from a Mediterranean mixed forest in central Portugal," *Eur J Forest Res*, vol. 144, pp. 925-940, 2025, doi: 10.1007/s10342-025-01772-7

[15] I. T. Bueno, C. A. Silva, K. Anderson-Teixeira, L. Magee, C. Zheng, E. N. Broadbent, et al., "Aboveground biomass and tree mortality revealed through multi-scale LiDAR analysis," *Remote Sensing*, vol. 17, no. 5, 2025, doi: 10.3390/rs17050796

[16] C. Xu, M. Förster, P. Beckschäfer, U. Talkner, C. Klinck, and B. Kleinschmit, "Modeling European beech defoliation at a regional scale gradient in Germany from northern lowlands to central uplands using geo-ecological parameters, Sentinel-2 and National Forest Condition Survey data," *Forest Ecology and Management*, vol. 576, p. 122383, 2025, doi: 10.1016/j.foreco.2024.122383

[17] Y. Wang, M. Lehtomäki, X. Liang, J. Pyörälä, A. Kukko, A. Jaakkola, et al., "Is field-measured tree height as reliable as believed – a comparison study of tree height estimates from field measurement, airborne laser scanning and terrestrial laser scanning in a boreal forest," *ISPRS Journal of Photogrammetry and Remote Sensing*, vol. 147, pp. 132–145, doi: 10.1016/j.isprsjprs.2018.11.008

[18] C. E. Van Wagner, "The line intersect method in forest fuel sampling," *Forest Science*, vol. 14, no. 1, pp. 20–26, 1968, doi: 10.1093/forestscience/14.1.20

[19] H. Vacik, A. Egger, G. Koch, and H. Kirchmeir, "Totholzerhebung im Rahmen der Hemerobiebewertung in Südtirols Wäldern," *Cbl. f. d. ges. Forstwesen*, vol. 117, no. 2, pp. 115–132, 2000

[20] S. Fraver, M. J. Ducey, C. W. Woodall, A. W. D'Amato, A. M. Milo, and B. J. Palik, "Influence of transect length and downed woody debris abundance on precision of the line-intersect sampling method," *Forest Ecosystems*, vol. 5, no. 1, 2018, doi: 10.1186/s40663-018-0156-9

[21] H. Kirchmeier and S. Mayrhofer, "Erhaltungszustand der Buchenwälder im Nationalpark - Unversehrtheit," in Natürliche Buchenwälder des Nationalparks Kalkalpen, in Schriftenreihe Nationalpark Kalkalpen, vol. 16. , Molln, Austria, 2016, pp. 115-127, available: https://www.zobodat.at/pdf/NP-Kalkalpen-Schriftenreihe_16_0001-0159.pdf

[22] B. Commarmot, U.-B. Brändli, F. Hamor, and V. Lavnyy, "Inventory of the largest primeval beech forest in Europe. A Swiss-Ukrainian scientific adventure," Swiss Federal Research Institute WSL, Birmensdorf, L'viv, 69 p., 2013, available: https://www.wsl.ch/de/publikationen/inventory-of-the-largest-primeval-beech-forest-in-europe/

[23] H. Luo, C. Wang, C. Wen, Z. Chen, D. Zai, Y. Yu, et al., "Semantic labeling of mobile LiDAR point clouds via active learning and higher order MRF," *IEEE Trans. Geosci. Remote Sensing*, vol. 56, no. 7, pp. 3631–3644, 2018, doi: 10.1109/TGRS.2018.2802935

[24] X. Liang, V. Kankare, X. Yu, J. Hyyppä, and M. Holopainen, "Automated stem curve measurement using terrestrial laser scanning," *IEEE Trans. Geosci. Remote Sensing*, vol. 52, no. 3, pp. 1739–1748, 2014, doi: 10.1109/TGRS.2013.2253783

[25] T. P. Pitkänen, P. Raumonen, X. Liang, M. Lehtomäki, and A. Kangas, "Improving TLS-based stem volume estimates by field measurements," *Computers and Electronics in Agriculture*, vol. 180, p. 105882, 2021, doi: 10.1016/j.compag.2020.105882

[26] Y. Wang, J. Pyörälä, X. Liang, M. Lehtomäki, A. Kukko, X. Yu, et al., "In situ biomass estimation at tree and plot levels: what did data record and what did algorithms derive from terrestrial and aerial point clouds in boreal forest," *Remote Sensing of Environment*, vol. 232, p. 111309, 2019, doi: 10.1016/j.rse.2019.111309

[27] K. Olschofsky, V. Mues, and M. Köhl, "Operational assessment of aboveground tree volume and biomass by terrestrial laser scanning," *Computers and Electronics in Agriculture*, vol. 127, pp. 699–707, 2016, doi: 10.1016/j.compag.2016.07.030

[28] Y. Cao, J. G. C. Ball, D. A. Coomes, L. Steinmeier, N. Knapp, P. Wilkes, et al., "Benchmarking airborne laser scanning tree segmentation algorithms in broadleaf forests shows high accuracy only for canopy trees," *International Journal of Applied Earth Observation and Geoinformation*, vol. 123, p. 103490, 2023, doi: 10.1016/j.jag.2023.103490

[29] M. Abegg, R. Bösch, D. Kükenbrink, and F. Morsdorf, "Tree volume estimation with terrestrial laser scanning — testing for bias in a 3D virtual environment," *Agricultural and Forest Meteorology*, vol. 331, p. 109348, 2023, doi: 10.1016/j.agrformet.2023.109348

[30] N. Marchi, F. Pirotti, and E. Lingua, "Airborne and terrestrial laser scanning data for the assessment of standing and lying deadwood: current situation and new perspectives," *Remote Sensing*, vol. 10, no. 9, p. 1356, 2018, doi: 10.3390/rs10091356.

ACKNOWLEDGEMENT:

We gratefully acknowledge funding from the Office of the Vorarlberg State Government, Department of Environmental and Climate Protection (IVe), as well as project financing from the Austrian Forest Fund.
Special thanks to Vanessa Berger, Hannah Rathke and Daniel Nussbaumer for their support in field assessment and laser scanning, to the company Umweltdata GmbH for the technical support and the provision of the laser scanner and to the Romanian company Forest Design SRL for processing the TLS data.

We sincerely appreciate Martin Bösch (at that time Natura 2000 regional manager at inatura) for introducing us to the Rohrach Natural Forest Reserve and providing technical assistance. Finally, we extend our gratitude to Cornelia Peter (Department of Environmental and Climate Protection) for providing and preparing the data from 1995-1996.

ABOUT THE AUTHORS

Larissa Posch, E.C.O.
Institute of Ecology
Klagenfurt, Austria
E-Mail: posch@e-c-o.at

Hanns Kirchmeir, E.C.O.
Institute of Ecology,
Klagenfurt, Austria

Klaus Steinbauer, E.C.O.
Institute of Ecology,
Klagenfurt, Austria

Markus Hollaus
Department of Geodesy and Geoinformation, TU Wien, Vienna, Austria

BACK TO CONTENT

Short Notes

Development and field testing of a portable eDNA water sampler

Pierre Hohenberger, Johanna Marion Schulz, Alexander Blum, Vid Švara

ABSTRACT

One of the methods currently revolutionizing biodiversity assessment is the analysis of environmental DNA (eDNA). Here we present a prototype of a semi-automatic sampler for water eDNA collection. The sampler is a portable, affordable, battery-powered device that supports hands-free filtration using peristaltic pumps and allows for the processing of multiple water samples under field conditions.

The prototype system consists of commonly available components including an ESP32 microcontroller, a 3D-printed battery adapter, voltage converters, and two peristaltic pumps. The system is controlled by a simple push-button starting a 20-minute sampling cycle. The filtration setup ensures that contamination is avoided by placing the filter before the pump in the water flow path.

Initial field testing was conducted at Lake Silbersee in Carinthia, Austria, where successful filtrations were carried out using different filters. Concentration measurements of extracted eDNA samples ranged from 9.8 to 24.0 ng/µL, confirming that the device can collect eDNA for water biodiversity assessment. Tests also revealed that filters became clogged after 1 L of filtration in the given water source, supporting the decision to limit operation time.

Future improvements to the prototype may be possible by adding further pump capacity, a display, data logging, and a web-based interface to further increase usability and automation.

KEYWORDS

- eDNA
- environmental monitoring
- water sampler
- portable device

Entwicklung und Felderprobung eines tragbaren eDNA-Wasserprobenehmers

ZUSAMMENFASSUNG

Eine der Methoden, die derzeit die Bewertung der biologischen Vielfalt revolutionieren, ist die Analyse von Umwelt-DNA (eDNA). Hier stellen wir den Prototyp eines halbautomatischen Probenehmers für Wasser-eDNA vor. Der Probenehmer ist ein tragbares, erschwingliches, batteriebetriebenes Gerät, das eine freihändige Filtration mit peristaltischen Pumpen unterstützt und die Verarbeitung mehrerer Wasserproben unter Feldbedingungen ermöglicht.

Der Prototyp besteht aus handelsüblichen Komponenten wie einem ESP32-Mikrocontroller, einem 3D-gedruckten Batterieadapter, Spannungswandlern und zwei peristaltischen Pumpen. Das System wird über einen einfachen Druckknopf gesteuert, der einen 20-minütigen Probenahmezyklus startet. Der Filteraufbau stellt sicher, dass Verunreinigungen vermieden werden, indem der Filter vor der Pumpe im Wasserflussweg platziert wird.

Erste Feldversuche wurden am Silbersee in Kärnten, Österreich, durchgeführt, wo erfolgreiche Filtrationen mit verschiedenen Filtern stattfanden. Die Konzentrationsmessungen der extrahierten eDNA-Proben reichten von 9,8 bis 24,0 ng/µl und bestätigten, dass das Gerät eDNA für die Bewertung der biologischen Vielfalt im Wasser sammeln kann. Die Tests zeigten auch, dass die Filter nach 1 Liter Filtration in der gegebenen Wasserquelle verstopft waren, was die Entscheidung, die Betriebszeit zu begrenzen, bestätigte.

Zukünftige Verbesserungen des Prototyps könnten durch weitere Pumpenanwendungen, ein Display, Datenprotokollierung und eine webbasierte Schnittstelle möglich sein, um die Benutzerfreundlichkeit und Automatisierung weiter zu erhöhen.

INTRODUCTION

Environmental DNA (eDNA) sampling is an increasingly important method in biodiversity monitoring, allowing the detection of organisms based on genetic material present in environmental samples, including water or soil [1], [2]. eDNA sampling techniques mostly rely on manual filtration using syringes, which can be labor-intensive and prone to contamination [3]. The growing demand for reliable, efficient, and field-deployable systems has led to the development of portable eDNA samplers [4], [5]. However, these devices are often large, difficult to transport, reliant on specific filter systems, and expensive, making them inaccessible to many users.

In this paper we present a semi-automatic, battery-powered sampler developed as part of a research internship during the MSc Study program System Design at Carinthia University of Applied Sciences. The project was initiated in response to the need for a lightweight, user-friendly, and robust device that can operate without external infrastructure in remote locations. The aim of the project was to develop a system that supports hands-free filtration via peristaltic pumps and is capable of processing multiple water samples in parallel. The sampler should allow the use of various filter types and include features such as predefined operation times to prevent overloading or clogging of the filter.

The development of the portable eDNA sampler followed a structured, iterative process. First, a functional concept was designed based on the requirements for autonomous eDNA sampling in remote environments. The system was planned to operate with minimal user interaction, using a microcontroller, two peristaltic pumps, and a standard 18 V power tool battery. Splash protection, field portability, and ease of use were also considered in the design.

Based on this concept, the first prototype was assembled. 3D printing was used for selected components of the prototype. All electronic components were installed in splash-resistant housing, providing adequate protection against light rain and moisture during fieldwork. Initial functionality was tested step-by-step on the workbench.

Before field deployment, preliminary tests were carried out in a controlled aquarium environment populated with fish and aquatic plants. These tests verified the system's basic performance under realistic conditions and helped optimize tubing layout and flow rates.

The completed prototype was then tested under natural conditions in the field. Water samples were collected using both the automated sampler and a manual syringe method for comparison. The filtered samples were analyzed in the laboratory to assess DNA concentrations and evaluate the performance and sample quality of the system.

METHODS

The core system consists of an ESP32-WROOM-32E microcontroller, two peristaltic pumps, a toggle switch, two push-buttons, relay modules, and two voltage converters. Power is supplied by an 18 V Makita battery via a 3D-printed adapter. The voltage converters reduce the voltage to 12 V for the pumps and 5 V for the controller. All components are mounted in a splash-resistant plastic housing, providing protection against light rain and moisture during field use. A modular internal layout and a prototyping board with screw terminals allow for easy access and future modifications.

A schematic overview of the wiring setup is provided in Supplementary Figure 1, and a photo of the assembled prototype is shown in Figure 1.

Each pump is controlled independently by pressing a corresponding button, which starts a 20-minute filtration cycle. This duration is based on preliminary tests that showed filter clogging after pumping of approximately 1 L of lake water. Water is drawn through a filter placed upstream of the pump to prevent contamination of internal tubing. After sampling, filters are removed and stored on ice.

The microcontroller is programmed using Arduino IDE software. The control logic includes a simple timer function for automated pump shutdown after 20 minutes.

Field testing took place on March 27, 2025, at Lake Silbersee (Villach, Austria), a freshwater lake located in the Alps-Adriatic region. Four water samples were collected using glass fiber filters with a pore size of 0.7 µm and the sampler prototype: three water samples were filtered using the peristaltic pumps, and one sample was processed manually

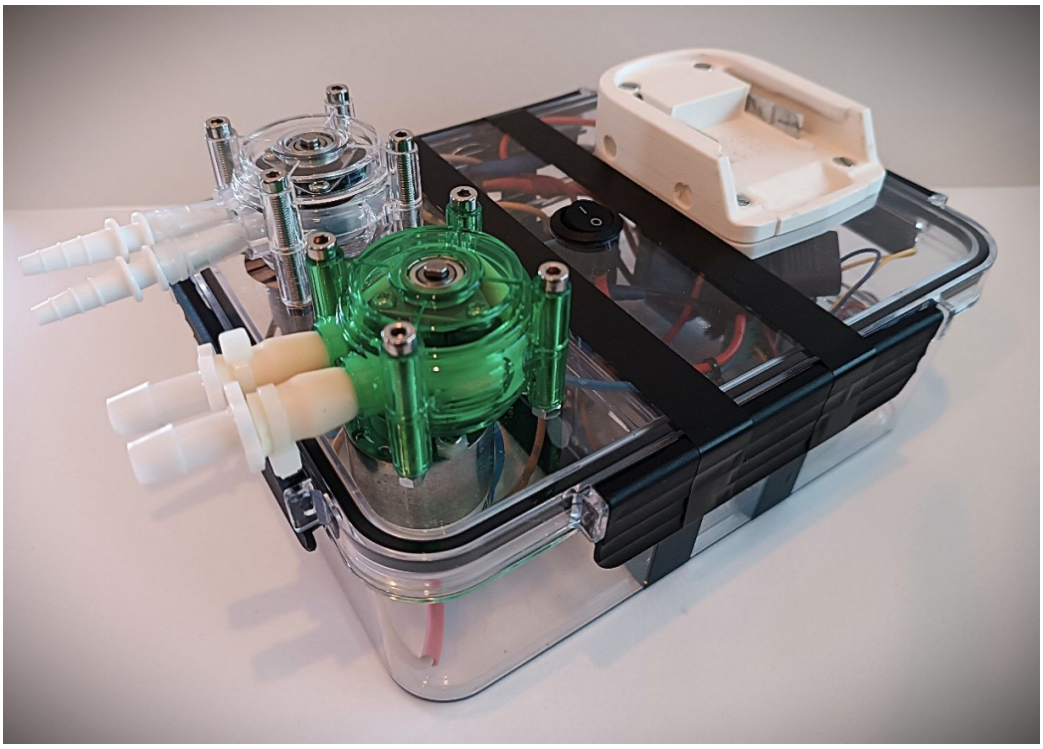


Fig. 1

Figure 1:
Prototype of the portable eDNA water sampler in housing. Source: Own image

Abbildung 1:
Prototyp des tragbaren eDNA-Wassersamplers in einem Gehäuse. Quelle: Eigenes Bild

with a syringe for comparison. After the filtration process, the filters were stored in tubes containing 1.5 µL ATL extraction buffer (Qiagen, Hilden, Germany). Two control samples were included: a negative field control and a DNA extraction blank using only the extraction buffer. DNA was extracted from all filters on April 17, 2025, using the DNeasy Blood & Tissue Kit (Qiagen, Hilden, Germany) with a 2 h Proteinase K incubation step, and the final sample elution volume was 100 µL (2 × 50 µL). For all samples and controls containing filters, 500 µL were used for the extraction; for all controls that did not contain filters, 200 µL were used. An inhibitor removal step was performed according to the manufacturer's instructions using the Inhibitor Removal Kit (Zymo Research, CA, USA). All samples and final DNA extracts were stored at –20 °C prior to and post analysis. DNA concentrations were measured using a Qubit fluorometer (Thermo Fisher Scientific, MA, USA).

RESULTS

The field test demonstrated that the prototype is capable of filtering approximately 1 L of lake water within 20 minutes using standard eDNA filter cartridges. During operation, the peristaltic pumps functioned reliably under battery power. All four filtered samples (three using the device, one using a syringe) yielded measurable amounts of eDNA. Filter clogging occurred consistently after pumping around 1 L of filtered water.

Tab. 1

Sample code	Filtration method	Starting volume (µl)	Concentration (ng/µl)
P1	Pump	500	9.8
P2	Pump	500	24.0
P3	Pump	500	17.0
S4	Syringe	500	24.0
K5	Sampling control	500	0.0
EK	Extraction control	200	0.0

Table 1:
Overview of filtered samples and corresponding eDNA concentrations

Tabelle 1:
Übersicht der gefilterten Proben und entsprechenden eDNA-Konzentrationen

The concentration of extracted DNA varied between 9.8 ng/µL and 24.0 ng/µL (Table 1). Notably, the highest concentrations were recorded in samples P2 and S4, both reaching 24.0 ng/µL. The concentration of DNA measured in the samples was of the same order of magnitude for the syringe and the pump samples. Syringe-based filtration performed comparably to the automated system. No significant difference was observed between the pump-filter combinations in terms of sample yield, suggesting that the system works reliably across different filter types, provided they are compatible in size and flow resistance. The negative controls (field control and extraction blank) showed 0.0 ng/µL, indicating the absence of contamination during sample handling and processing.

DISCUSSION

The major advantage of the system is its portability and ease of use. Unlike most commercial systems, which require supervision and often depend on external power sources, the prototype operates autonomously for a predefined time and is powered by a common 18 V tool battery. This makes the system especially suitable for fieldwork in remote areas with limited infrastructure.

The results of the field tests confirm that the developed eDNA sampler can successfully collect environmental DNA from freshwater environments. The measured DNA concentrations are within the expected range for aquatic eDNA studies and demonstrate the system's practical usability under field conditions. The agreement between automated and manual filtration (syringe) further supports the validity of the approach and confirms that the prototype is suitable for producing high-quality samples. In addition to DNA yield, user observations during field deployment confirmed that the handling of the prototype can be done without significant previous experience, and the splash-resistant housing protects the electronics from the elements. However, filter clogging occurred consistently after around 1 L of filtered water, justifying the decision to limit pump operation to 20 minutes per cycle.

The absence of contamination in the control samples indicates that the upstream filter placement is effective. This design choice reduces the need for internal cleaning and simplifies reuse. However, the current version lacks advanced features such as data logging or sample tracking, which could enhance traceability in large-scale sampling efforts.

Despite the successful performance of the sampler, the field test also highlighted practical challenges associated with the transport and handling of additional sampling equipment. Items such as filters, gloves, tweezers, waste bags, and cooling containers need to be transported and accessed efficiently under varying weather and terrain conditions. The current housing of the sampler itself is a functional but provisional prototype and could be further optimized to enhance waterproofing, durability, and usability in rugged environments.

Potential further improvements include adding a user interface (e.g., LCD display), implementing real-time monitoring of flow rates or pressure, and introducing remote connectivity (e.g., via Wi-Fi) for device control and data access. These features could be integrated in future iterations depending on field testing feedback and specific use case requirements.

The lack of an integrated or standardized transport solution for all required components was a limiting factor during field use. In response, a theoretical concept for a modular transport system—based on a hard plastic case with backpack straps—was developed. This approach could significantly improve handling efficiency and operational readiness in

the field. Future iterations of the project should explore optimized storage and organization solutions that support rapid deployment and help minimize the risk of contamination or equipment loss.

REFERENCES

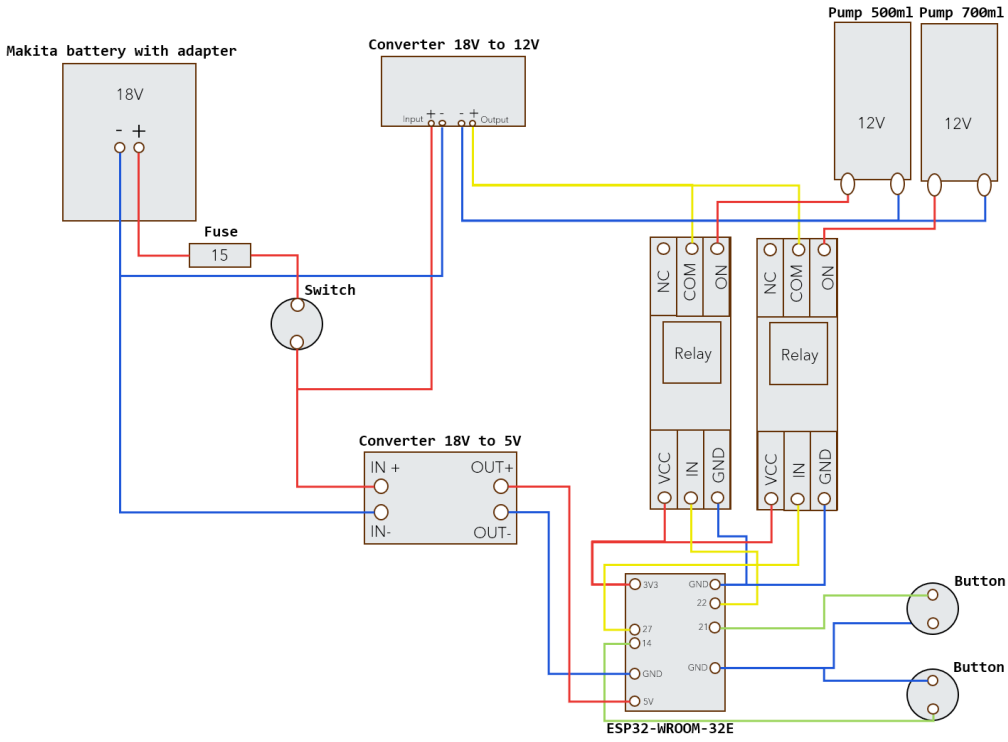
[1] G. F. Ficetola, C. Miaud, F. Pompanon, and P. Taberlet, "Species detection using environmental DNA from water samples," *Biol. Lett.*, vol. 4, no. 4, pp. 423–425, 2008, doi: https://doi.org/10.1098/rsbl.2008.0118

[2] P. Taberlet, E. Coissac, F. Pompanon, C. Brochmann, and E. Willerslev, "Towards next-generation biodiversity assessment using DNA metabarcoding," *Mol. Ecol.*, vol. 21, no. 8, pp. 2045–2050, 2012, doi: https://doi.org/10.1111/j.1365-294X.2012.05470.x

[3] K. Bruce et al., "A practical guide to DNA-based methods for biodiversity assessment," Advanced Books, 2021, doi: https://doi.org/10.3897/ab.e68634

[4] A. C. Thomas, J. Howard, P. L. Nguyen, T. A. Seimon, and C. S. Goldberg, "eDNA Sampler: A fully integrated environmental DNA sampling system," *Methods Ecol. Evol.*, vol. 9, no. 6, pp. 1379–1385, 2018, doi: https://doi.org/10.1111/2041-210X.12994

[5] N. Formel, I. C. Enochs, C. Sinigalliano, S. R. Anderson, and L. R. Thompson, "Subsurface automated samplers for eDNA (SASe) for biological monitoring and research," *HardwareX*, vol. 10, p. e00239, 2021, doi: https://doi.org/10.1016/j.ohx.2021.e00239



Supplementary Fig. 1

Supplementary Figure 1: Wiring diagram of the portable eDNA sampler. Source: Own image Ergänzende

Ergänzende Abbildung 1: *Schaltplan für den tragbaren eDNA-Probenehmer. Quelle: Eigenes Bild*

ABOUT THE AUTHORS

Pierre Hohenberger
Carinthia University of Applied Sciences
Europastraße 4
A-9524 Villach, Austria
E-Mail: p.hohenberger@fh-kaernten.at

Johanna Marion Schulz
Carinthia University of Applied Sciences
UNESCO Chair on Sustainable Management of Conservation Areas
Europastraße 4, A-9524 Villach, Austria

Alexander Blum
Carinthia University of Applied Sciences
Europastraße 4, A-9524 Villach, Austria
Carinthia University of Applied Sciences
UNESCO Chair on Sustainable Management of Conservation Areas
Europastraße 4
A-9524 Villach, Austria

Vid Švara, Dr. rer. Nat., Senior Researcher
UNESCO Chair on Management of Conservation Areas
Carinthia University of Applied Sciences
Europastrasse 4,
9524 Villach, Carinthia
Austria
ORCID 0000-0002-7100-9518

BACK TO CONTENT

Establishment of the Miyawaki forest at Carinthia University of Applied Sciences in Villach

Mojca Nastran, Anna Hollerer, Stefan Ruess, Daniel Dalton

ABSTRACT

The Miyawaki method offers a fast and effective nature-based solution for the restoration of ecosystems, especially in urban areas. Developed by Akira Miyawaki, the approach relies on dense planting of native species to create diverse, multi-layered forest ecosystems, resulting in a so-called Miyawaki Forest (MF). In April 2025, an MF was created on the campus of Carinthia University of Applied Sciences (CUAS) in Villach as part of the Interreg IT-AT project BioBox to promote urban biodiversity, especially for pollinators and birds. Following soil analysis, an area of 91 m² was prepared by plowing and enrichment with straw and compost. Inspired by the species composition of local riparian forests along the Drava River, nearly 300 saplings of native trees and shrubs were planted in three vertical layers by 16 volunteers. The MF at CUAS will serve as an outdoor laboratory for the students to monitor soil, growth and biodiversity. Although they are still rare in Austria, MF — like the CUAS pilot project — demonstrate the potential of small-scale urban forests to increase biodiversity, improve ecosystem services and engage communities. The Miyawaki method offers significant long-term environmental benefits, including better air and soil quality, urban cooling and carbon sequestration.

KEYWORDS

- Miyawaki forest
- tiny forest
- potential natural vegetation
- CUAS
- reforestation

Anlage eines Miyawaki-Waldes an der Fachhochschule Kärnten in Villach

ZUSAMMENFASSUNG

Die Miyawaki-Methode bietet eine schnelle und effektive, naturorientierte Lösung für die Wiederherstellung von Ökosystemen, insbesondere in städtischen Gebieten. Entwickelt von Akira Miyawaki, basiert der Ansatz auf der dichten Bepflanzung einheimischer Arten, um vielfältige, mehrschichtige Waldökosysteme zu schaffen, die als sogenannte Miyawaki-Wälder (MW) bekannt sind. Im April 2025 wurde auf dem Campus der Fachhochschule Kärnten (FHK) in Villach im Rahmen des Interreg IT-AT-Projekts BioBox ein MW angelegt, um die städtische Biodiversität, insbesondere für Bestäuber und Vögel, zu fördern. Nach einer Bodenanalyse wurde eine Fläche von ca. 91 m² durch Pflügen und Anreicherung mit Stroh und Kompost vorbereitet. Inspiriert von der Artenzusammensetzung lokaler Auwälder entlang der Drau pflanzten 16 Freiwillige ca. 300 Setzlinge einheimischer Bäume und Sträucher in drei vertikalen Schichten. Der MW wird als Freiluftlabor genutzt, in dem Studierende Boden, Wachstum und Biodiversität untersuchen und überwachen. Obwohl Miyawaki-Wälder in Österreich bislang nur vereinzelt realisiert wurden, illustriert das Pilotprojekt der FHK das Potenzial kleinräumiger Stadtwälder zur Förderung der Biodiversität, zur Verbesserung ökologischer Funktionen und zur Einbindung lokaler Gemeinschaften. Die Miyawaki-Methode bietet bedeutende langfristige Umweltvorteile, darunter eine bessere Luft- und Bodenqualität, städtische Kühlung und Kohlenstoffbindung.

INTRODUCTION

A Miyawaki forest (MF), also known as a tiny forest or pocket forest, is derived from a rapid reforestation method developed by the Japanese botanist Akira Miyawaki in the 1970s that has attracted worldwide attention. It represents a paradigm shift in ecological restoration as the Miyawaki method offers a fast and effective approach to establishing native forests in degraded or urban environments. An MF distinguishes itself through its emphasis on indigenous species, dense plantings, and soil preparation, fostering accelerated forest development and an increase in biodiversity [1]. An MF is established through dense planting of native trees and understory plants with application to restore degraded land or make urban areas more attractive and biodiverse. By mimicking natural forest ecosystems, a diverse, multi-layered and resilient plant community is created in which species support each other. This approach can be considered a nature-based solution and provides a fast, effective and sustainable way to restore native ecosystems that have been degraded or altered.

The selection of species for MF follows the principle of potential natural vegetation. The MF is intended to develop into a climax vegetation community that could develop and persist under the current climate and soil conditions in an area given there is no human influence, no disturbance, and assuming long-term natural succession [2]. Typically, more than 20 different native tree and shrub species are used, resulting in a multi-layered forest. The MF method accelerates forest development by planting a dense mixture of as many native mid-successional, late-successional, and climax species as possible in richly prepared soils, skipping early successional stages. Species are distributed over several structural levels (canopy, sub-canopy, understory trees, and shrubs) aiming to form a mature canopy within 20–30 years [3].

By design, MFs cover relatively small areas, from less than 100 m^2 up to several thousand m^2. These tiny forests are now very popular in urban areas because they fit into areas that are suitable for renaturalization. The planting phase involves a high-density arrangement, typically three to five seedlings per square meter, which encourages intense competition for resources among the plants, driving up growth and accelerating the natural selection process [4].

MF plantings have a high survival rate and grow at an annual rate of at least one vertical meter. After about three years, a completely self-sufficient, natural and indigenous forest will have developed that requires no further maintenance. MFs improve soil quality, prevent erosion, improve groundwater retention, significantly reduce heat and noise, improve air quality, and absorb up to 30 times more CO_2 than conventional monoculture plantations. In addition, they support the local fauna and do not require the use of chemical fertilizers [3], [5].

An MF utilizing the Miyawaki method was established in April 2025 on the Carinthia University of Applied Sciences (CUAS) campus in Villach as an implementation measure of the Interreg IT-AT project BioBox, with the goal of improving biodiversity in urban areas, and with particular focus to increase the diversity of pollinators and birds. The MF will also serve as a polygon for monitoring biodiversity and ecosystem services for CUAS students.

METHODS

When setting up the MF at CUAS, we adhered to the established steps [6]. We installed the MF planting area to the north of the main Villach campus building (46.611856 N, 13.882840 E). The area was configured as two half-circles and covered approximately 90 m^2. The soil was analysed, plowed and enriched with mature compost.

Since the area of the Drava River near the Villach campus is quite densely populated and the forests have been heavily modified, we were inspired by the nature reserves along the Drava [7] and various publications [8], [9], [10]. Most of the species planted in the CUAS MF can be found along large rivers in mixed riparian forests containing *Quercus robur, Ulmus laevis* and *Ulmus minor, Fraxinus excelsior* or *Fraxinus angustifolia* in a habitat type referred to as *Ulmenion minoris*. We selected several native flowering species of smaller trees and shrubs that attract insects and birds, thus increasing biodiversity and aesthetics.

On 23 April 2025, approximately 300 seedlings of native trees and shrubs were planted (Table 1). The planting was organized in a participatory manner. After planting, a thick mulch layer of wood chips was applied to retain moisture and control weeds. The planned maintenance included summer irrigation in the first year, which will be repeated in summer 2026. A low protective fence will be erected around the forest to prevent damage

to shoots and bark caused by wildlife (primarily rabbits) and to restrict pedestrian access during the early stage of growth.

Tab. 1

	Scientific name	Common name	Vertical layer	Maximum height (m)	No. of plants surveyed	No. of plants invoiced
1	*Cornus mas*	Cornelian cherry	1	5	9	10
2	*Cornus sanguinea*	common dogwood	1	4	14	15
3	*Corylus avellana*	hazel	1	4	7	5
4	*Crataegus monogyna*	common hawthorn	1	5	31	30
5	*Euonymus europaeus*	European spindle tree	1	4	30	30
6	*Prunus spinosa*	blackthorn	1	5	24	25
7	*Rhamnus frangula*	alder buckthorn	1	5	34	35
8	*Salix purpurea*	purple willow	1	3	26	28
9	*Sambucus nigra*	black elder	1	7	8	10
10	*Viburnum lantana*	wayfaring tree	1	4	15	15
11	*Viburnum opulus*	Guelder rose	1	4	17	18
12	*Weigela florida*	old-fashioned weigela	1	2	1	0
13	*Alnus glutinosa*	black alder	2	25	5	4
14	*Alnus incana*	grey alder	2	20	1	2
15	*Populus tremula*	quaking aspen	2	21	0	2
16	*Prunus padus*	bird cherry	2	10	22	20
17	*Salix alba*	white willow	2	25	11	10
18	*Taxus media* 'Hicksii'	common yew	2	15	14	15
19	*Fraxinus excelsior*	European ash	3	30	2	4
20	*Populus alba* 'Nivea'	white poplar	3	30	4	3
21	*Quercus robur*	English oak	3	40	3	3
22	*Ulmus laevis*	European white elm	3	35	11	12
		total			**289**	**296**

Table 1:
Species of trees and shrubs in three vertical levels. Layer 1 represents understory species, layer 2 represents sub-canopy species, and layer 3 represents canopy species.

Tabelle 1:
Arten von Bäumen und Sträuchern in drei vertikalen Schichten. Schicht 1 repräsentiert Unterwuchsarten, Schicht 2 repräsentiert Unterkronenarten, und Schicht 3 repräsentiert Kronenarten.

A low-altitude flight was conducted over the MF on 23 September 2025 using an uncrewed aerial vehicle (UAV), generating an orthophoto of the MF following the first growing season. A survey of the surviving plants was made in parallel to the UAV flight. Locations of each plant were approximated using QGIS software by placing color-coded points onto the orthophoto, and the resulting shapefile was exported into ArcGIS (Environmental Systems Research Institute, Inc., Redlands, CA, USA) for visualization.

RESULTS

According to the soil map of Austria, eutric cambisols are present along the Drava River at Villach [11]. The initial analysis of the vertical soil profile indicated a shallow organic horizon (3 cm depth), eutric brown soil (9 cm depth), underlaid by a predominantly sandy soil with clay admixtures, which is most likely a remnant of historical alluvial deposits from the Drava River (Figure 1). After plowing, we enriched the soil with 0.9 m^3 of mature compost with straw. With 16 student and staff volunteers (Figure 2), approximately 300 seedlings of 21 native tree and shrub species were planted. Planting took about two hours, after which 5.5 m^3 of mulch and wood chips were added (Figure 3). A total of 4,175 € was spent to establish the forest, covering the purchase of seedlings, compost, wood chips for mulching, and gloves. The costs do not include the fence, which will be installed later, or the volunteer work. A representative distribution of the plantings is shown (Figure 4).



Fig. 1

Figure 1:
Soil core sample from under the planned CUAS Miyawaki forest site, pre-planting stage

Abbildung 1:
Bodenkerprobe vom geplanten Standort des FHK-Miyawaki-Waldes, vor der Pflanzphase



Fig. 2

Figure 2:
Participatory planting (photo credit: Elisabeth Wiegele)

Abbildung 2:
Partizipative Pflanzung (Foto: Elisabeth Wiegele)



Fig. 3

Figure 3:
Planted CUAS tiny forest following the Miyawaki method

Abbildung 3:
Gepflanzter FHK-Miniwald nach der Miyawaki-Methode

DISCUSSION

Tiny forests are not yet widespread in Austria. The closest MF to our knowledge is in Maribor in Slovenia, established in 2020. As part of a pilot project “Wiener Wäldchen”, several tiny forests were planted in Vienna in 2022. In this respect, the CUAS MF will also serve to raise awareness among stakeholders about the benefits of urban forests, will increase local biodiversity, and will be a stepping stone between other green habitats in the city. It will also serve as a learning tool for students who will be able to measure and evaluate soil parameters, growth rates and biodiversity of flora and fauna over the years, especially in comparison to other empty or vegetated control plots in the neighborhood. Regular monitoring is planned.



Figure 4: Visualization of the Miyawaki Forest planting from above

Abbildung 4: *Visualisierung der Miyawaki-Waldpflanzung von oben*

Fig. 4

Despite some concerns about intensive site preparation, planting density, reduced genetic diversity, management required and low aesthetics in the early stages of forest establishment, the MF method offers numerous advantages. The importance of careful planning of the MF and ongoing research is emphasised to optimise the effectiveness of the tiny forest as a nature-based solution and to ensure its long-term success.

ACKNOWLEDGEMENTS

Funding for the Miyawaki Forest planting was provided through the Interreg IT-AT project BioBox, Project Number ITAT-27-008. We additionally thank the volunteers who conducted the site preparation and field plantings.

REFERENCES

[1] A. Miyawaki, "Restoration of urban green environments based on the theories of vegetation ecology," *Ecological Engineering*, vol. 11, no. 1-4, pp. 157-165, 1998, doi: 10.1016/S0925-8574(98)00033-0

[2] A. Chiarucci, M. B. Araújo, G. Decocq, C. Beierkuhnlein, and J. M. Fernández-Palacios, "The concept of potential natural vegetation: an epitaph?," *Journal of Vegetation Science*, vol. 21, no. 6, pp. 1172-1178, 2010, doi: 10.1111/j.1654-1103.2010.01218.x

[3] L. Butfoy, Miyawaki Method Handbook. Kent: Kent County Council, 2023

[4] J. C. Rodríguez and C. Sabogal, "Restoring degraded forest land with native tree species: The experience of "Bosques Amazónicos" in Ucayali, Peru," *Forests*, vol. 10, no. 10, p. 851, 2019, doi: 10.3390/f10100851

[5] M. L. Cárdenas, B. Pudifoot, C. L. Narraway, C. Pilat, V. Beumer, and D. B. Hayhow, "Nature-based solutions building urban resilience for people and the environment: Tiny Forest as a case study," *Quarterly Journal of Forestry*, vol. 116, no. 3, pp. 173-183, 2022

[6] V. E. Cambria, C. Fratarcangeli, G. Fanelli, V. C. Cuccaro, I. Panero, M. De Sanctis, et al., "Testing the Miyawaki method in Mediterranean urban areas through a standardised experimental design," *Botany*, vol. 102, no. 9, pp. 379-386, 2024, doi: 10.1139/cjb-2024-0045

[7] Drava - Natura 2000. "Riparian oak-ash-elm woodlands along large rivers," 2025, available: https://drava-natura.si/en/habitats/riparian-oak-ash-elm-woodlands-along-large-rivers (accessed 13 October, 2025).

[8] I. Dakskobler, L. Kutnar, and U. Šilc, "Poplavni, močvirni in obrežni gozdovi v Sloveniji: gozdovi vrb, jelš, dolgopecljatega bresta, velikega in ozkolistnega jesena, doba in rdečega bora ob rekah in potokih," 2013, available: https://www.gozdis.si/f/docs/Publikacije/51_Poplavni_gozdovi_Dakskobler_et_al_celotna_2013.pdf

[9] European Environment Agency, "Riparian mixed forests of *Quercus robur*, *Ulmus laevis* and *Ulmus minor*, *Fraxinus excelsior* or *Fraxinus angustifolia*, along the great rivers (*Ulmenion minoris*)," 2025, available: https://eunis.eea.europa.eu/habitats/10199 (accessed 13 October, 2025).

[10] M. A. Fischer, K. Oswald, and W. Adler, "Exkursionsflora für Österreich, Liechtenstein, Südtirol," Land Oberösterreich, Biologiezentrum der Oberösterr. Landesmuseen, 2008

[11] W. Rieck, "Bodenkarte von Osterreich. (Soil map of Austria)," Joint Research Centre, European Soil Data Centre, 1989, available: https://esdac.jrc.ec.europa.eu/content/bodenkarte-von-osterreich-soil-map-austria (accessed 13 October, 2025)

ABOUT THE AUTHORS

Mojca Nastran
Department of Forestry and Renewable Forest Resources
Biotechnical Faculty
University of Ljubljana
Slovenia
E-mail: mojca.nastran@bf.uni-lj.si

Anna Hollerer
Construction Needs Nature, Faculty of Engineering & IT Carinthia University of Applied Sciences, Austria

Stefan Ruess
Spatial Informatics for ENvironmental Applications, Faculty of Engineering & IT Carinthia University of Applied Sciences, Austria

Daniel Dalton
UNESCO Chair on Sustainable Management of Conservation Areas, Faculty of Engineering & IT, Carinthia University of Applied Sciences, Austria

BACK TO CONTENT

Restoring ecosystems, advancing science: The Metschacher Moos outdoor lab

Ilja Svetnik, Daniel Dalton, Gerfried Pirker, Michael Jungmeier

ABSTRACT

On the occasion of the realignment of research activities at the Metschacher Moos, this article compiles key information about the natural environment, land use history, previous scientific studies, and planned initiatives. The State of Carinthia maintained a long-term lease on the site, located in a side branch of the Glan Valley (Carinthia), to restore wet meadows that were drained in the 20th century. With the acquisition of the land by the Kärntner Sparkasse Foundation, these restoration efforts and scientific activities can now be continued.

This presents an opportunity to develop a research site dedicated to restoration and the application of biodiversity technologies (BiDiTechs). The project "S.O.S. Metschacher Moos," funded by the Austrian Biodiversity Fund, enabled initial measures to resume management activities, including control of invasive species, restoration of monitoring plots, and installation of a sensor network. Further research projects are underway, aiming to contribute to the assessment of biodiversity and ecosystem services in restoration initiatives.

KEYWORDS

- moor
- field lab
- restoration
- biodiversity monitoring
- technology
- sensor network

Ökosysteme renaturieren, Forschung ermöglichen: Das Outdoor Lab Metschacher Moos

ZUSAMMENFASSUNG

Anlässlich der Neuausrichtung der Forschungsvorhaben am Metschacher Moos werden in diesem Beitrag die wichtigsten Informationen zu Naturraum, Nutzungsgeschichte, bisherigen wissenschaftlichen Arbeiten sowie den geplanten Vorhaben zusammengestellt. Das Land Kärnten hatte das Gelände in einem Seitenarm des Glantales (Kärnten) langfristig gepachtet, um die im 20. Jahrhundert entwässerten Feuchtwiesen zu renaturieren. Mit dem Erwerb der Flächen durch die Kärntner Sparkasse Privatstiftung können diese Bemühungen und die wissenschaftlichen Arbeiten fortgeführt werden.

Es bietet sich die Möglichkeit, ein Forschungsgelände für Renaturierung und den Einsatz von Biodiversitäts-Technologien (BiDiTechs) zu entwickeln. Das Projekt „S.O.S. Metschacher Moos" des Österreichischen Biodiversitätsfonds ermöglichte erste Maßnahmen zur Wiederaufnahme des Managements, darunter die Kontrolle invasiver Arten, die Wiederherstellung von Monitoring-Plots und die Installation eines Sensornetzwerks. Weitere Forschungsvorhaben sind im Laufen; sie sollen einen Beitrag zur Erfassung von Biodiversität und Ökosystemleistungen in Renaturierungsvorhaben leisten.

INTRODUCTION

RESTORATION NEEDS AND NEW TECHNOLOGIES (BIDITECHS)

The necessity of restoring degraded ecosystems is undisputed [1], and the UN Decade on Ecosystem Restoration 2021–2030 aims to contribute to this effort through a collective multilateral initiative. As a European contribution to this global endeavor, the Restoration Law (Regulation (EU) 2022/869) was enacted in 2024. This regulation has sparked significant discussion across Europe (e.g., [2]), which has also had an impact on Austria (e.g., [3]). The regulation obliges EU member states to ensure that, "by 2050, degraded ecosystems and habitats are restored to a good condition" [3]. As a first step, member states are required to submit restoration plans outlining the current data, planned measures, and priorities at sites.

The long-term nature and scale of this initiative present not only political, financial, and organizational challenges, but also significant ecological, technical, and scientific issues. Effective planning and monitoring of progress require appropriate technical tools. The systematic assessment of biodiversity and ecosystem services facilitates the development of new technologies. Additionally, it is essential to manage and process vast amounts of data across administrative and national boundaries and to represent them in time series.

Dalton et al. [4] have categorized and described a wide range of technologies (BiDiTechs, see [5]) that are evolving at a remarkable pace. This rapid development, often referred to as a "technology leap," is characterized by parallel advancements in different technologies that interact with one another, further accelerating progress. The most important technologies for biodiversity monitoring are found in the fields of earth observation (for ecosystems and habitats), optical and acoustic sensors (for species and populations), and genetic methods (molecular biology techniques, such as eDNA, for assessing genetic diversity and microorganisms).

However, there is a significant gap between the theoretically possible applications of these technologies and their practical implementation. This gap is due to challenges such as reliability, energy supply, weather resistance, insufficient and unreliable reference data, technical interfaces, and data transmission rates, among others. In general, there is a lack of reliable workflows, quality assurance tools, and user expertise. This highlights the need to test technologies, devices, and workflows in dedicated experimental sites.

The requirements for an experimental site include a relevant ecological research question– which in the case of Metschacher Moos is related to the restoration of a wetland–appropriate supporting infrastructures, favorable logistical and legal conditions including stable ownership structures, as well as high-quality and well-documented reference data.

These factors enable the swift validation of results, which is crucial for the testing and development of instruments. It is essential that the test site be available for an extended period and, ideally, can already reference historical data. This allows for better contextualization and calibration of results.

Such a test site is planned to be gradually developed at Metschacher Moos. It will serve as an outdoor lab for research and education that is conceptualized in this article.

THE RESEARCH SITE METSCHACHER MOOS: FROM WETLAND TO FARMLAND AND BACK

At the beginning of the 20th century, the extensive peatlands of the Glan Valley were considered the largest moorland in Carinthia [6]. Today, these peatlands have been almost entirely destroyed, with only a few remnant areas remaining. The Metschacher Moos, a wetland located in a side branch of the Glan Valley, was drained during the interwar period, converted into arable land, and intensively farmed. The drainage system consisted of three ditches and clay pipes laid in a herringbone pattern. Over time, the collapse of these pipes led to the gradual rewetting of the area. Between 1990 and 2020, the State of Carinthia leased this 14.6-hectare area and removed it from agricultural use. A long-term research project was initiated to observe secondary succession on the fallow wetland and to study vegetation development on former peat soils that had been used as farmland [6], [7], [8].



Fig.1

Figure 1:
The valley floor at Metschach. The side arm of the Glan Valley between Zweikirchen and Maria Feicht is intensively used for agriculture. The Metschacher Moos has developed into an important refuge for fauna and flora; it is connected to the surrounding area through several rows of shrubs and hedges. The image shows the Metschacher Moos (elevation 520 m) behind the power pole in the middle ground of the picture, looking eastward, with the Ulrichsberg mountain (elevation 1,022 m) in the background. (Photo: Michael Jungmeier)

Abbildung 1:
Der Talboden von Metschach. Der Seitenarm des Glantales zwischen Zweikirchen und Maria Feicht ist landwirtschaftlich intensiv genutzt. Das Metschacher Moos hat sich zu einem wichtigen Rückzugsort für Fauna und Flora entwickelt; es ist über mehrere Gehölzzeilen mit dem Umland vernetzt. Das Bild zeigt das Metschacher Moos (SH 520 m) im Bildmittelgrund hinter dem Strommasten, mit Blickrichtung Osten, im Hintergrund der Ulrichsberg (SH 1.022 m). (Foto: Michael Jungmeier)

After the lease with the State of Carinthia had ended, the land changed ownership. In October 2023, the parcel owner attempted to convert the area back into farmland, partially plowing it. In response to this imminent threat, the Kärntner Sparkasse Foundation purchased the land with significant financial investment to preserve it for biodiversity conservation and research.

STARTER PROJECT S.O.S. METSCHACHER MOOS

Upon acquisition by the Kärntner Sparkasse Foundation, parts of the Metschacher Moos were plowed, invasive species such as goldenrod (*Solidago* spp.) were spreading, individual trees had fallen, and the majority of the significant monitoring plots were lost. The project *S.O.S. Metschacher Moos: Emergency Measures for the Restoration of a Degraded Habitat* (financed by the Austrian Biodiversity Fund) enabled critical immediate actions to secure the ecological and scientific potential of the area, including the restoration of grassland habitats, monitoring and control of invasive species, rehabilitation of damaged long-term monitoring plots, continuation of monitoring, and the installation of a sensor network. Additionally, the foundations for long-term management were established through an assessment of the hydrological situation, the development of a management plan, and the creation of a monitoring concept. Selected restoration measures were implemented, such as the establishment of succession areas, the resumption of maintenance mowing, and targeted individual interventions (for example, nesting aids for birds, bats, and wild bees). By the conclusion of the project in autumn 2025, key measures will have been implemented, putting the area back on the path to restoration. A detailed management plan ensures that the site will be maintained as a grassland ecosystem through mowing and grazing [9]. A follow-up project will explore gentle rewetting measures that naturally avoid any impacts on neighboring properties [10].

OUTDOOR LAB OF I.C.E.B.

On October 13, 2023, an agreement was signed between Carinthia University of Applied Sciences and the Kärntner Sparkasse Foundation to develop research and educational infrastructure at Metschacher Moos. This agreement establishes the legal framework for the long-term restoration of the area and secures research opportunities for the future. The site will serve as a platform for developing, testing, and calibrating methods and technologies for assessing biodiversity and ecosystem services.

The outdoor lab is operated by the university's Interdisciplinary Centre for Ecosystem Services (I.C.E.B.), which was established in 2024. The center's mission is to "make biodiversity measurable" while focusing on the development and testing of relevant technologies. Together with other test sites, particularly the transnational UNESCO World Heritage site "Ancient and Primeval Beech Forests of the Carpathians and Other Regions of Europe" (https://whc.unesco.org/en/list/1133/), the Metschacher Moos will enable the testing and deployment of biodiversity technologies (BiDiTecs) in various environments.

RESEARCH ACTIVITIES 1990 – 2025

TIME SERIES AND INVENTORIES

During the lease period by the State of Carinthia between 1990 and 2020, the area was repeatedly the subject of scientific research, particularly in the 1990s. Long-term monitoring of vegetational succession formed the backbone of these studies and was conducted, with interruptions, from 1990 to 2025 (see [7], [8], [11], [12], [13], [14]). An early comprehensive overview of various taxa, including plants, vegetation ecology, succession,



Fig. 2

Figure 2:
Outdoor Lab at the start of the 2025 growing season: The central strip of shrubs marks a drainage ditch. The northern area (on the right) has been mulched. It displays the typical patches of fallow vegetation, which arise due to patterns of random dominance by individual species. These patterns change with the seasons. The southern area (on the left) has been rotary tilled to control invasive plant species and is now undergoing succession again. (Photo: Ilja Svetnik)

Abbildung 2:
Outdoor Lab am Beginn der Vegetationsperiode 2025. Der zentrale Gehölzstreifen markiert einen Entwässerungsgraben. Die Nordfläche (rechts) ist geschlegelt. Sie zeigt die typischen Patches der Brachevegetation, bedingt durch die Muster zufällige Dominanzen einzelner Arten entstehen. Die Muster wechseln mit den Jahreszeiten. Die Südfläche (links) ist zur Bekämpfung der Neophyten gefräst und unterliegt nunmehr wieder der Sukzession. (Foto: Ilja Svetnik)

mollusks, spiders, butterflies, selected ground beetles, caddisflies, macrozoobenthos, birds, amphibians, reptiles, and mammals, was provided by Wieser & Jungmeier [6]. Bogner & Golob [15] compared the biodiversity development in Metschach with other fallow areas.

Specialized studies focused on specific taxa, such as true bugs [16], [17], [18], spiders [19], bats [20], and butterflies [21]. Köstl et al. [13] presented an interim evaluation of the years 1990 to 2020, noting that the anticipated development toward wet meadow vegetation had not yet occurred. They attributed this to ecological site factors, particularly nutrient availability and water supply, which had so far prevented the establishment of ecologically significant species and communities. They emphasized that the transformation of wet farmland into ecologically valuable areas requires long timeframes (see [22]). Similarly, Steinbauer et al. [14] highlighted the long-term perspective of renaturation and showed that prior land use (e.g., maize cultivation in the northern area and mixed crops in the southern area) continued to influence the site even after decades of fallow.

The findings suggest that establishing near-natural vegetation units at the site requires extended time periods. To support ecological restoration, future management efforts must prioritize ensuring an adequate water supply and maintaining suitable nutrient conditions.

RECENT RESEARCH ACTIVITIES AND PROJECTS

Currently, 29 vegetation-ecological plots are established at Metschacher Moos along three transects. Furthermore, four groundwater monitoring wells have been installed, along with 40 soil TMS4 Soil Logger sensors (TOMST s.r.o., Prague, Czech Republic) to measure temperature and moisture (Figure 3). In addition, six points have been designated for acoustic sensors, and five points have been designated for physicochemical and eDNA sampling of the soil. Research activities are already underway and are planned to be gradually expanded.

Furthermore, in order to promote native species of birds, bats and insects, several nesting aids and boxes have been installed in different location both for continued monitoring and educational purposes. The fields have undergone tilling and mowing. Seeds of local



Fig. 3

Figure 3: Installation of groundwater monitoring wells. To enable continuous long-term monitoring of the groundwater level, a total of four gauges were installed within the research area in frame of the project S.O.S. Metschacher Moos. (Photo: Ilja Svetnik)

Abbildung 3: *Setzen von Grundwasserpegeln. Im Rahmen des Projekte Metschacher Moos wurden zur laufenden langfristigen Beobachtung des Grundwasserspiegels im Forschungsgelände insgesamt vier Pegel gesetzt. (Foto Ilja Svetnik)*

natural grasses and flowering plants have been sown onto the southern area, which is more heavily impacted by neophytes than the northern area. The fields will continue to receive extensive management from local farmers–both with machinery and cattle–in order to promote local flora and prevent the spread of invasive species.

BioMonitor4CAP: The Outdoor Lab in Metschach is part of the Horizon Europe project "BioMonitor4CAP," which addresses ways to systematically monitor agricultural

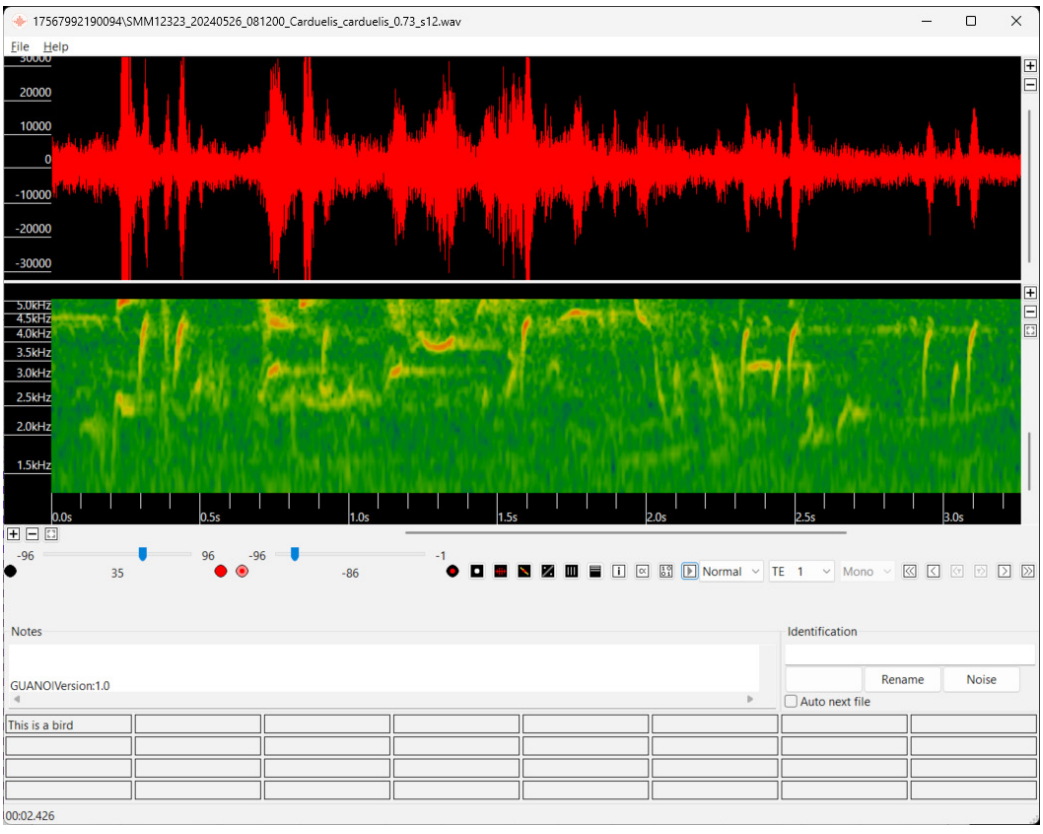


Fig.4

Figure 4: Spectrogram of a call of *Carduelis carduelis*. The European goldfinch, as identified by the BirdNet algorithm and verified by experts, is a characteristic bird of the site. This call was recorded in the frame of the project BioMonitor4CAP using a Song Meter Micro acoustic recording device at Metschacher Moos on 26 May 2024 at 8:12 a.m. (Source: own data, rendered by Kaleidoscope software, Wildlife Acoustics, Inc.)

Abbildung 4: *Spektrogramm eines Rufs von Carduelis carduelis. Der Stieglitz, identifiziert durch den BirdNet-Algorithmus und von Experten verifiziert, ist ein charakteristischer Vogel des Standorts Metschach. Dieser Ruf wurde im Rahmen des Projektes BioMonitor4CAP am 26. Mai 2024 um 8:12 Uhr im Metschacher Moos mit einem akustischen Aufnahmegerät vom Typ Song Meter Micro aufgezeichnet. (Quelle: Eigene Daten, dargestellt mit der Kaleidoscope-Software, Wildlife Acoustics, Inc.)*

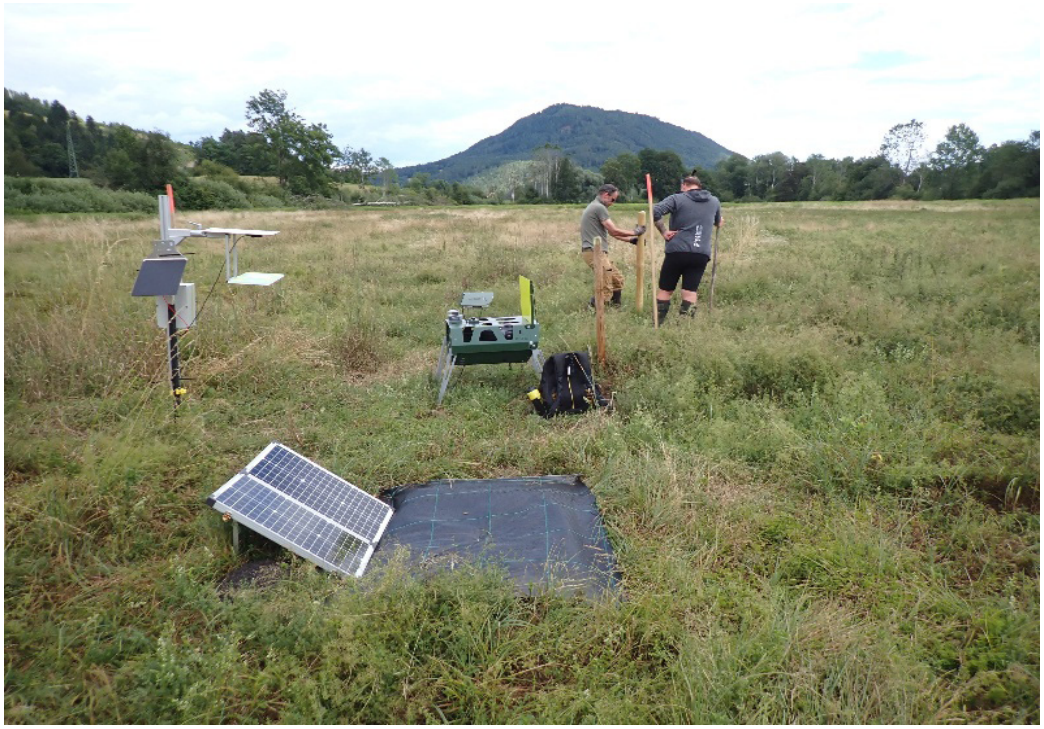


Fig. 5

Figure 5:
Automated insect monitoring. As part of the BioMonitor4CAP project, various methods for monitoring insects are being tested: Insect Detect (shown on the left), Diopsis Insect Camera (center), and the setup of a time lapse camera (in the background on the right).
(Photo: Ilja Sventik)

Abbildung 5:
Automatisierte Erfassung von Insekten. Im Rahmen des Projektes BioMonitor4CAP werden verschiedene Möglichkeiten zur Erfassung von Insekten getestet: Insect Detect (im Bild links), Diopsis Insect Camera (Bildmitte) und die Montage einer Zeitrafferaufnahmekamera (im Bild rechts hinten).
(Foto: Ilja Sventik)

biodiversity and thereby contribute to the further development of the Common Agricultural Policy (CAP) of European states. The Metschacher Moos serves as a study area where various methods are employed, including remote sensing (satellites, drones), automated recording of bird songs using AudioMoth and Song Meter (Wildlife Acoustics, Inc, Maynard, MA, USA) devices (Figure 4), and insect monitoring using camera traps such as Insect Detect and Diopsis (Figure 5), as well as eDNA collection from the soil. The results are expected to be available in 2026.

BioDivTech Lab: As part of a project funded by the Austrian Research Promotion Agency (FFG), the I.C.E.B. is currently developing research infrastructure for the coming decade (see [5]). One module of this infrastructure is being implemented in Metschach. In addition to advanced biodiversity sensors, a database for species referencing and a climate station are being established. The climate station is intended to be integrated into the European LTER (Long-Term Ecological Research) network program in the medium term, thereby becoming part of a European research infrastructure [23].

Further Monitoring Efforts: Biodiversity monitoring in the area is to be continued or initiated. This aims to continuously document the overall development of the area. In addition to the continuation of vegetation ecological monitoring, plans include the continuation of the EU Grassland Butterfly Index [24], [25] (see https://viel-falter.at/monitoring-en/) and the establishment of a transect for the Farmland Bird Index [26]. The monitoring efforts will be designed and conducted in accordance with the international standards for biodiversity monitoring in Protected Areas and OECMs set by the IUCN [27], [28].

FUTURE PERSPECTIVES: TOWARD A COLLABORATIVE RESEARCH SITE

This article aims to provide an initial overview of the establishment of the Outdoor Lab at Metschacher Moos. The scientific results of the current research projects, particularly with regard to the BiDiTechs, are expected to be available soon and will offer deeper insights. The scientific infrastructure will continue to be developed, and the restoration

measures outlined in the management plan will be implemented step by step.
According to the agreement between the Kärntner Sparkasse Foundation and Carinthia University of Applied Sciences, the following priorities have been defined for research activities. In particular, the focus shall be on: a) Developing and maintaining a research site for biodiversity and ecosystem services; b) Applying, testing, and developing methods and tools for long-term environmental monitoring; c) Investigating specific aspects of biodiversity, ecosystem services, as well as ecosystem restoration and rehabilitation; and d) Making research results visible through publications and educational formats.
The Metschacher Moos is also open for activities of other research and educational institutions, with the aim of fostering the collaborative development and use of the site. Future research activities will adhere to the following principles:

- Open Data: All environmental data will be made available for scientific reuse in accordance with the FAIR data sharing principles (metadata, primary data, results). Only sensitive data (e.g., nesting sites of rare species) will be excluded from this.
- Open Access: It will be ensured that relevant results are published and made publicly accessible. Wherever possible, this will be done through open-access publications. Access to the Metschacher Moos site will also be granted to research and educational institutions other than Carinthia University of Applied Sciences, in coordination with the university.
- Minimum Impact: The research site will be subjected to natural development as much as possible, based on the management and maintenance plan. Research and educational activities will be conducted with special consideration for sensitive species and habitats. New research projects must not compromise the outcomes of ongoing activities.

The Metschacher Moos thus serves as a unique platform for collaborative, open, and sustainable research and education, contributing to the understanding and preservation of biodiversity and ecosystem services.

REFERENCES

[1] C. R. Nelson, J. G. Hallett, A. E. Romero Montoya, A. Andrade, C. Besacier, V. Boerger, et al., "Standards of practice to guide ecosystem restoration – a contribution to the United Nations Decade on Ecosystem Restoration 2021-2030," Rome, FAO, Washington, DC, SER, Gland, Switzerland, IUCN CEM, 2024, doi: 10.4060/cc9106en

[2] A. Cliquet, A. Aragão, M. Meertens, H. Schoukens, and K. Decleer, "The negotiation process of the EU Nature Restoration Law Proposal: Bringing nature back in Europe against the backdrop of political turmoil?" *Restor. Ecol.*, vol. 32, no. 5, p. e14158, 2024, doi: 10.1111/rec.14158

[3] M. Jungmeier, "Wellen und Muster der europäischen Naturschutzpolitik in Kärnten – Das Beispiel Renaturierungsverordnung (RnV)," in *Kärntner Jahrbuch für Politik* 2024, Klagenfurt am Wörthersee: Hermagoras, K. Anderwald, K. Hren, and K. Stainer-Hämmerle, Eds., pp. 231–241, 2024, available: https://www.jahrbuchkaernten.at/fileadmin/jahrbuch/jahrbuecher/Jahrbuch_Politik_Kaernten_2024.pdf

[4] D. T. Dalton, K. Pascher, V. Berger, K. Steinbauer, and M. Jungmeier, "Novel Technologies and Their Application for Protected Area Management: A Supporting Approach in Biodiversity Monitoring," in *Protected Area Management - Recent Advances*, IntechOpen, M. N. Suratman, Ed., 2022, doi: 10.5772/intechopen.99889

[5] M. Jungmeier, A. Paulitsch-Fuchs, G. Paulus, and M. Schneider, "BioDivTech Lab – conceptualizing a new research infrastructure for biodiversity monitoring," *Carinthia Nature Tech*, vol. 2, no. 1, pp. 29–32, 2025, available: https://phaidra.fh-kaernten.at/detail/o:54

[6] C. Wieser and M. Jungmeier,"Bracheprojekt "Metschach" – Naturschutzprogramm zur Rückführung von Ackerland in Feuchtwiesen: Ergebnisse der Jahre 1990-1992," Amt der Kärntner Landesregierung, *Naturschutz in Kärnten*, vol. 13, Klagenfurt am Wörthersee, 1994, available: https://e-c-o.at/files/publications/downloads/L02734_1994_Wieser_Jungmeier_Bracheprojekt_Metschach_compressed.pdf

[7] C. Keusch, H. Kirchmeir, and M. Jungmeier, "Vegetationsentwicklung auf Feuchtbrachen - Das Projekt Metschach 1990 bis 2006," *Carinthia II Teil 2*, vol. 199, no. 119, pp. 413–432, 2009, available: https://www.zobodat.at/pdf/CAR_199_119_0413-0432.pdf

[8] A. Fuchs, V. Berger, K. Steinbauer, T. Köstl, D. Wuttej, and M. Jungmeier, "The long-term effects of monoculture maize cultivation on plant diversity," *Phytocoenologia*, vol. 50, no. 4, pp. 397–408, 2021, doi: 10.1127/phyto/2021/0382

[9] Arge NATURSCHUTZ, "Managementplan Metschach – Bericht 2024," Arge NATURSCHUTZ, Klagenfurt am Wörthersee, no. PN-2025/10/675-2, 2025

[10] eb&p Umweltbüro GmbH, "Metschacher Moos Hydrogeologische Grundlagen – Technischer Bericht," eb&p Umweltbüro GmbH, Klagenfurt am Wörthersee, no. HYMA-24, 29 p., 2024

[11] G. Dullnig, H. Kirchmeir, and M. Jungmeier, "Zur Vegetationsentwicklung auf Feuchtbrachen - das Projekt Metschach 1990 bis 1999," *Carinthia II Teil 2*, vol. 191, no. 111, pp. 465–495, 2001, available online at https://www.zobodat.at/pdf/CAR_191_111_0465-0495.pdf

[12] M. Jungmeier and C. Wieser, "Bracheprojekt „Metschach" Naturschutzprogramm zur Rückführung von Ackerland in Feuchtwiesen." *Carinthia II Teil 2*, vol. 183, no. 103, pp. 223–230, 1993, available: https://www.zobodat.at/pdf/CAR_183_103_0223-0230.pdf

[13] T. Köstl, D. Wuttej, V. Berger, K. Steinbauer, A. Fuchs, and M. Jungmeier, "Vegetationsuntersuchung Metschach – 1990-2020," E.C.O. Institute for Ecology, Amt der Kärntner Landesregierung, Klagenfurt am Wörthersee, 52 p., 2020

[14] K. Steinbauer, V. Berger, T. Köstl, D. Wuttej, H. Kirchmeir, and M. Jungmeier, "Abgrenzung von Vegetationseinheiten anhand multitemporaler Luftbilder am Beispiel von Feuchtbrachen," In T. Lumetsberger and A. Höltl (Eds.): *19. Österreichische Botanik-Tagung*, 23–25 September 2021, Donau-Universität Krems, p. 22, 2021, available: https://door.donau-uni.ac.at/detail/o:1409

[15] Bogner & Golob KEG, "Biodiversität auf Stilllegungsflächen: Zusammenhänge zwischen Artenschutz und Landwirtschaft – Endbericht," Amt der Kärntner Landesregierung, Büro für Ökologie und Landwirtschaft, Klagenfurt am Wörthersee, 211 p., 2003

[16] T. Friess, "Die Wanzenfauna (Heteroptera) mehrjähriger Ackerbrachen mit Saumbiotopen im Glanfeld (Kärnten)" *Carinthia II Teil 2*, vol. 189, no. 109, pp. 335–352, 1999, available: https://www.zobodat.at/pdf/CAR_189_109_0335-0352.pdf

[17] T. Friess, "Beitrag zur Kenntnis der an Grau-, Grün- und Schwarzerlen (*Alnus* spp.) vorkommenden Heteropteren in Südösterreich (Steiermark, Kärnten)," *Beiträge zur Entomofaunistik*, vol. 1, pp. 57–71, 2000, available: https://www.zobodat.at/pdf/BEF_1_0057-0071.pdf

[18] T. Friess, "Fallow fields and nature conservation: Evaluation of protective measures on the example of the heteropteran fauna in Carinthia, Austria (Insecta: Heteroptera)," *Entomological Society of Austria*, vol. 9, pp. 8–10, 2003, available: https://www.zobodat.at/pdf/ENTAU_0009_0008-0010.pdf

[19] C. Komposch, "Bemerkenswerte Spinnen aus Südost-Österreich I (Arachnida: Araneae)," *Carinthia II Teil 2*, vol. 190, no. 110, pp. 343–380, 2000, available: https://www.zobodat.at/pdf/CAR_190_110_0343-0380.pdf

[20] D. Wieser, "Ergebnisse der Batcordererhebung des Kärntner Landesmuseums an heimischen Fledermäusen 2015 (Mammalia: Chiroptera)," *Rudolfinum - Jahrbuch des Landesmuseums für Kärnten*, 2015, pp. 371–383, available: https://www.zobodat.at/pdf/Rudolfinum_2015_0371-0383.pdf

[21] P. Huemer and C. Wieser, „Neufunde von Schmetterlingen aus dem Gebiet des Bracheprojektes „Metschach" (Zweikirchen) (Lepidoptera)," *Carinthia II Teil 2*, vol. 187, no. 107, pp. 395–399, 1997, available: https://www.zobodat.at/pdf/CAR_187_107_0395-0399.pdf

[22] K.-F. Schreiber, "Grundzüge der Sukzession in 20-jährigen Grünland-Bracheversuchen in Baden-Württemberg," *Forstw. Cbl.* vol. 116, pp. 243–258, 1997, doi: 10.1007/BF02766901

[23] Directorate-General for Research and Innovation, "ERIC practical guidelines. Legal framework for a European Research Infrastructure Consortium," Revised, European Commission: Luxembourg (KI-01-25-077-EN-N), 2025, available: https://op.europa.eu/en/publication-detail/-/publication/c8ca2717-15c4-11f0-b1a3-01aa75ed71a1/language-en

[24] C. M. van Swaay, R. Schmucki, D. B. Roy, E. Dennis, S. Collins, R. Fox, et al., "EU Grassland Butterfly Indicator 1990-2023 Technical report", *Butterfly Conservation Europe & EMBRACE/eBMS & Vlinderstichting report VS2025.014*, Version v3, 2025, doi: 10.5281/zenodo.17174718

[25] J. Rüdisser, F. Barkmann, and M. Huss, "Tagfalter-Monitoring Metschacher Moos Jahresbericht 2025," University of Innsbruck, Innsbruck, 2025

[26] N. Teufelbauer and B. Seaman,"Farmland Bird Index für Österreich: Indikator 2023 bis 2029," BMLUK, Vienna, 2024, available online at https://assets.ctfassets.net/2oszne1tuxgg/17MCMmQOSsxbYx1QhJMbOI/c46a08bb5031187124ddafdbeccc43fc/2024_Bericht_Farmland_Bird_Index_2023.pdf

[27] D. T. Dalton, V. Berger, V. Adams, J. Botha, S. Halloy, H. Kirchmeir, et al., "A conceptual framework for biodiversity monitoring programs in conservation areas," *Sustainability*, vol. 15, no. 8, p. 6779, 2023, doi: 10.3390/su15086779

[28] D. Dalton, V. Berger, H. Kirchmeir, V. Adams, J. Botha, S. Halloy, et al., "A framework for monitoring biodiversity in protected areas and other effective area-based conservation measures: concepts, methods and technologies," International Union for Conservation of Nature, IUCN WCPA Technical Report Series no. 7, 2024, doi: 10.2305/HRAP7908.

ACKNOWLEDGEMENT

We would like to express our gratitude to the landowner, the Kärntner Sparkasse Foundation, which acquired the area and is making it available for long-term restoration and research purposes. Our thanks also go to the neighbors and the municipality of Liebenfels for their constructive collaboration. Last but not least, we extend our appreciation to the State of Carinthia, which recognized the need for restoration as early as the late 1980s, initiated action by leasing the area in 1990, and preserved the site for decades. We would like to express our sincere thanks and recognition for these efforts as well. The research activities are funded by different sources, including *S.O.S. Metschacher Moos* (Austrian Biodiversity Fund), *BioMonitor4CAP* (Horizon Europe Project Number 101081964) and *BioDivTech Lab* (Austrian Research Promotion Agency FFG).

DANK

Wir bedanken uns bei der Grundeigentümerin Kärntner Sparkasse Privatstiftung, welche die Fläche erworben hat und für Renaturierungs- und Forschungszwecke langfristig zur Verfügung stellt. Unser Dank gilt den Nachbarn und der Gemeinde Liebensfels für die konstruktive Zusammenarbeit. Das Land Kärnten hat bereits am Ende 1980iger Jahre die Renaturierungsnotwendigkeit erkannt, mit der Anpachtung 1990 einen Impuls gesetzt und die Fläche über Jahrzehnte erhalten. Auch dafür sollen Dank und Anerkennung zum Ausdruck gebracht sein. Die Forschungsaktivitäten finanzieren sich aus unterschiedlichen Quellen wie etwa den Projekten *S.O.S. Metschacher Moos* (Österreichischer Biodiversitätsfonds), *BioMonitor4CAP* (Horizon Europe, Projektnummer 101081964) und *BioDivTech Lab* (Österreichische Forschungsförderungsgesellschaft FFG).

ABOUT THE AUTHORS

Ilja Svetnik, MSc
Junior Researcher
UNESCO Chair on Sustainable Management of Conservation Areas
Carinthia University of Applied Sciences
Europastrasse 4
A-9524 Villach/St. Magdalen
i.svetnik@fh-kaernten.at

Daniel Dalton
Senior Researcher
UNESCO Chair on Sustainable Management of Conservation Areas
Carinthia University of Applied Sciences
Europastrasse 4
A-9524 Villach/St. Magdalen, ORCID
0000-0001-8267-1155

Gerfried Pirker
UNESCO Chair on Sustainable Management of Conservation Areas
Carinthia University of Applied Sciences
Europastraße 4
9524 Villach, Austria

FH-Prof. Mag. Dr. Michael Jungmeier
UNESCO Chair on Sustainable Management of Conservation Areas
Carinthia University of Applied Sciences
Europastraße 4
9524 Villach, Austria
ORCID
0000-0003-4510-2118

BACK TO CONTENT

Book Reviews

Handbuch Naturschutzfachkraft: a guide to getting things done in conservation

Julia Zierler

ABOUT THE PUBLISHERS AND AUTHORS



'Handbuch Naturschutzfachkraft' – or translated, the 'Handbook of Nature Conservation Engineering' – was written by an interdisciplinary team of authors consisting of experienced experts in science, administration, and practice. The aim of the editors Elisabeth Wiegele, Michael Jungmeier and Martin Schneider (Carinthia University of Applied Sciences) and its 54 authors is to create a practice-oriented reference that can be used both for training and everyday work. Contributors attach great importance to a holistic view of nature conservation and emphasize the importance of communication, cooperation, and legal background knowledge.

CONTENT AND STRUCTURE

The book is divided into several main chapters: the basics of nature conservation, the legal framework, methodological expertise, communication and public relations, project management and practical case studies. Each of the ten chapters begins with an introduction and concludes with practical exercises or checklists.

The authors explain key terms and principles of nature conservation across the 662 pages of the book, including biodiversity, ecosystem services and sustainable development. One focus is on the current legal framework, in particular the Federal Nature Conservation Act of Germany and other relevant EU directives. Methods for mapping, assessment and monitoring are clearly explained, supplemented by numerous illustrations and tables.

STRENGTHS AND WEAKNESSES

The high practical relevance of the book's topics is particularly noteworthy. Case studies and checklists facilitate implementation in everyday working life. The book demonstrates, for example, how using appropriate amphibian protection fences and temporary barriers at construction sites can help safeguard migrating toads and frogs from hazards during their main movement periods.

The work integrates scientific, legal, and communicative aspects and thus promotes a comprehensive understanding. The authors address current topics such as climate change, invasive species and digitalization. The topics have regional relevance, especially for the Alps-Adriatic region, as most case studies feature a Carinthian example. The clear structure, understandable language, and numerous illustrations make the book accessible even for less experienced conservationists.

This accessibility, while helpful to attract interest in the individual topics, may also be the book's biggest weakness. Due to the simplified language, the depth of individual chapters sometimes falls short of expectations. Supplementary specialist literature is recommended for specialized questions. Furthermore, the book's focus is strongly on Austria and Austrian law. International aspects are only dealt with marginally. Some content, particularly on legal principles, is repeated in various chapters.

RELEVANCE FOR THE FIELD OF NATURE CONSERVATION

The 'Handbuch Naturschutzfachkraft' closes an important gap between theory and practice. It serves as a guide for career starters but also offers experienced professionals a valuable orientation aid for new challenges. The book is particularly relevant for training and further education, as it was compiled with these activities in mind. The chapters convey the requirements for modern nature conservation specialists in a practical and understandable way.

By emphasizing communication and project management, the handbook helps to strengthen the often-underestimated 'soft' skills in nature conservation. The practical examples promote the implementation of nature conservation measures on site and support cooperation with authorities, associations and the public.

CONCLUSION

The 'Handbuch Naturschutzfachkraft' is a highly recommended reference for anyone working in or interested in nature conservation. Despite minor weaknesses, its relevance is convincing due to its practicality, wealth of topics, and holistic approach. It makes an important contribution to the professionalization of the field and should not be missing from any specialist library.

ORIGINAL TITLE:

[1] E. Wiegele, M. Jungmeier, M. Schneider (Eds.), Handbuch Naturschutzfachkraft, Praktischer Naturschutz für Baustellen, Betriebsgelände und Infrastrukturen, Fraunhofer IRB Verlag, ISBN 978-3-7388-0598-7, 2022

ABOUT THE AUTHOR

Julia Zierler, MSc
Formerly at UNESCO Chair on Sustainable Management of Conservation Areas, currently working as project manager Klima- und Energiemodellregion Murraum Leoben
E-Mail: zierler@kampus.at

BACK TO CONTENT

Monitoring biodiversity: Hitting the nail on the head with *Conservation Technology*

Daniel Dalton

REVIEW:

The book *Conservation Technology* was published in 2021 by Oxford University Press (Oxford, UK) [1]. Edited by conservation gurus Serge A. Wich and Alex K. Piel, and with contributions from 39 renowned experts in their respective fields, this book is a master class on the state of modern-day technology-based biodiversity monitoring.

The purpose of this review is to provide a brief summary explaining the ways in which this information-dense book is relevant for the state-of-the-art of various fields of biodiversity monitoring today. In recent years global treaties and international agreements have highlighted a call to action to conserve our planet's fragile biodiversity in an attempt to mitigate the worst effects of the current biodiversity crisis, the so-called 'sixth extinction' that is driven by human activities [2]. The authors do an effective job at showing practical examples of how biodiversity monitoring can contribute to reaching the goals of these agreements, particularly through leveraging for the greater good of conservation the immense technological advances that we are experiencing today.

Conservation Technology provides a contemporary view on high-tech biodiversity monitoring techniques and remains perhaps the most comprehensive volume on the subject. While no longer a new resource, almost all topics in the book are as salient today as at the time of publication. *Conservation Technology* is written for university-level students and practitioners of conservation research and management. The book provides 13 independent and attention-grabbing chapters, but not based on the typical doom-and-gloom surrounding the issues of biodiversity loss, nor on the hype of the latest technological fads. Rather, the topics focus on techniques to gather relevant information about species behaviors, population dynamics, and other interesting biological phenomena. Authors of individual chapters are experts in their respective domains; one key strength is that, as a compendium, the book provides a highly interdisciplinary view into the diverse facets of biodiversity monitoring. Both of the editors are co-authors of multiple chapters, lending strength to their qualified knowledge on conservation biology.

Let's face it: countless academic reviews and books cover many of today's usual go-to technologies, and this book covers them, too. These include camera trapping, acoustic monitoring, environmental DNA collection, and using drones and animal-borne trackers to monitor wildlife or habitats. But this book enlists some true experts in these fields, while also introducing lesser-known state-of-the-art technologies that will likely play a larger role in the coming years. Such approaches include in-depth reviews on computer vision and artificial intelligence, applied case studies of SMART software implementation, valuation of tablet- and cell phone-based data collection, field techniques, and laboratory analysis of animal and ecosystem health. Critically, the book dedicates significant space on the societal implications of current technologies, future trends on personal privacy, and the potential impacts on human social dynamics. Many chapters outline challenges to current work flows, with suggestions on how to improve technologies in the near future for the benefit of nature. This book provides the space for authors to go into detail on the implementation of covered technologies. Rich with schematic diagrams and illustrative photos, a second or even third



Conservation Technology © Oxford Publishing Limited
ISBN: 9780198850243
This content is excluded from all forms of open access licence, including Creative Commons, and the content may not be reused without the permission of Oxford University Press – details of how to obtain permission can be found at https://global.oup.com/academic/rights/permissions/?cc=gb&lang=en&
Reproduced with permission of the Licensor through PLSclear.

read of the chapters provides additional pieces of knowledge or relatable experiences that help the reader to become fully immersed in each topic. I often found myself searching for a fact that I had read days earlier, only to get sidetracked by another feature that did not fully sink in upon the first read. One could argue that the detail in each chapter is too much to take in, but in my opinion, this is the strength of the book format: one really has the opportunity to digest the details of the topic and not just a summary. To expand one's knowledge requires pushing this limit, particularly when considering the target audience.

Especially in light that *Conservation Technology* has been available for four years, and the rapid pace of today's digital advancements, the relevance of the book is impressively pertinent for the current state of conservation research. However, despite its strengths, the book does have some weaknesses. The list of authors is geographically unbalanced, with most authors affiliated with institutions in the Global North. In this way, the book is a reflection of the inequities that plague conservation in general today. Some chapters specifically address the global imbalance of access to technologies and make a clear-eyed argument for greater inclusiveness. For example, a number of open-source technologies are described, including methods to reduce barriers to their implementation. Open access data sharing is emphasized, improving access to information for people living in resource-poor regions of the earth.

Another weak point of the book is its lack of analysis or discussion on marine ecosystem biodiversity. In retrospect, an additional chapter or two specifically providing an overview on monitoring sea life would have been welcome. On the other hand, focusing on terrestrial ecosystems and species may have been an editorial decision, leaving open an opportunity for the community of marine ecologists to provide a similar overview and outlook on monitoring pelagic species and ecosystems.

In summary, *Conservation Technology* delivers a highly interesting read on a host of prescient issues in biodiversity monitoring in the digital age. This book provides a strong springboard particularly for young scientists to understand the issues involved in biodiversity monitoring, giving a detailed overview on today's key technologies–as well as some uncommon ones–and the social considerations involved in their use. While the scope is on real-world implementation of state-of-the-art approaches, it remains relevant as well for developers of new technologies and policy makers. This book is a must-read for practitioners and academics alike; the conservation movement depends on leveraging these technologies effectively, as we risk the effects of ecosystem collapse without sound monitoring and management practices.

REFERENCES:

[1] S. A. Wich and A. K. Piel (Eds.), "Conservation technology," Oxford University Press, Oxford, UK, 297 p., 2021, doi: 10.1093/oso/9780198850243.001.0001

[2] E. Kolbert, "The sixth extinction: an unnatural history," Bloomsbury Publishing, London, UK, 319 p., 2015, paperback edition, ISBN 9781408851241

ABOUT THE AUTHOR

Daniel Dalton
UNESCO Chair on Sustainable Management of Conservation Areas
Carinthia University of Applied Sciences
Europastrasse 4
A-9524 Villach/St. Magdalen
E-Mail: d.dalton@fh-kaernten.at

BACK TO CONTENT

"Tage der Biodiversität 2025" – Collection of abstracts

Franz Hoelzl



REVIEW:

The abstract volume for the "Tage der Biodiversität 2025," hosted by the University of Natural Resources and Life Sciences (BOKU) Vienna, Austria from February 25-28, 2025, is a collection of recent scientific developments and points out different directions for the future of biodiversity research and conservation, predominantly from studies conducted in Austria [1]. This book of abstracts is more than a simple compilation of summaries, as it demonstrates how Austrian scientists and practitioners are combining innovative technologies and state-of-the-art methods to combat the escalating biodiversity crisis.
The depth of Austrian biodiversity research is underscored by the scope of the addressed challenges. The volume covers a great variation of habitats from the nation's largest ecosystems (forests) - which cover 48% of the country - to critical aquatic and dry habitats and even agricultural landscapes. Furthermore, it is a great assemblage of ideas and innovations to protect the environment and all its inhabitants for future generations.
The abstract volume is logically structured by the five main sessions of the conference:

1) *Measures of transformation: nature restoration*
   This topic primarily addresses connectivity of habitats and restoration of ecosystems. It furthermore deals with implementing conservation strategies to preserve and promote biodiversity.

2) *Competencies & quality control: from species knowledge to monitoring*
   This part shows the importance of new methods for biodiversity research and the shift towards technology-based biodiversity assessments, while it also highlights the demand for classical taxonomic experts (taxonomists, geographers) to interpret the massive datasets generated by the new technologies such as eDNA analysis, remote sensing, camera trapping, and passive acoustic monitoring.

3) *Together with society: outreach and education*
   This topic emphasizes the indispensable role of public engagement, citizen science, and education for sustainable development.

4) *Challenges of sustainability: conflicting goals, synergies, key issues, biodiversity, and climate*
   This crucial thematic area addresses complex conflicts, particularly the tension between conservation goals and economic demands. It explores topics from trade-offs between maximizing carbon storage and preserving biodiversity to potential negative impacts and necessary management strategies for the expansion of photovoltaic and wind energy infrastructure on biodiversity.

5) *Free and open topics*
   This category covers diverse, interdisciplinary topics, including the profound connection between soil biodiversity and One Health or the importance of genetic diversity in agriculture and livestock breeding.

Overall, the volume confirms the vital and multifaceted nature of Austrian biodiversity research. The work not only documents the existing crises (e.g., long-term species decline; loss of genetic diversity in rare species) but also gives examples for developing actionable, evidence-based strategies to protect biodiversity in line with international directives. Additionally, many contributions to this collection of abstracts deal with technologies that are of great interest to readers, authors, and editorial members of *Carinthia Nature Tech*.

In summary, the "Tage der Biodiversität 2025" abstract volume gives a great overview of the state of Austrian biodiversity research, its strategic implementation on new technologies, and the urgent, complex challenges across the country's ecosystems. Furthermore, it not only shows how conservationists are using new technologies but also how they have to grapple with complex policy mandates such as the EU Nature Restoration Law, while actively forging new partnerships between science and society.

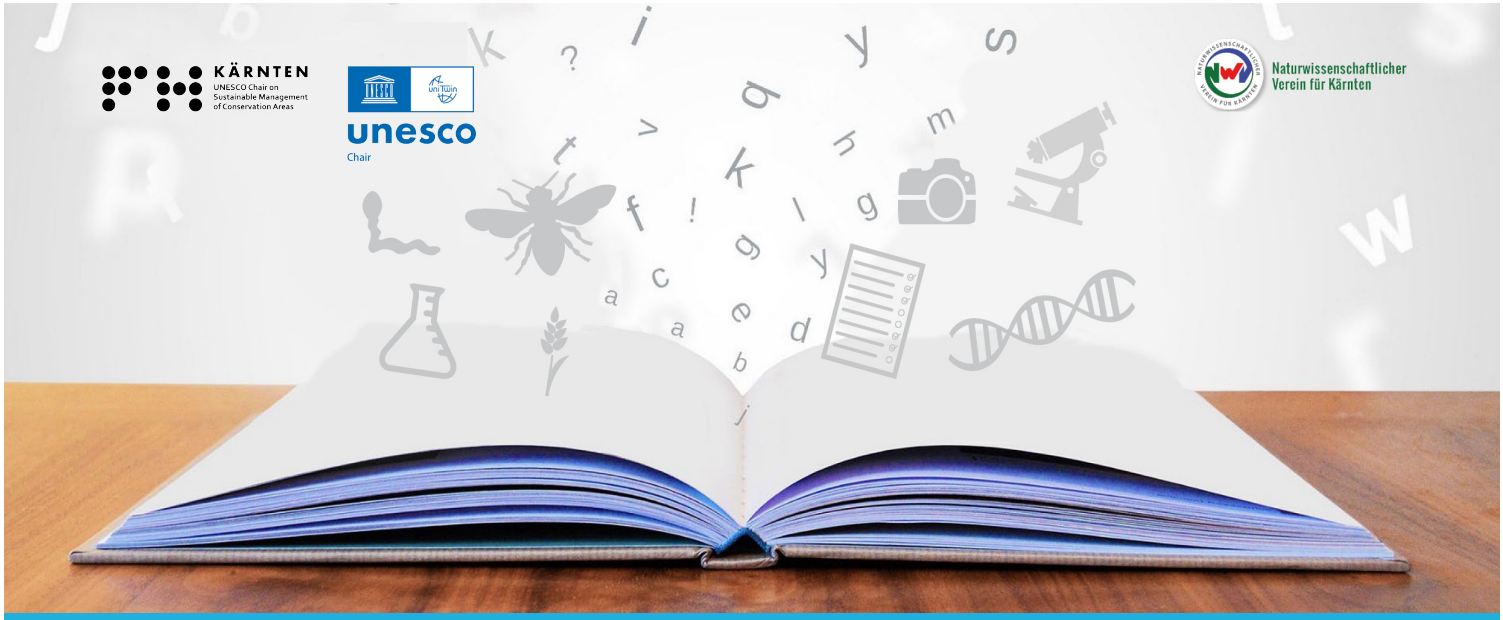
ORIGINAL TITLE:

[1] University of Natural Resources and Life Sciences, "ABSTRACTS: Tage der Biodiversität 2025," Biodiversity Days Conference, Vienna, Austria, 218 p., 2025, available: *https://biodiversitaetstage.boku.ac.at/wp-content/uploads/2025/02/TdB25_Abstractband.pdf*

ABOUT THE AUTHOR

Franz Hoelzl, PhD
UNESCO Chair
on Sustainable
Management of
Conservation Areas
Carinthia University
of Applied Sciences
Austria
f.hoelzl@fh-kaernten.at

BACK TO CONTENT



Carinthia Nature Tech Author Guidelines

Revised 2/4/2025

General Requirements

The journal Carinthia Nature Tech is organized into key sections: 1) Preface, 2) Scientific Articles: *Full Articles*, 3) Scientific Articles: *Short Articles*, 4) *Short Notes*, 5) *Book Reviews*. Two issues of Carinthia Nature Tech will be published annually. Only previously unpublished articles may be accepted. The editors may propose changes to the text based on feedback from the reviewers. Alterations will be discussed with the authors. Carinthia Nature Tech will use third party tools to check submitted texts for plagiarism. Plagiarism reports will be kept as part of the documentation process of the paper submission. Any detection of plagiarism will lead to an immediate rejection of the submission.

The articles must have a clear connection to the Alps-Adriatic Region. At least one contributing author or the study area must be directly connected to the region. The connection to the area must be clear through linking author affiliations or study locations to Carinthia. The Editorial Office will verify this connection at the time of manuscript submission.

Manuscripts submitted for publication as scientific articles undergo a double-blind peer review. This means that for *Full Articles* and *Short Articles* neither the authors nor the reviewers will be able to know each other's identities at the time of review. Submissions must avoid self-identifying language including reference to "our previous findings" or similar wording. Author names, affiliations, contact addresses, ORCID, and short biographies (max. 500 characters including spaces) need to be provided in the title page template. For scientific articles please include a minimum of 4 keywords that define the thematic area of your article. The template can be downloaded from the homepage.

Submissions should be provided in .doc, .docx, or .txt format. Manuscripts should be structured as follows: Abstract, Introduction, Methods, Results, Discussion, (Conclusions), References. If a submitted manuscript deviates from this structure, the corresponding author is encouraged to provide a short explanation for the deviation. Please refer to all tables, figures, and pictures in numerical order **following the references at the end of the text.** Figures, tables, and pictures can alternatively be provided as separate documents at the time of submission.

Graphics should be submitted as .png, .jpg, or .tiff formats, or embedded in .doc, .docx formats. Images should be provided in high quality resolution (300 dpi or greater). Videos should be provided as .mp4 files. Diagrams should be submitted as .xlsx. Supplementary materials should be accessible in a commonly used file type.

References should be provided in the IEEE citation style (https://journals.ieeeauthorcenter.ieee.org/your-role-in-article-production/ieee-editorial-style-manual/) and listed at the end of the paper. Footnotes may not be used in the text. The metric system should be used for all measurements. Numerical units should conform to the International System of Units (SI).

Authors are fully responsible for the contents and opinions expressed in their contribution. A declaration from the authors attesting to the originality of the work needs to be uploaded. You can find the template of the declaration on the homepage. If reproducing copyrighted materials such as photographs, illustrations, or other materials, written permissions from the copyright owners must be provided at the time of manuscript submission. An author's description template will be provided, where authors are required to fill in their names, affiliations, contact addresses, and short biographies (max. 100 words).

Submission and review process: Authors are invited to submit their manuscripts to dalton@cuas.at.

Identifier and indexation Carinthia Nature Tech will be identifiable via a unique ISSN. In addition, each accepted peer reviewed article will receive a DOI. Authors are requested to provide their ORCID so that articles can be directly linked to the authors. Full text downloads and access to supplementary materials will be provided.

Format of Scientific Articles

Full Articles: Full Articles are intended to showcase relevant and novel research findings of general scientific interest. *Full Articles* should have a strong focus on methods that advance the state-of-theart of the scientific research community. Submitted manuscripts should be 40,000 to 60,000 characters long, including spaces. Title, abstract, keywords, references, and table and figure captions count towards the character limit. *Full Articles* should be written in American English, with the title, tables, figures, and captions in both English and German. A German-language executive summary of 1,500 – 2,500 characters must be included. Exceptions to the character count restrictions will be considered by the Editorial Office on a case-by-case basis. For non-German speaking authors, the editorial office offers assistance in the German translation of the executive summary and description of tables, figures and captions.

Short Articles: Short Articles are intended to showcase promising results, approaches or projects that may be at an interim stage of research. Submitted manuscripts should be 20,000 to 40,000 characters long, including spaces. Title, abstract, keywords, references, and table and figure captions count towards the character limit. Articles should be written in American English, with the title, tables, figures, and captions in both English and German. A German-language executive summary of about 1,000 characters must be included. Exceptions to the character count restrictions will be considered by the Editorial Office on a case-by-case basis. For non-German speaking authors, the Editorial Office offers assistance in the German translation of the executive summary and description of tables, figures and captions.

Format of Short Notes

The *Short Notes* section is dedicated to research reports featuring projects carried out by early career researchers, students and practitioners. The purpose of *Short Notes* is to disseminate research results or preliminary project results at a low threshold. Contributions in this section should be 10,000 to 20,000 characters long, including spaces. Title, abstract, keywords, references, and table and figure captions count towards the character limit and should follow the same formatting as for *Scientific Articles*. *Short Notes* should be written in American English, with the title, tables, figures, and captions in both English and German. A German-language executive summary of 500 – 1,500 characters must be included. Exceptions to the character count restrictions will be considered by the Editorial Office on a case-by-case basis. For non-German speaking authors, the Editorial Office offers assistance in the German translation of the executive summary and description of tables, figures and captions. *Short Notes* will not be indexed and will not receive DOIs.

Format of Book Reviews

The *Book Reviews* section is intended to evaluate new stand-alone publications in the field of technologies in nature conservation and with a connection to the Alps-Adriatic Region. Each book review should be 3,500 – 8,000 characters long, including spaces, with a German-language abstract of 200 – 500 characters, including spaces. It should include summarizing information identifying authors and editors, title of the book, year published, the name of the publisher, and a link or reference to the original source. The review should provide a brief summary of the book. Critical analysis of the strengths and weaknesses of the book, comparison to other works in its field, and its overall relevance for the intended audience should be prominent in the review. *Book Reviews* will be managed within the editorial office and evaluated by the Editorial Office. *Book Reviews* will not be indexed and will not receive DOIs.